ABSTRACT

XU, XU. An Investigation on the Interactivity between Suspended-load Backpack and Human Gait. (Under the direction of Dr. Simon M. Hsiang.)

Rome et al. (2005) proposed a suspended-load backpack to scavenge energy through human walking. The relative movement between the load and the backpack frame can generate up to 7 watt of electrical power. The aim of this study was 1) to build a physical model for such a backpack which is capable of predicting the amount of the scavenged energy and the ground reaction force (GRF) based on different walking speeds and load weight, and 2) to evaluate the effects of the suspended-load backpack on the temporal and kinetic parameters of human gait.

The proposed physical model was a combination of an inverted pendulum model and a base excitation model, which, respectively, describe the oscillation of the torso during walking and the oscillation of the load excited by the movement of the torso. The index representing the scavenged energy in this model was the relative velocity between the load and the backpack frame. The model showed that the amount of scavenged energy and the ground reaction force are not monotonic with the walking speed and the load weight. The monotonicity depended on the damping coefficient of the backpack system.

An experiment was conducted to validate the accuracy of the model and to examine the effects of the suspended-load backpack on the human gait. Ten male subjects carrying a suspended-load backpack walked on a treadmill. The movements of the torso and the load were captured. The temporal and kinetic gait parameters were recorded. The results showed that 1) there was an agreement between the experiment data and the

predicted value from the model, where the absolute percentage error is 24.2%, 2) with the suspended-load backpack the normalized push-off force (NPOF) decreased when the walking speed increased, which is contradictory to the effect of a conventional backpack on NPOF, and 3) the suspended-load backpack had the same effect as a conventional backpack on cycle time (CT), single support time (SST), double support time (DST), normalized weight acceptance force (NWAF), and normalized mid-stance force (NMSF). These results provided some quantitative insight into the movement of the suspended-load backpack during walking and the response of the gait to the suspended-load backpack.

An Investigation on the Interactivity between Suspended-load Backpack and Human Gait

by
Xu Xu

A dissertation submitted to the Graduate Faculty of
North Carolina State University
in partial fulfillment of the
requirements for the Degree of
Doctor of Philosophy

Industrial Engineering

Raleigh, North Carolina

2008

APPROVED BY:

_____	_____
David A. Dickey, Ph.D.	David B. Kaber, Ph.D.
_____	_____
Gary A. Mirka, Ph.D.	Simon M. Hsiang, Ph.D. Chair of Advisory Committee

BIOGRAPHY

Xu Xu was born in 1983 and grew up in Beijing, China. He grew up with his parents, Xuezeng Wu and Aixue Zhang. Xu Xu graduated from Tsinghua University in 2004 with a degree of Bachelor of Science. He came to the United States and started his graduate studies in the Department of Industrial and Systems Engineering in North Carolina State University. In 2006, He received a degree of Master of Science under the direction of Dr. Gary Mirka. At present, he works as a research assistant for Dr. Simon Hsiang.

ACKNOWLEDGEMENTS

I would like to express my sincere thanks to my research advisor, Dr. Simon Hsiang, for his academic and philosophical advice and guidance. I would like to thank Dr. Gary Mirka, Dr. David Kaber, and Dr. David Dickey for serving on my committee and the suggestion they gave on my work. Thanks are also extended to my fellow graduate students, especially Xuezhong Wang and Tao Zhang, who have always been a reliable source of assistances and support.

TABLE OF CONTENTS

LIST OF FIGURES

LIST OF TABLES

1 Introduction

The cell phone, laptop computer, walkman CD player, and iPod — these gadgets have become our daily wardrobes and symbolize the new mobility of modern human beings. All of these gadgets would not function without batteries. As we approach an era of robotics in military operations (e.g., unmanned aerial vehicles), the need to have reliable electric battery sources is also necessary for handheld remote controls for soldiers. On the other hand, the large size and low capacity of batteries lowers the portability of these mobile devices and produces potential problems for the environment due to improper battery disposal. To counteract this issue, harvesting energy from everyday activities to generate power has been explored for more than a decade. Recently, a suspended-load backpack generator was invited to harvest up to 8 watt of electrical power from human walking (Rome, Flynn et al. 2005), which is sufficient to drive most portable electrical devices. However, the mechanisms of this backpack generator and the interaction between the backpack and person has not been fully investigated. It is only known that when walking speed increases, the amount of useful energy will rise with enlarged joint loading. At this point, the quantitative relationship between walking and harvested energy and the potential risk of the suspended-load backpack on the walking pattern remain unclear. The trade-off between scavenged energy and biomechanical influence is not fully known, either. Thus, before practically applying such a backpack device, the mechanism in such a backpack generator needs to be clarified.

In the current research, the mutual influence between the backpack and those who carry it will be investigated. The main goals are (1) to determine the amount of harvested energy for any specific walking speed and mass of pack, (2) to examine the effect of

suspended-load backpacks on gait parameters, and (3) to evaluate the potential trade-off between the benefit of energy harvesting and the cost of joint loading. A concise introduction is presented in the following sections and the objectives of this research are identified in Section 1.4.

1.1 Human Walking

As a characteristic of human beings, human walking is a type of body movement by which people can move themselves from one position to another. Compared with quadripedal walking, the bipedal walking of human beings needs greater balance control because they cannot provide the stability with three limbs on the ground as well as quadripedal animals. Whittle (1996) defined human walking as "a method of locomotion involving the use of the two legs alternatively to provide both support and propulsion," and Inman et al. (2006) defined it as "a process of locomotion in which the erect, moving body is supported by first one leg and then the other."

Due to the bipedal plantigrade type of human walking, the center of mass (CoM) of the body falls and rises with each step and leaves a smooth, sinusoidal curve when projected on the sagittal plane. Specifically, CoM falls to the lowest point in elevation when both feet contact with the ground and reach the highest point at the middle of the stance with a single foot on the ground. With respect to this energy consumption, such a vertical oscillation of the CoM may waste the energy because the oscillation cannot take us from one point to another. Interestingly, the mechanism of our body is capable of reducing the energy waste and facilitates optimal energy consumption. Saunders et al. (1953) proposed six gait characteristics of human walking (see section 2.1 for details) by which the displacement of CoM is minimized.

For better understanding of human movement, many models have been proposed using the laws of physics and engineering methods in the last several decades. In general, in a biomechanical model the human body is treated as a rigid multi-linkage system with forces and moments that are only applied on the joints between the rods. Therefore, most research on human movement models represents each leg as one rigid rod or two linked rods (femur and tibia), and human walking is simplified to an inverted pendulum. With the initial condition of each link and the external excitation, the movement of each link can be predicted by physical laws. Among these models, some focus on the maximum walking speed (Alexander 1976; McGeer 1990) some on the prediction of energy consumption with different walking speed (Alexander 1976), and some on the ground reaction force during walking (Mochon and McMahon 1980; Mochon and McMahon 1980). However, none of these models fully investigates the relationship between the vertical displacement and the walking parameters from a biomechanical perspective.

In the current research, a more detailed picture of human walking and gait analysis is demonstrated in Section 2, and a model on estimating the vertical displacement of the torso is proposed and validated in Section 3.

1.2 Backpack

A Backpack is a pack or carrier for a piece of equipment that is designed to be strapped on the user's back for carrying a load, and it is widely used by schoolchildren, recreational hikers, military, and astronauts (Figure 1). It was estimated that about 40 million students and 28 million outdoor enthusiasts use backpacks to carry school materials or outdoor equipment (Kinoshita 1985; Pascoe and Pascoe 1999). The early backpack had a cloth sack secured by straps over the shoulders because the shoulder

(including the deltoid and scapula) is a better fit for supporting load weight compared with the hands. In the last several decades, the design of the backpack has fundamentally changed with the use of frames and hip-belts by which the load weight is mainly distributed on hips and stabilized by shoulder straps (Bloom and Woodhull-McNeal 1987). This change improves the potential of load carrying since in principle the CoM of load should be placed close to the CoM of the body (Legg and Mahanty 1985; Stuempfle, Drury et al. 2004).

Figure 1 Backpacks for schoolchildren, recreational hikers, soldiers, and astronaut.

However, the backpack itself may lead to injuries or acute medical problems. Knapik et al.(1996) reviewed 117 articles (from 1947 to 1995) on load carriage with packs and stated that it was associated with stresses and strains on various joints and soft tissues. Numerous studies have investigated the effect of backpacks on human walking through physiological and biomechanical measures. It is well known that oxygen consumption, as an expression of energy expenditure, increased as the weight of the load increased (Datta and Ramanathan 1971; Soule, Pandolf et al. 1978; Legg and Mahanty 1985). The three-dimensional ground reaction forces also increased in proportion with an

increase on load (Kinoshita 1985). For a better understanding on the effects of load carriage, a comprehensive literature review is presented in Section 2.

1.3 Energy Scavenging

Nowadays, the demands of battery capacity keeps increasing since more and more mobile devices are involved in our daily life. However in the past fifteen years, while the CPU speed increased by one thousand times, battery capacity only doubled (Paradiso and Starner 2005). As a result, many electronics (e.g., radios, laptop computers, GPS) need to change their batteries frequently when the power supply is not available in some remote areas. Furthermore, cadmium and mercury in the battery could seriously pollute the environment.

Because of these limitations with batteries, some studies focus on how to scavenge waste energy from human movement to recharge the batteries. Starner (1996) conducted research on estimating the energy generated by body heat, breath, blood pressure, upper limb motion, and walking. He proposed that 5-8 watts of power might be recovered from daily movement without stressing the user, which is sufficient for most portable devices. In the research of Rome et al. (2005), a suspended-load backpack was invited to generate up to 18 watts mechanical power or 8 watts electrical power during human walking (Figure 2). To date no models have been developed to predict the amount of energy extracted from human walking. The investigation presented in this study introduces a biomechanical model to estimate the energy generated from the suspended-load backpack presented in the research of Rome et al. A broader literature review on energy scavenging from human movement is presented in Section 2.

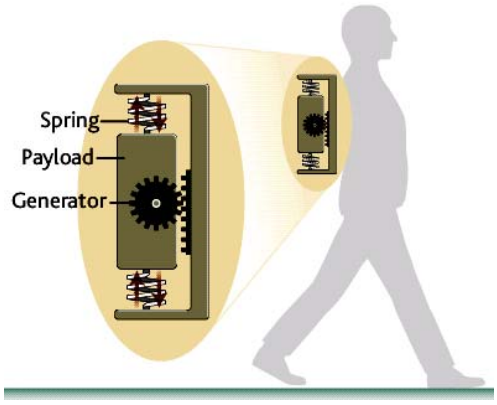

Figure 2 Energy harvesting backpack (adopted from Kuo, 2005)

1.4 Objectives

Human walking is accompanied by oscillation of the torso. This oscillation is transferred from the torso to the backpack during load carriage. With a suspended-load backpack, the mechanical energy of the backpack oscillation can be extracted and transformed into electrical energy. It is known that walking pattern may influence the amount of scavenged energy, and carrying a backpack can change human gait. Thus, there is an interaction between the suspended-load backpack and the gait. The objectives of this study are:

- To build a model to predict the mechanical energy generated by the suspended-load backpack based on the stiffness coefficient, damping coefficient, the mass of payload, and the amplitude of base excitation.
- To investigate the effect of the suspended-load backpack on the gait parameters.
- To investigate if there is any trade-off between energy production and safety in the use of a backpack.

2 Background

2.1 Gait Pattern and Ground Reaction Forces

During human walking, one leg serves as a support and the other leg moves forward to a new support site. Then, the two legs alternatively reverse their roles. Since walking is a repetitious sequence of body motion, the gait cycle is defined as the time interval between two successive occurrences of one of the repetitive events (Whittle 1996). Roughly, one gait cycle consists of two periods: stance phase and swing phase. Stance phase begins with the initial contact and is the period during which the foot contacts the ground. Swing phase begins with the toe off of the ground and is the period during which the leg is in the air and moves forward. In one gait cycle, the stance phase lasts about 60% of the cycle, and the swing phase is about 40% (Murray, Drought et al. 1964). However, the duration of these phase intervals varies and has an inverse relationship with the walking velocity (Andriacchi, Ogle et al. 1977).

The sum of the time from initial contact to toe off of both feet is longer than one gait cycle, due to the initial contact of one foot while the other foot is still on the ground. Therefore there is a period of double support during the stance phase that accounts for 10% of one gait cycle (Perry 1992; Whittle 1996). Accordingly, during the swing phase only one foot has contact with ground and this is the period of single support. As opposed to running, in walking, at least one foot is in contact with the ground to transfer body weight from one foot to the other. During running, the double support phase disappears, and between steps there is a flight phase.

In normal walking, the CoM can be approximated with a sinusoidal curve when projected on the sagittal plane (Inman 1966; Rose and Gamble 2006). The total amount of this vertical displacement is about 4 to 5 cm at a usual speed of walking (Saunders, Inman et al. 1953; Inman 1966). The crest of this oscillation appears at the mid-stance of the support limb, and the valley appears during the middle of double support (Rose and Gamble 2006). As a simple model of this phenomenon, a bipedal locomotion in which the lower extremities are represented by rigid levers is presented (Saunders, Inman et al. 1953). With a bipedal model, the radius of arc equals to the length of the leg. However, such locomotion results in a severe acceleration at the intersection point of two consecutive arcs, since there is a sudden change in the direction of velocity of the CoM. Consequently, Saunders et al. (1953) identified six determinants used to minimize the movement of the CoM of body and to reduce the energy usage during walking.

The first determinant is that the pelvis twists about the vertical axis during the gait cycle and brings each hip joint forward, by which less flexion and extension of hip is required. The effect of pelvic rotation is to reduce the radius of the arc of the locus of the CoM in the bipedal model. This reduction in the angular displacement of flexion and extension leads to a reduction in the vertical movement of the hip. The second determinant is that the pelvis is oblique downwards in the coronal plane on the side of the swing leg. When the hip of the stance leg is on the highest point, the pelvis lists downwards and reduces the height of the hip of the swing leg. Since the height of torso is the average of the two hips, the list of the pelvis reduces the vertical excursion of the torso. During the stance phase, the mechanisms of the knee, ankle and feet adjust the effective length of the leg to lower the vertical displacement of the hip. Such adjustments

are the third, fourth and fifth determinant of gait. Flexion of the knee of the support limb at mid-stance reduces the height of the crest of the locus, while the ankle and foot increase the effective leg length at the start of the stance phase and elevate the valley of the locus of CoM. The sixth determinant is that by keeping the walking base narrow, the lateral displacement of the pelvis is reduced. If the lower extremities were parallel to one another, the body would need to list half the interval between the axes of the hip joint. Due to the tibiofemoral angle and adduction at the hip, this excessive displacement is reduced and less lateral movement is needed to preserve balance. Figure 3 demonstrates the sum of the effects of six determinants and it is clear that the movement of the troso is approximately a sinusoidal curve of low amplitude. More detailed analyses and modeling of walking determinants will be presented in Section 3.

Figure 3 The sum of the effects of several determinants is a sinusoidal curve of low amplitude (Saunder 1953, Rose and Gamble 2006)

During human walking, the drop of body weight yields ground reaction force, which is a three dimensional vector that includes vertical, lateral and fore-aft force. These forces are opposite in direction and equal in intensity to those applied on the ground. The

horizontal shear force is relatively very small. Lateral component of force is less than 10% of body weight, and fore-aft shear force is equivalent to less than 25% of body weight (Perry 1992). Figure 4 shows vertical ground reaction force for three consecutive steps, and Figure 5 demonstrates some common nomenclature on gait analysis. From Figure 5, it is clear that the vertical force of ground reaction force shows a characteristic of double hump. The first peak occurs during the early stance in response to the weight acceptance. The valley representing the reduction of downward force is created by the rise of CoM, when the body moves forward over the weight-bearing foot. The second peak occurs in late stance and indicates the lowering of the body CoM, as body weight falls down.

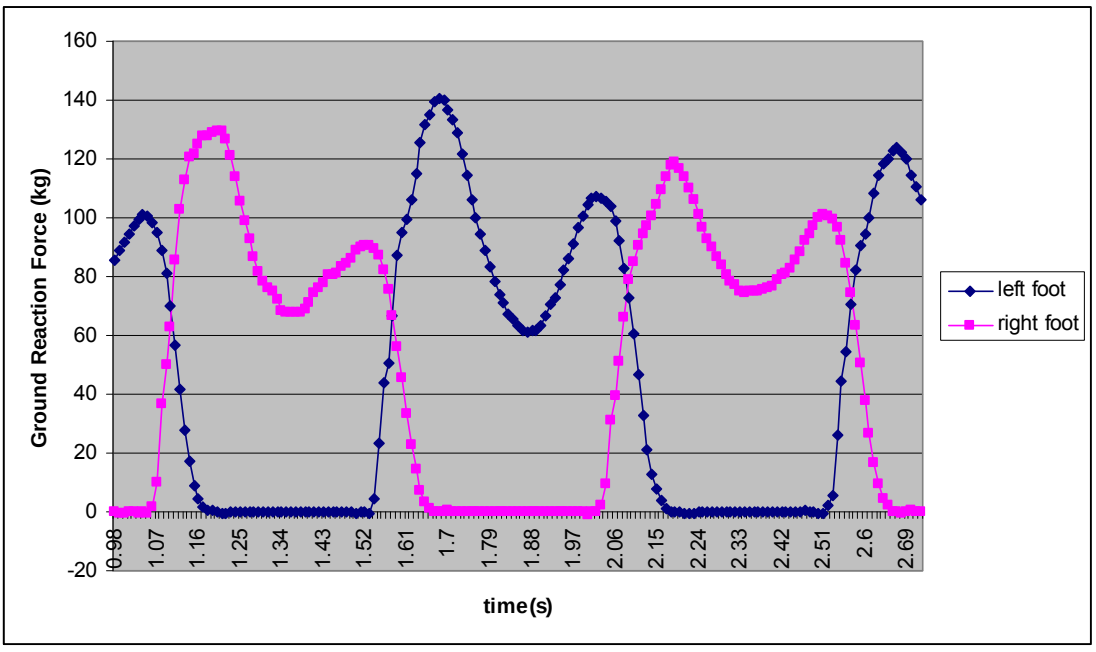

Figure 4 Vertical ground reaction force profile for three consecutive steps

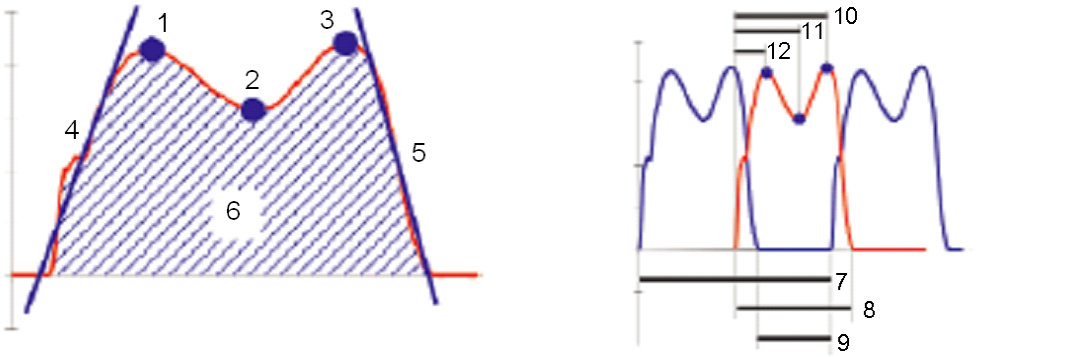

Force Parameters

1. First peak force
2. Mid support force
3. Second peak force
4. Weight acceptance rate
5. Push-off rate
6. Impulse
7. Stride time
8. Contact time
9. Single-support time
10. Time to second peak
11. Time to mid-support
12. Time to first peak

Figure 5 Some commonly used gait parameters (adopted from the manual of Gaitway Instrumented Treadmill)

At a walking speed of 82 m/min (3.1 mph), the value of the peaks is about 110% of body weight and the value in the valley is about 80% of body weight (Perry 1992). The maximum and minimum vertical force changes with different walking speeds. Walking with a slow speed reduce the peaks and increase the valleys. Conversely, fast walking results in a large peak-valley deviation from body weight. Summing the ground reaction forces of the left and right foot together yields the curve that represents the total ground reaction force applied on the human body. From Figure 4, it is clear that the shape of this curve is similar to a sine wave and the reason will be explained below in Section 3.1.

2.2 Study on Load Carriage with Backpack

There have been many studies investigating the effect of backpack load carriage during human walking. Knapik et al.'s review on load carriages (1996) revealed that many medical problems, such as foot blisters, stress fractures, knee pain and low-back pain, may be associated with load carriage. The military also recognized that during long

marching load carrying could lead to some clinical disorders because of the heavy loads (Kinoshita 1985). However, though a heavy load may be a potential risk factor for these injuries, Haisman (1988) stated that it would be hard to define the maximal load level because of widely varying circumstances. Some studies also reveled interesting results. The oxygen consumption divided by the load weight is almost constant for the load from 35 kg to 70 kg (Soule, Pandolf et al. 1978), and the muscle activity of erector spinae is even lower during light load carriage compared with the unloaded condition (Bobet and Norman 1984; Harman, Han et al. 1992). In addition, it is found that the backpacks systematically reduce the performance of other tasks such as short sprint, vertical jump and obstacle courses from the perspective of the military (Holewijn and Lotens 1992). In the following sections, several physiological and biomechanical studies are reviewed.

2.2.1 Physiological Studies

Datta and Ramanathan (1971) conducted a comparison among seven modes of carrying on the horizontal plane. Seven subjects walked at 5 km/hour and carried 30 kg load with seven different carrying conditions, which were (1) head, (2) rucksack, (3) double pack, (4) rice bag, (5) Sherpa, (6) yoke, and (7) hands. The observation on oxygen consumption and pulse rate revealed that the carrying mode significantly influenced the energy expenditure and cardio-respiratory response of the subjects. Within these seven modes, the double pack is the most efficient in energy cost and had least impact on the cardio-respiratory system, while two-hands is the most uneconomical mode and the most unfavorable. The calculation showed that when the energy expenditure of the double pack was 100 (the baseline), head and hand was 103.3 and 144.1, respectively. The

authors believed that the differences in the isometric tension of muscles could be a major cause for the variation in the values of the energy expenditure. Therefore, in terms of backpack design, the static work of muscle might need to be minimized to reduce energy consumption.

In contrast, Legg and Mahanty (1985) compared effects of five modes of carrying load on cardio-respiratory, metabolic and subjective response. Five subjects carried 35% of body weight using the following method: backpack with frame, backpack without frame, half load in backpack and half in waist belt, half in backpack and half in front pack, and total load in the trunk jacket. The results indicated that though carrying a heavy load had a significant effect on physiological measurements, which included oxygen consumption, minute ventilation, and heart rate, the way load was carried did not. However, the questionnaire showed that distributing the load half in backpack and half in front pack was much more comfortable compared with single backpack load. Therefore, the authors stated that the measurements in their study were probably not able to detect the difference over the five modes of load carrying in terms of physiology.

Soule et al. (1978) examined energy expenditure using different walking speeds and load weight. Fourteen subjects carrying 35, 40, 45, and 50 kg walked for 20 minutes on a treadmill at 3.2, 4.8 or 6.4 km/hour. Another ten subjects carrying 60, 65 or 70 kg walked for 45 minutes at the same speed. Since carrying the three heaviest loads cost about 90% of maximal oxygen consumption, most subjects could not complete the 45 minutes of walking. As expected, total expenditure increased significantly for each load with increasing walking speed and was approximately doubled as the speed was doubled from 3.2 to 6.4 km/hour. However, as the net energy expenditure was expressed as the

increased oxygen consumption divided by the weight of load, it showed a consistency at each speed as the loads ranged from 35 to 70 kg. However, the within-subject variability increased for lighter subjects at a higher speed. The authors concluded that increased energy expenditure was associated more with increased walking speed than increased load.

Evans et al. (1980) studied the effect of self-paced walking with load on physiology. Six male subjects and six female subjects performed self-paced walking on four different terrains with no external load, 10 kg, and 20 kg. It was seen that the external load had no effect on energy expenditure for female subjects, regardless of being expressed in watt or the percentage of maximal oxygen uptake. However, when expressed in maximal oxygen uptake, it was always about 45% for all subjects and conditions. It was also shown that the heart rates for all load conditions were similar and around 140 to 152 beat/minute. The authors believed that with self-paced walking the subjects maintained a similar relative cost level regardless of the loads by adjusting the self-pacing rate to achieve this cost level.

In a follow up study, Levine et al. (1982) examined the effect of training on prolonged (17.07 km) self-paced loaded walking. Twelve subjects were chosen for participation with half of them engaged in some form of regular aerobic activity. The result showed that walking velocity and predicted energy expenditure (watt) did not decline over time, regardless of the weight of load (no load, 10 kg and 20 kg). However, the walking speed was significantly decreased as the weight of load increased. In terms of relative energy expenditure, the percentage of maximal oxygen uptake was significantly

different between the trained and the untrained subjects, while the mean heart rate for untrained subjects was greater than that for the trained subjects.

Stuempfle et al. (2004) investigated the effect of the center of gravity of load on physiological response. Ten female subjects carried 25% of their body weight with a backpack and the load was placed in the high (T1~T6), medium (T7~T12), or low position (L1~L5). Oxygen consumption and minute ventilation of the high location were significantly lower than those at a low location. This result was consistent with the investigations conducted by Obusek et al. (1997), in which it was shown that the lowest metabolic cost occurred when the 25 kg load was positioned on the highest and closest to the body location. The author concluded that the load in the high position was close to the center of gravity of the body and generated relatively small movements. .

The physiological studies mentioned above indicated that load carriage with backpack had strong effect on the pattern of human walking. Generally speaking, the external load in backpack increases the energy expenditure during walking with respect to the oxygen consumption. Table 1 summarizes the experiment conditions of these studies and may provide some reference for the current research. As reviewed in the next section, considerable biomechanical studies have investigated the mechanism that may change energy expenditure.

Table 1 Experimental conditions for some physiological research

Authors and year	Speed (km/h)	Duration / Length	Load
Datta and Ramanathan (1971)	5	1 km	30 kg
Legg and Mahanty (1985)	4.5	60 min	35% bodyweight
Soule et al. (1978)	3.2 / 4.8 / 6.4	20 min	35 to 50 kg
Evan et al. (1980)	self-paced	1.3 to 1.6 km	10 to 20 kg
Levine et al. (1982)	self-paced	4 to 4.7 km	10 to 20 kg
Stuempfle et al. (2004)	5.1	10 min	20% body weight

2.2.2 Biomechanical Studies

2.2.2.1 Studies on Fundamental Gait Parameters

Martin and Nelson (1986) conducted research on the effect of carrying loads on walking patterns of men and women using high speed cinematography. Eleven men and eleven women carried five different military loads (0.8 kg, 9.5 kg, 17.7 kg, 30.0 kg, and 36.8 kg) and the latter two load conditions involved a framed backpack system for balanced-weight. Some temporal and kinematic characteristics of walking (stride length, stride rate, single-support time, double-support time, and the forward inclination of the torso) were measured. The results demonstrated that when males and females carried similar loads walking patterns were significantly different. The authors stated that this was due to the difference on stature and leg length between the male and female subjects. With respect to the effect of the backpack frame, the results showed that forward inclination of the torso significantly increased when the backpack was carried. Since the backpack added load entirely on the posterior aspect of the torso, an increase in the forward lean of the torso was necessary to offset this additional moment. However, the author stated that the amount of additional stress placed on the spine was unknown because the overall effect of carrying load and forward-leaning position was not clear.

Kinoshita (1985) examined the effect of different loads of weight on biomechanical parameters of human walking. Ten male subjects experienced external loading of 20% and 40% body weight with a backpack system, which corresponded with the effect of light loads and heavy loads. Three-dimensional ground reaction force was

measured with fixed walking speed at 4.5 km/hour and normalized by individual subject mass. In terms of gait patterns, single and double support periods in one gait cycle were significantly changed by the increased load. The percentage of double support period lengthened as load increased, and, accordingly, the percentage of single support period shortened since the total cycle time for all conditions were similar. The authors admitted that these results were not consistent with previous findings derived by Smith et al. (1960), in which neither the double nor single support periods made a significant difference with an increased load. Kinoshita believed that this discrepancy was mainly due to the walking speed, as found in the previous research, the subjects could freely choose their speed for each condition. It was also found that the ground reaction force in all directions increased in proportion to the increased system mass, which proved that the increased force was primarily due to the static effect rather than the dynamic properties of the system.

Charteris (1998) conducted research on the effect of backpack loading and walking speed on foot-floor contact pattern. Forty-five male subjects walked on a 40 meters walkway carrying 20%, 30%, 40%, 50 or 60% of their body weight at a constant speed. The subject personally selected this speed when 60% of their body weight was loaded. With the increased backpack load, the increased tendency for double-support time was considerable. The author believed that this increased double-support time would decrease the possibility of falling down and reduce the mechanical stress exerted on each lower extremity. It was also found that increasing the load in the backpack did not have a significant effect on cadence, stride length, and swing time. To compare the effect of walking speed and load level, the subjects were asked to walk unburdened at 3km/hour to

8 km/hour in 1km/hour increment in another test. The result indicated that the decrease in make-contact time (heel contacting with ground to hallux contacting with ground) with increased loading was similar to the effect of increased walking speed. The lengthened break-contact time (heel rise to hallux rise) with progressive loading had the opposite tendency to the effect of increased walking speed. In addition, the author stated that since all subjects in this experiment were bare-footed, the initiatory description on foot-floor contact pattern may need to be adjusted when footwear was used.

Wang et al. (2001) evaluated the effect of book backpacks on gait pattern and accumulated ground reaction force per stride and per meter. The accumulated force index was expressed as the integral of mean force divided by total mass on time. Thirty subjects experienced walking unloaded and walking with 15% of their body weight load in the backpack. The cadence was either self-selected by the subjects or fixed at 55.5 steps/minute by a metronome. According to the experimental procedures, only the ground reaction force of the left foot was recorded by the force plate. With respect to the kinematics' variables, carrying the load with book backpack had a significant effect on average walking speed while walking cadence did not. The results showed that single support time was reduced and double support time was increased, which was also consistent with Kinoshita (1985). In terms of kinetic variables, walking cadence did not have an effect on peak force nor the time to reach peak force. The single support impulse (the index of accumulated single support force) significantly decreased and the double support impulse increased when carrying the load. The authors believed the changes on accumulated force indices were helpful for distributing the load on both legs and reducing stress applied to a single lower limb. After normalizing by the stride length,

only the index of accumulated double support force had a significant change when the load was carried. The authors emphasized that the advantage of evaluating the load stress per meter is that it could be used for a between-subject comparison when stride dynamics were self-modified by the subjects.

Attwells et al. (2006) studied the influence of carrying heavy loads on posture and gait of soldiers. Twenty male soldiers were recruited and experienced four different conditions, which included 7.95 kg rifle, 15.95 kg webbing, 39.95 kg backpack, and 50.05 kg light antitank weapon. Seventeen active markers were placed on the body to identify movements of the lower limb, torso, head and backpack. Participants walked at a self-selected speed. The results showed that as the load weight increased, stride length had a decreased trend and the double support period increased. The authors believed that increased double support period could provide greater stability to reduce the possibility of losing balance. They also found that for lower limbs, the maximum angle of ankle, knee's range of motion, and the femur angle had both insignificantly and significantly increased when load was added. For the upper body, the torso and craniovertebral angles had a significant change with added load. Finally, the authors concluded that the rational design goal for military load carriage systems should minimize these biomechanical changes.

2.2.2.2 Studies on Kinetics, Kinematics, and Muscle Activities

Pierrynowsi et al. (1981) performed a study on mechanical energy of human segments with backpacks. Six male subjects experienced five different backpack loads ranging from 15 kg to 34 kg. They walked upon a level treadmill at 5.54 km/hour. For the biomechanical analysis, the subject and load were modeled as a linked system with 15 rigid segments connected by pin joints. The total segment energy at each point in time

was calculated as the summation of potential and kinetic energy. The internal mechanical work per stride for each segment significantly changed as soon as the subjects were loaded, but no additional change was observed for increasing loads. Therefore, the authors concluded that there were no considerable gait pattern adjustments while the loads became heavier. The results also showed that among each segment the legs exhibited the greatest energy changes, followed by the torso, and the majority of total body energy exchange resulted from these leg energies. In addition, since it was assumed that the backpack frame was fixed with the torso, the energy exchange of the torso and load would be in phase. However, in this research the torso energy did not change systematically with an increased load. One possible reason is that the relative movement between the backpack frame and torso weakened the energy transfer between them.

Bobet and Norman (1984) investigated the effects of load placement on back muscle activity during load carriage. Eleven subjects walked on a level surface at a velocity of 5.6 km/hour carrying a load of 19.5 kg in two different load placements (below mid-back or above shoulder level). Erector spinae EMG and trapezius EMG were measured, since backpackers often notice fatigue and soreness in this region. The average amplitude of the EMG signal was calculated and expressed relative to the EMG amplitude during unloaded conditions for that muscle. The results showed that EMG for the lower load placement was significantly lower than those for a high load placement. The EMG of erector spinae for both placements was less than that for unloaded walking. Therefore the author believed that the additional load could decrease the activity level of erector spinae, compared with unloaded walking. EMG of the trapezius for high placement was slightly above unloaded condition, while that for low placement was a

little below. One possible explanation given by the authors is that the moment generated by head, arms, and torso without the load is located forward of the lumbosacral joint and had to be balanced by the activity of erector spinae. With a loaded backpack, the moment of load partly compensates the moment of the upper body and consequently reduces the activity of the erector spinae. With a high placement, the dynamic moment generated by the load increased and larger muscle activities were required to offset this increase through shoulder straps and hip belts. The authors concluded that a mid-back placement should be preferable.

Bloom and Woodhull-McNeal (1987) examined the effect of internal-frame and external-frame backpack on postural adjustments while standing. Nine female and seven male subjects carried 14 kg and 19kg loads, respectively, which corresponded to 27% of body weight on average. The positions of joints of the ankles, knees, hips, and shoulders were marked and measured relative to the ankles. It was found that with either of two backpacks, the subject leaned forward and the positions of knees, hips, and shoulders significantly changed. The center of gravity of the whole body with load did not move significantly with either backpack, while the partial center of gravity of the upper body moved backward. Therefore, the authors believed that although the subjects were able to maintain the overall balance while carrying loads with either type of backpack, the center of gravity above the hips cannot be perfectly controlled. The comparison between the two types of backpacks indicated that the internal-frame backpack influenced the posture of subjects more than the external-frame backpack. The position of all measured joints moved forward for an internal-frame backpack, while the center of gravity above the knees was moved back. The authors stated this was a compromise between the need to

balance load and the need not to bend the torso too much. In addition, although male subjects preferred the internal-frame backpack while female subjects preferred the other type, the results showed that the position of joints of male subjects did not have a significant difference compared with that of female subjects while wearing either type of backpack.

Hsiang and Chang (2002) studied the effect of gait speed and load carrying condition on the reliability of ground reaction forces. Fifteen subjects experienced three walking speeds and five loading conditions (no-load, backpack, front-back double pack, front-pack, and two-hand carrying). Without perturbing the gait cycles of the subjects, several kinetic parameters of ground reaction force were measured and the first four statistical moments of these parameters were calculated. The results indicated that adding load to various parts of the body and increasing walking speed increased the magnitude of weight acceptance and push-off magnitude. The load also significantly increased weight acceptance rate and push-off rate, regardless of the location of the load. In terms of statistical moments, the two-hand carrying condition led to significantly higher values of standard deviation, skewness, and kurtosis of weight acceptance rate than the other load locations. Center of pressure velocity was not sensitive to the changes in speed and loading conditions. The authors concluded that higher walking speeds and loading conditions that moved the center of gravity from its common position had an adverse effect on the variability and the reliability of the gait pattern. This could be reflected in the higher moments of the distributions of several kinetic variables.

Ren et al. (2005) studied the biomechanical effect of load carriage dynamics during human walking using both computational modeling and gait measurement. All

body segments were assumed to be rigid body and only the movements in the sagittal plane were considered. An inverse dynamics approach was adopted for predicting changes in the joint force and joint moment. The pack interface force was used as input, rather than ground reactions in conventional applications. To describe the nonlinear property of the interaction between pack and torso, a nonlinear model with three cubic polynomials of position, velocity, and acceleration of the backpack was used to calculate the tangential pack interface force. The coefficient of each term in this nonlinear model was determined by the type of backpack and loading condition. Two subjects carrying a backpack were selected to provide kinematics input data for the motion of each body segment. The simulation results showed that under the assumption that only linear elastic and linear damping components were considered in the pack suspension model, mechanical energy expenditure decreased little with reduced stiffness and enlarged damping ratio of the pack interface. It was also found that decreasing the stiffness reduced the peak value of vertical pack force and skin pressure under the shoulder straps. However this effect was not significant on lower limb joints due to the load being relatively small compared with body weight. The authors concluded that a soft pack suspension system could reduce the risk of possibility of rucksack palsy and lower limb injuries.

Smith et al. (2006) studied the effect of carrying an unframed backpack on pelvic motion. Thirty female college students participated in three conditions which included walking without a backpack, unilaterally carrying a backpack with 15% of body weight, and carrying a backpack over both shoulders. Reflective markers were placed on the subject at the sacrum, anterior superior iliac spine, distal aspect of femurs, patella, middle

point of tibias, lateral malleolus, calcaneus, and forefoot. Pelvic tilt, pelvic rotation, and pelvic obliquity were measured as dependent variables in this research. The results indicated that angle of pelvic tilt increased under the condition of wearing unilateral or bilateral backpack for college-age females. As compared to not wearing a backpack, pelvic obliquity and rotation ranges of motion decreased while wearing a backpack, and pelvic tilt range of motion did not change. The angle of pelvic obliquity and rotation were similar over all three conditions, though increased obliquity was expected when carrying the backpack unilaterally compared to normal walking. The authors stated that based on the changes of pelvic motion, postural deviations may happen in female college student after long-term carriage.

To summarize, many studies quantitatively examined the effect of backpacks in terms of biomechanics. It is clear that the temporal gait parameters, ground reaction force, motion of segments, and muscle activities can be influenced by the configuration of the backpack. Table 2 summarizes all these dependent variables mentioned in the section above. These variables will be used as the references for the experiment design of the current research. On the other hand, since the suspended-load backpack is a very novel invention, none of these papers investigated the effect of such backpack. It is not clear whether a suspended-load backpack has the same effects as a regular backpack on gait parameters. To systematically predict how suspended-load backpacks affect gait pattern, a biomechanical model should be built to analyze the interaction between human body and backpack and the potential risk on human movement.

Table 2 Dependent Variables of some Biomechanics Research on the effect of Backpack

Authors and year	Dependent Variables
	Fundamental Gait Parameters:
Martin and Nelson (1986)	Stride length, Cadence, Single-support time, Double-support time
Kinoshita (1985)	step length, single-support time, double-support time, Three-dimension GRFs
Charteris (1998)	Single-support time, Double-support time. Heel to hallux time
Wang et al. (2001)	Stride length, Cadence, Single-support time, Double-support time, Time to reach peak GRF
Attwells et al. (2006)	Stride length, Double support time, Joint range of Motion
	Kinetics, Kinematics, and Muscle Activities:
Pierrynowsi et al. (1981)	Body segment energy
Bobet and Norman (1984)	Erector spinae and trapezius EMG
Bloom and Woodhull (1987)	Positions of ankles, knees, hips, and shoulders
Hsiang and Chang (2002)	Weight acceptance, Push-off, Mid-stance, Weight acceptance rate, Push-off rate
Ren et al. (2005)	Simulated GRFs
Smith et al. (2006)	Pelvic motion

2.3 Energy Scavenging

Because of the prevalence of mobile devices, such as cell phones, PDAs, and laptop computers, in the past two decades, the demand of the capacity of batteries has increased. However, in terms of the increasing performance of laptop computers, the increasing trend for battery energy is slow compared with CPU speed, wireless transfer speed, disk capacity, etc. (Paradiso and Starner 2005). Since traditional batteries limit the breakthrough of battery capacity, some other power supply methods were devised for energy harvesting. For instance, RFID tags derive energy inductively and capacitively from electromagnetic radiation, and some wristwatches use thermoelectric modules to drive the clock from the temperature difference between the human wrist and environment.

Another source of energy harvesting is the movement of human beings. With a hand-operated generator and a 30-second wind, a windup radio plays for approximately half hour at normal volume and a wind up flashlight gives approximately 20 minutes of bright light. Such devices require the use of human limbs to provide extra energy, which is finally converted into electrical energy. However such methods of power generation are accompanied by obvious movements, which could be very irritating to users. To avoid these annoying extra movements, human walking is a natural form of motion that can be used to extract energy. Starner (1996) stated that during normal walking, 67 watts of power is available in the heel movement of a 68 kg person walking at 2 steps per second. One way for scavenging this energy is placing piezoelectric crystals in the sole, by which electricity is generated from compressing the shoes during human walking (Shenck and Paradiso 2001). However, since the displacement needs to be very small to maintain walking balance, only less than 1 watt can be generated.

An alternative method to scavenging energy from human walking is to use a backpack generator. Rome et al. (2005) developed a suspended-load backpack, which converts mechanical energy from the vertical displacement of carried loads to electricity during normal walking. During walking, owing to the periodic movement of the CoM of the human body, the payload in a backpack has to go up and down the same vertical distance with a considerable amount of mechanical energy transferred. For a 36 kg payload, approximately 35 watts of power is available from this vertical movement. To scavenge this energy, the authors believed that decoupling the load from the human body would allow the differential movement between the load and the body, which is necessary for extracting mechanical energy and producing electrical energy. Six subjects

walked at speeds ranging from of 4.0 to 6.4 km/hour while carrying 20, 29, and 38 kg payloads in addition to the fixed weight of the backpack frame. The result showed that electrical power increased with walking speed and the weight of load in the backpack. With a 38 kg load, the suspended-load backpack gave 4.5 cm relative movement of the load with respect to the backpack frame and the linear movement drove a generator up to 5000 rpm with a rack. The average electrical power of the generator was 5.6 W and the maximum electrical power output obtained was 7.37 W on flat ground. Furthermore, in the case of walking on a 10% incline, electrical energy for a given load and speed was equal to or greater than that on the flat. The efficiency of conversion of mechanical energy to electrical energy was between 30% and 40% over the range of load and walking speed. The authors also compared the metabolic difference between the spring-based backpack and regular backpack, which did not have relative movement or energy generation. Given that the mechanical power input to the generator is 12.15 W, the anticipated increase in metabolic input is 48.6 W, since the maximum efficiency of mechanical power production by human muscle is about 25%. However, while comparing with the regular backpack, the increase in metabolic rate was only about 19.1 W, which is less than the predicted value. To explain this result, some initial kinematic analyses were conducted. The averaged vertical movement of the hip joint decreased 11.9 mm for the suspended backpack compared with the regular backpack, and the reduction in the peak force exerted by the load onto the person was about 11.8%.

Although the exact mechanism of the metabolic compensation was not clear, Kuo (2005) gave an explanation for this phenomenon. During the step-to-step transition of normal walking, both legs contact the ground and the ground reaction force is exerted on

each leg. The leading leg performs negative work on the CoM and the trailing leg performs positive work. Since the negative work is dissipated as energy loss, an equal magnitude of positive work has to be performed by the trailing leg to balance this energy loss and maintain the walking speed. Both positive and negative work contributes to the overall metabolic cost of normal walking. In the case of a suspended backpack, the load exerts a fluctuating force on the human body. Assuming the energetic cost of the pendulum phase (when only one leg contacts ground) is insensitive to additional load, and the step-to-step transition is more sensitive, the suspended payload can be beneficial on energy consumption and comfort, due to the payload exerting more downward force during the pendulum swing phase and less during step-to-step transition. The author mentioned that to confirm this hypothesis the actual phasing of the suspended backpack relative to the backpack frame needs to be measured.

2.4 Dynamics of Physical System

2.4.1 Base Excitation Model

Before discussing the model application to a backpack generator and gait pattern, a brief overview of some fundamentals of dynamic systems in the physics field will be provided in this section.

As described by White and Tauber (1969), a system is a set of interacting elements. A physical system can be thought of as a combination of interacting physical components which contain matters and energy. The input-output behavior of a physical system can be considered as the system response, which is directly determined by the

properties of the system. The elements of a practical engineering system may be quite complex. However, in most cases a mechanical system can be decomposed of masses, springs, and dampers, in which masses and springs are energy-storing elements and dampers are energy dissipating elements. Usually a mechanical system is a man-made system and includes the concept of optimizing certain parameters such as cost, efficiency, or reliability. By using these basic concepts, some measurements of the elements in a system can be modeled in terms of kinetics and kinematics.

Hooke's Law states that the amount by which a material body is deformed is linearly related to the force causing the deformation. Therefore the force produced by a linear spring is equal to the spring stiffness (k) multiplied by the elongated distance. This force is in the direction that opposes the displacement.

$$f_k = -k(x - x_0) \tag{0-1}$$

For viscous damping, the force exerted by a dashpot is equal to the damping coefficient multiplied by the relative velocity between the two ends of the dashpot, and acts in the opposite direction.

$$f_c = -c(\dot{x} - \dot{x}_0) \tag{0-2}$$

Newton's Second Law of Motion states that the sum of all forces applied to a constant mass is equal to the mass multiplied by the acceleration of that mass:

$$\sum f = m\ddot{x} \tag{0-3}$$

The dynamics of a system can be analyzed by summing all individual forces acting on the mass and applying Newton's Second Law. Consider the system below (Figure 6), where

a mechanical system with a mass of *m*, a spring with a stiffness of *k*, and a dashpot with a damping coefficient of *c*, is illustrated.

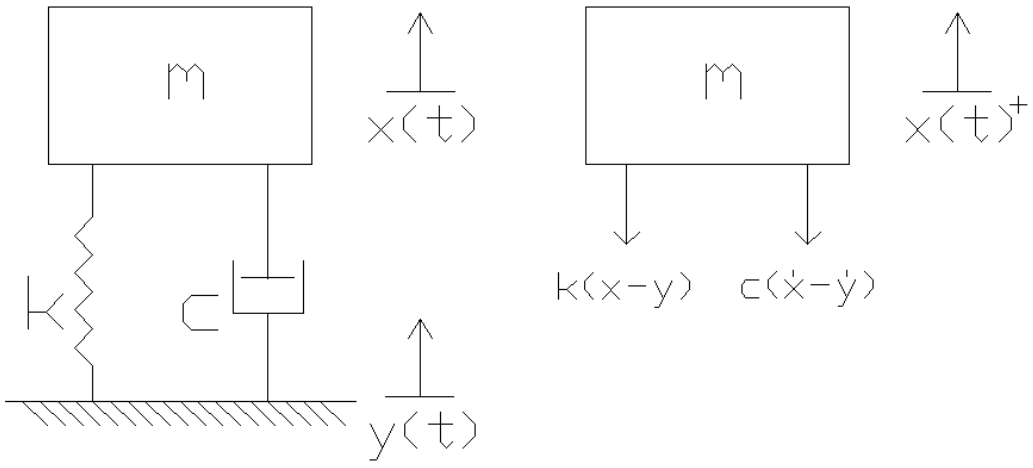

Figure 6 A simple base excitation mechanical system (assuming no gravity)

Assume the system is excited by the motion of its support and the base moves harmonically, that is,

$$y(t) = Y \sin \omega_b t \tag{0-4}$$

where Y denotes the amplitude of the base vibration and ω_b represents the frequency of the base oscillation.

Summing the relevant forces on the mass m and using Newton's second law and assuming there are no gravitational forces in this example,

$$m\ddot{x} + c(\dot{x} - \dot{y}) + k(x - y) = 0 \tag{0-5}$$

Substitution of y(t) from (0-4) into (0-5) gives

$$m\ddot{x} + c\dot{x} + kx = cY\omega_b \cos \omega_b t + kY \sin \omega_b t \tag{0-6}$$

(0-6) is a second-order linear non-homogeneous differential equation with constant coefficients describing the system's behavior. It's also commonly represented in terms of the damping ratio and natural frequency ω_n:

$$\ddot{x} + 2\zeta\omega_n\dot{x} + \omega_n^2 x = 2\zeta\omega_n\omega_b Y\cos\omega_b t + \omega_n^2 Y\sin\omega_b t \tag{0-7}$$

Where $\omega_n = \sqrt{\frac{k}{m}}$ and $\zeta = \frac{c}{2\sqrt{km}}$

Since (0-7) is a linear non-homogeneous equation, its solution is the sum of the homogeneous solution and a particular solution. For an underdamped system ($0 < \zeta < 1$), the homogeneous solution is

$$x_h(t) = Ae^{-\zeta\omega_n t}\sin(\omega_d t + \phi) \tag{0-8}$$

where

$$\omega_d = \omega_n\sqrt{1-\zeta^2}$$

$$A = \sqrt{x_0^2 + \left(\frac{\dot{x}_0 + \zeta\omega_n x_0}{\omega_d}\right)^2}$$

$$\phi = \tan^{-1}\frac{x_0\omega_d}{\dot{x}_0 + \zeta\omega_n x_0}$$

x_0 and $\dot{x}_0$ are the initial displacement and velocity.

The approach to solve the particular solution of the above differential equation (0-7) is to use the linearity of this equation. The particular solution will be the sum of the particular solution assuming the input is $2\zeta\omega_n\omega_b Y\cos\omega_b t$ only, denoted by x_p^1, and the

particular solution assuming the input is $\omega_n^2 Y \sin \omega_b t$ only, denoted by x_p^2. The solution of x_p^1 is

$$x_p^1 = \frac{2\zeta\omega_n\omega_b Y}{\sqrt{(\omega_n^2 - \omega_b^2)^2 + (2\zeta\omega_n\omega_b)^2}} \cos\left(\omega_b t - \theta_1\right) \tag{0-9}$$

where

$$\theta_1 = \tan^{-1} \frac{2\zeta\omega_n\omega_b}{\omega_n^2 - \omega_b^2}$$

As mentioned by Inman (2001), the range of the arctangent function used in the phase delay calculation is between $0 \le \theta \le \pi$, rather than $-\pi/2 \le \theta \le \pi/2$, as assumed for normal arctangent function.

The solution of x_p^2 is

$$x_p^2 = \frac{\omega_n^2 Y}{\sqrt{(\omega_n^2 - \omega_b^2)^2 + (2\zeta\omega_n\omega_b)^2}} \sin\left(\omega_b t - \theta_1\right) \tag{0-10}$$

From the principle of linear superposition, x_p equals to the sum of x_p^1 and x_p^2. Adding (0-9) and (0-10) yields

$$x_p(t) = \omega_n Y \left[\frac{\omega_n^2 + (2\zeta\omega_b)^2}{(\omega_n^2 - \omega_b^2)^2 + (2\zeta\omega_n\omega_b)^2} \right]^{\frac{1}{2}} \cos(\omega_b t - \theta_1 - \theta_2) \tag{0-11}$$

where

$$\theta_2 = \tan^{-1} \frac{\omega_n}{2\zeta\omega_b}$$

The total solution is the sum of homogeneous solution (0-8) and particular solution (0-11):

$$x(t) = \omega_n Y \left[\frac{\omega_n^2 + (2\zeta\omega_b)^2}{(\omega_n^2 - \omega_b^2)^2 + (2\zeta\omega_n\omega_b)^2} \right]^{\frac{1}{2}} \cos(\omega_b t - \theta_1 - \theta_2) + Ae^{-\zeta\omega_n t} \sin(\omega_d t + \phi) \quad \text{(0-12)}$$

Figure 7 illustrates the dynamic response of a base excitation system.

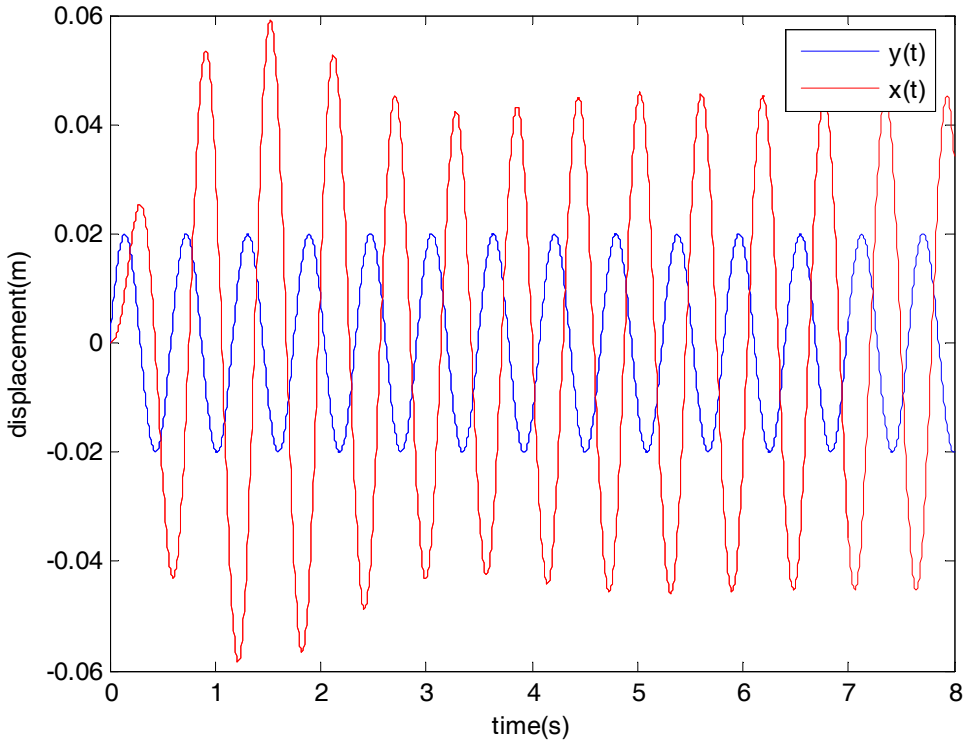

Figure 7 Base excitation system where m=30 kg, k=2500 N/m, c=50 N·sec/m, x(0)=0, and x'(0)=0

Since the homogeneous solution decays exponentially and the current research focuses on the stable condition, the homogeneous solution can be ignored and only the particular solution is left. Therefore,

$$x(t) = \omega_n Y \left[\frac{\omega_n^2 + (2\zeta\omega_b)^2}{(\omega_n^2 - \omega_b^2)^2 + (2\zeta\omega_n\omega_b)^2} \right]^{\frac{1}{2}} \cos(\omega_b t - \theta_1 - \theta_2) \quad \text{(0-13)}$$

The magnitude of the particular solution X can be expressed as

$$X = Y\left[\frac{1+(2\zeta r)^2}{(1-r^2)^2+(2\zeta r)^2}\right]^{\frac{1}{2}} \tag{0-14}$$

where

$$r = \frac{\omega_b}{\omega_n}$$

Then, the ratio of the maximum response magnitude to the maximum input displacement is

$$\frac{X}{Y} = \left[\frac{1+(2\zeta r)^2}{(1-r^2)^2+(2\zeta r)^2}\right]^{\frac{1}{2}} \tag{0-15}$$

Figure 8 illustrates the relationship between displacement transmissibility X/Y and frequency ratio ω_b / ω_n, with several different damping ratios. For $r < \sqrt{2}$, the displacement transmissibility is larger than 1 and increases as damping ratio decreased, which means the amplitude of the excited mass is greater than the amplitude of base and increasing when the viscosity is reduced . For $r > \sqrt{2}$, the displacement transmissibility is smaller than 1.

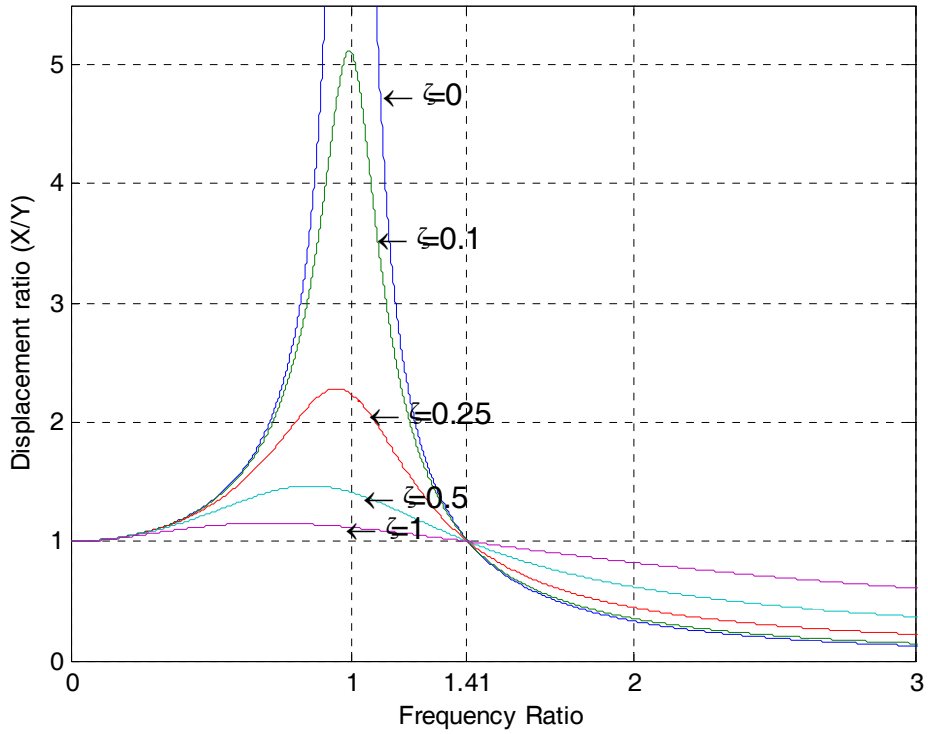

Figure 8 Displacement transmissibility vs. frequency ratio, with different damping ratio

With the definition of r, equation (0-9) and (0-11) yield

$$\theta_1 = \tan^{-1}\frac{2\zeta r}{1-r^2} \tag{0-16}$$

$$\theta_2 = \tan^{-1}\frac{1}{2\zeta r} \tag{0-17}$$

By comparing the expression of the base movement (0-4) and the excited mass movement (0-13), the phase delay between them can be written as:

$$\theta = \tan^{-1}\frac{2\zeta r}{1-r^2} + \tan^{-1}\frac{1}{2\zeta r} - \frac{\pi}{2} \tag{0-18}$$

where $\pi/2$ represents the phase shift when base movement is expressed by a cosine function.

Figure 9 demonstrates the phase delay vs. frequency ratio ω_b / ω_n with different damping ratios. Considering the case that $\zeta = 0$, which means the viscosity is ignored. The equation (0-15) degrades to

$$\frac{X}{Y} = \frac{1}{\left|1 - r^2\right|} \tag{0-19}$$

From (0-16) and (0-17),

$$\theta_1 = \begin{cases} 0 & \text{if } \omega_n^2 > \omega_b^2 \\ -\pi & \text{if } \omega_n^2 < \omega_b^2 \end{cases} \tag{0-20}$$

$$\theta_2 = \frac{\pi}{2} \tag{0-21}$$

Therefore, the response would be either in phase or in anti-phase with the excitation, given $\zeta = 0$.

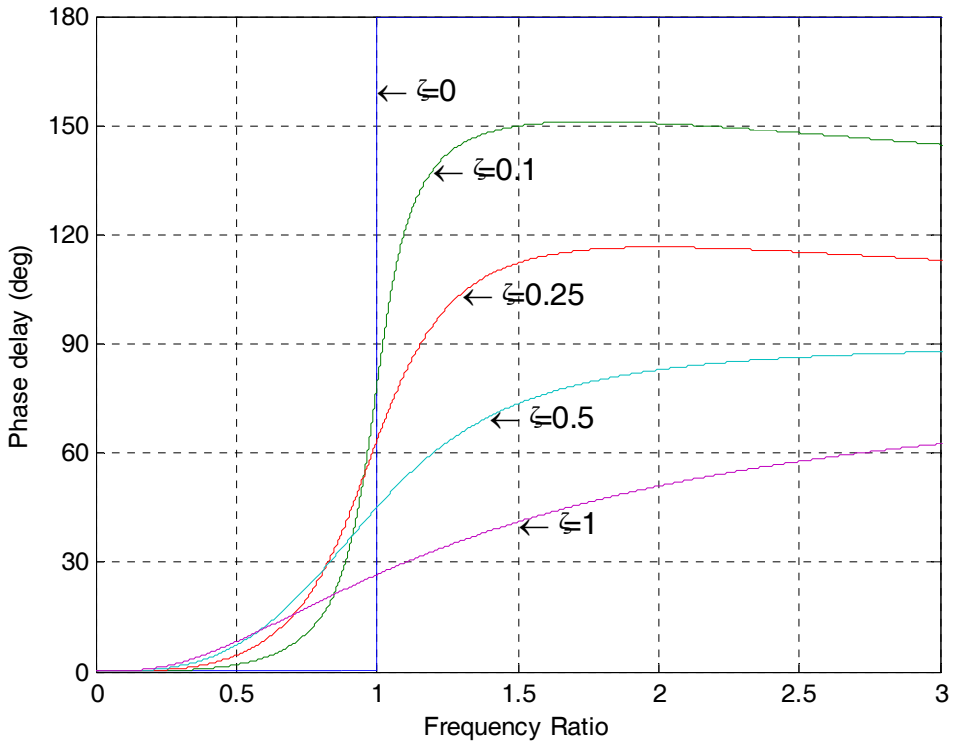

Figure 9 Phase delay vs. frequency ratio with different damping ratio

The force $F(t)$ transmitted to the base/mass is from the spring and damper. With Newton's Second Law of Motion,

$$F(t) = -m\ddot{x} \tag{0-22}$$

Differentiating the equation (0-13) and substituting in to equation (0-22) yields

$$F(t) = m\omega_b^2 \omega_n Y \left[\frac{\omega_n^2 + (2\zeta\omega_b)^2}{(\omega_n^2 - \omega_b^2)^2 + (2\zeta\omega_n\omega_b)^2} \right]^{\frac{1}{2}} \cos(\omega_b t - \theta_1 - \theta_2) \tag{0-23}$$

Using the frequency ratio r, the magnitude of this transmitted force F_T is

$$F_T = kYr^2 \left[\frac{1 + (2\zeta r)^2}{(1 - r^2)^2 + (2\zeta r)^2} \right]^{\frac{1}{2}} \tag{0-24}$$

where F_T is the magnitude of the transmitted force.

Being similar to the displacement transmissibility, force transmissibility (also called normalized force) is defined as:

$$\frac{F_T}{kY} = r^2 \left[\frac{1+(2\zeta r)^2}{(1-r^2)^2+(2\zeta r)^2} \right]^{\frac{1}{2}} \tag{0-25}$$

Figure 10 illustrates the force transmissibility as frequency ratio varies from 0 to 3 and damping ratio varies from 0 to 1.

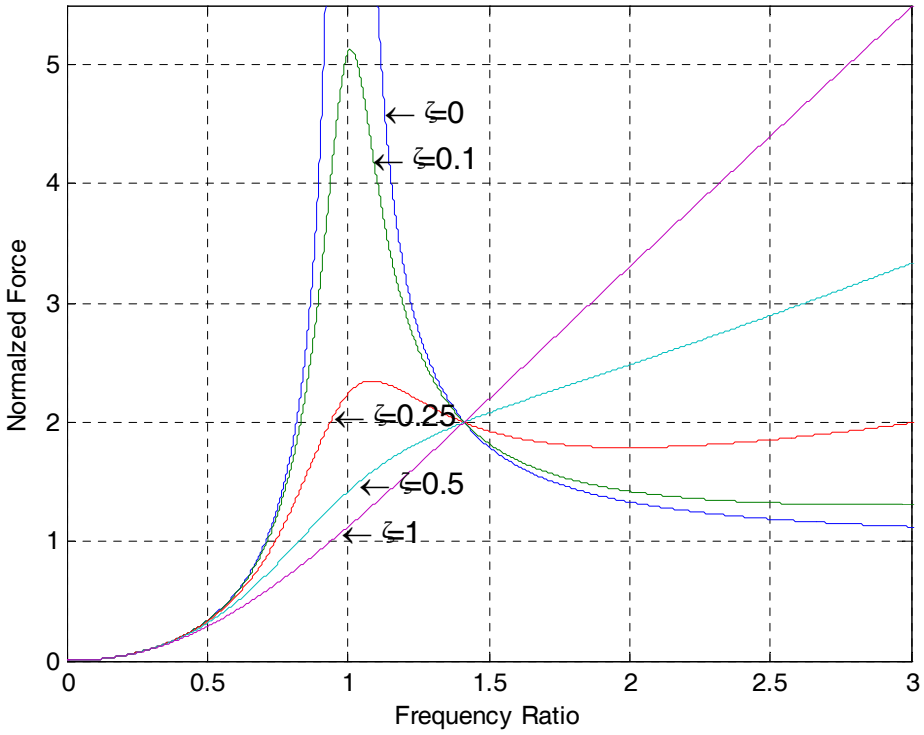

Figure 10 Frequency ratio vs. Normalized Force

If $\zeta = 0$, equation (0-24) degrades to

$$F_T = \frac{kYr^2}{\left|1-r^2\right|} \tag{0-26}$$

The transmitted force is either in phase or in antiphase with the excitation, given $\zeta = 0$.

As mentioned in Section 2.1, the CoM draw a sinusoidal curve, when projected on the sagittal plane during human walking. Therefore this sinusoidal movement can be treated as the oscillation of the base in the base excitation model. The springs and frictions in the backpack generator then are the stiffness coefficient and the damping ratio in that model. Thus, in this study people carrying a backpack generator is simplified to a base excitation model. Results from a pilot study illustrate how gait patterns influence the sinusoidal movement of CoM and the interaction between the backpack generator and gait pattern are presented in chapter 4.

2.4.2 Lumped Models of Human Walking

Many mathematical models of human walking have been proposed for a better understanding of human movement. The most concise model of walking is the minimal biped model (Alexander 1976; Alexander 1995; Gard, Miff et al. 2004; Srinivasan and Ruina 2006), by which Alexander explained the upper limit to the speed of walking. Considering this model behaves as an inverted pendulum during single support, the centripetal acceleration cannot exceed the acceleration of gravity when the supporting leg is vertical. With this constraint, he stated that the maximum possible speed of normal walking is 3m/s, which is very close to the realistic peak velocity of human walking. This model also revealed some walking mechanisms with respect to the energetics of walking. During the single support phase the potential energy gained from the rise of mass is equal

to the loss of kinetic energy and no work is performed in this period. Thus work has to be performed during double support phase to compensate for the loss of the vertical component of the velocity.

Synthetic wheel models are another type of mathematical model of human walking. The evidence from electromyographic studies shows that muscle activity is very little in the leg when the leg is in the swing phase of walking (Mochon and McMahon 1980; Alexander 1995). Therefore a pendulum can be used to model the passive movement of the swing leg. McGeer (1990) first analyzed the kinematics property of the rimless wheel and concluded that rim removal was not very efficienct due to large energy dissipation. He then devised the synthetic wheel of which each leg is a rod connected to a wheel and a torso mass is located at the hips, as a large point mass. The radius of curvature of feet is exactly equal to the leg length. While the rim of the support leg is on the ground, the swing leg moves forward with constant angular velocity. Thus, the support can seamlessly join from one rim to the next and a continuous rim is synthesized from two legs. Because the stance leg is a section of wheel, the hips move steadily along the ground at a constant speed under the assumption that the mass of the swing leg is too small to disturb the motion of the hips. Thus, the trajectory of the hips is parallel to the ground without vertical displacement and the swing leg moves as an unforced pendulum. Since this model does not require energy input to keep it moving, it cannot be used to analyze the energy transfer and consumption. Because this model did not consider the vertical displacement of torso and the energy transfer during walking, it is not applicable for the current research on energy harvesting. As commented by Alexander (1995), the

stride period of this model is about two seconds, which corresponds to an extremely slow walk. Thus, the model cannot explain the cadence of walking unless at low speeds.

Since the synthetic model of human walking is not able to show the energy dissipation or represent the vertical displacement of the hip, it was adjusted to include a relatively large mass on the leg and to have smaller feet whose radius of curvature is less than the leg length. Mochon and McMahon (1980a) proposed a mathematical model of the single support phase of human walking. The lower extremities were represented by three rigid links, one for the stance leg and two for the thigh and shank of the swing leg. They assumed that muscles generated the initial position and velocity of the limbs at the end of the double support phase and did not act or generate force during the swing phase. This assumption was consistent with the concept of push-off which suggested that the force generated by the back leg accelerated the whole body. But Perry (1992) stated that the term push-off should be replaced by roll-off because the pre-swing of the back leg was purely passive and did not have any effect on the acceleration of the body. In the research of Mochon and McMahon (1980a), they believed that the push-off accounts for the adjustment of the initial state of each step, and only gravity contributes to the movement of the whole mechanical system during the swing phase. The kinetic energy and the potential energy exchanged during the movement and the total mechanical energy kept constant, which indicates that this model was a ballistic model. The movements of the links were described by Lagrange's equations and the trajectories of ground reaction force showed that this model was very similar to the inverted pendulum model, except that it had a more strict range for swing time. After being compared with previous experimental data, it was found that with different leg lengths the calculated range of

time of swing phase was very close to the measured range. However, the vertical ground reaction force did not have the same general shape as those found in experiments for the support foot. The experimental data indicated that the minimum ground reaction force happened at mid stance, when the ballistic model predicted the maximum force.

In the following study, Mochon and McMahon (1980b) improved their ballistic model by adding knee flexion of the stance leg and pelvic rotation. The model then consisted of four links representing the thighs and shanks of two legs. The mass of the foot was modeled as a point mass at the ankle joint rather than contained in the mass of shank. To get rid of the collapse of the stance leg at mid-swing phase, it was assumed that the knee angle of the stance leg was related to the shank angle of the swing leg. The solution of Lagrange's equations indicated that the swing time reduced as the step length increased, which was compatible with the experimental observation. The vertical ground reaction force was not improved by this adjusted model and the predicted maximum force still happened at mid stance. Therefore the authors stated that neither the heel nor the knee flexion contributed to the shape of the vertical force in normal walking. The results also showed that the vertical movement of the CoM of the body decreased with knee flexion, which means the exchange of potential and kinetic energies reduced. This then increased the walking speed. The authors also took into account the pelvic rotation in their improved model and stated that the rotation of the pelvis did not change the system dynamics in that it rotated at a nearly constant angular speed. In addition, the authors mentioned that the last two determinants of human gait, pelvic tilt and lateral pelvic displacement, did not have significant effects on the swing phase of the ballistic model.

Selles et al. (2001) conducted a comparison on the predictive validity of ballistic models of human walking. The authors stated that it was not clear on whether the differences in the characteristics of ballistic models yielded different simulated outcomes and how accurately the models can predict kinematics of the swing phase. Six subjects walked along a 15-meter straight course and the kinematics and anthropometry data of the lower extremities were measured. Walking speed was then normalized by subject's leg length. For comparison, numerical simulations based on a ballistic model were calculated for each subject. Average root mean square error was used to compare the experimental and simulated time series. Although the previous research (Mochon and McMahon 1980a; Mochon and McMahon 1980b) demonstrated that there was a similarity between ballistic models and experimental data at comfortable walking speed, the results showed statistically significant difference in terms of time series of joint angle, swing time, and step length. Selles et al believed that this difference was due to the muscle activity during the swing phase and suggested that any forces and moments on knee and hip generated by muscles should be incorporated in the dynamic models. Furthermore, since tendons and muscles were elastic, Selles et al thought the passive effect of the joint also needed to be considered. With respect to the current research, although the ballistic model is able to roughly predict the movement of the lower extremities, load carriage violates the assumption that the system is only influenced by gravity. Therefore, the ballistic model becomes inapplicable to the current research.

As mentioned by Alexander (1995), the legs with sufficient mass are able to change the torso velocity during the swing phase, and the smaller feet make the torso rise and fall as observed. This vertical displacement of the torso and the interaction between

leg and torso also make the legs swing faster. Like the minimal bipedal model, the adjusted ballistic model shows that the energy is dissipated during the heel strike and indicates that if the initial position started with leg angle and speeds on some certain range it would quickly reach a steady state by which the model is able to withstand distribution.

Some research also focused on the optimization of gait with respect to the energy dissipation. Alexander (1980; 1992) used truncated Fourier series with two terms to describe the pattern of ground reaction force so that this description was compatible for both human walking and running. The leg was modeled as a set of torque actuators placed on the hip and a linear actuator that could lengthen or shorten with a spring. The variables were the stride duration and the ground reaction shape, which depended on whether walking or running was chosen. Considering that both positive and negative work contributes to the overall metabolic cost, the objective function was to minimize the summation of the positive and negative work done by all actuators. The results indicated that as the walking speed increases the running minimum became more global while the walking minimum became less economical. Therefore, there must be a critical speed at which a person switches between walking and running for minimizing the energy cost. However, the author stated that this critical speed could not be obtained explicitly with the defined method. In the current research, the walking cadence is actually the exciting frequency of the backpack. The exciting frequency approaches to the natural frequency of the suspended-load backpack as the force exerted on the torso increases. Therefore, the natural frequency of the backpack would intervene on minimization of energy cost.

Kay and Warren (1998) proposed that the oscillatory component of human walking could be modeled as a limit-cycle, because the amplitude and the frequency of leg motion was relatively constant and if interrupted they returned to a stable state. As a simple dynamical equation, a van der Pol oscillator was then adopted to describe the vertical oscillation of human walking. When not forced by the system input, the van der Pol will oscillate at a fixed frequency regardless of the initial condition and perturbations on the state variable. However, the authors also mentioned that human walking is not exactly a limit-cycle attractor. During walking, each stride has a different vertical amplitude and frequency so that the same state in the system cannot be repeated again. The phase plane locus is actually a collection of many similar cycles rather than a stable closed cycle generated by a van der Pol oscillator. In addition, since the nonlinear term of van der Pol is relatively small for describing human walking, the oscillator degrades to an approximate sinusoidal curve. Therefore, in the current research, only the linear oscillator will be considered to describe the torso motion during walking.

Collectively, the above models (Table 3) strived to simulate the real body movement in detail and to explain the mechanism of human walking. Although (compared with the complex human body movement) these models are very simple, some fundamental understanding of walking has been revealed. However none of them addressed human walking with a backpack or backpack generator. To investigate the effect of the backpack generator, the movement of the torso and the interaction between human body and backpack needs to be considered. Pilot work on this interaction and a tentative model of human carrying a backpack generator are presented in the next section.

Table 3 List of important human walking biomechanical models

Authors and year	Advantage	Disadvantage
Alexander (1976), Gard et al. (2004), Srinivasan and Ruina (2006)	A simple but representative biomechanics model. Explained the upper limit to the walking speed	Only considered one determinant of the human walking
Mochon and McMahon (1980a),(1980b), Selles et al. (2001)	Passive walking model, muscles only generated the initial position and velocity	Ground reaction force and joint angles are not consistent with measured data
McGeer (1990)	Described the swing phase of walking	The trajectory of hip joint is parallel to the ground, which is inconsistent with the human walking
Alexander (1992)	Explained the pattern of force exerted on the ground	No kinematics analysis on human body
Kay and Warren (1998)	Described the oscillation as a limit-cycle	Still not accurate, degrade to sinusoid with small ε

3 Pilot Work

One male subject (age: 26, weight: 74.5 kg, height: 177cm, leg length: 94 cm) was tested for the model validation.

3.1 Model Development for Energy Harvesting of Gait

3.1.1 Vertical Displacement of the Torso and Suspended-load Backpack

In a gait cycle, the leg can be modeled as an inverse pendulum and the movement of CoM would be an arc trajectory in the contact period (McMahon and Cheng 1990). Therefore the CoM of human fluctuates upward and downward in the vertical plane while walking. Figure 11 illustrates the relation between step length and trajectory of vertical displacement of CoM.

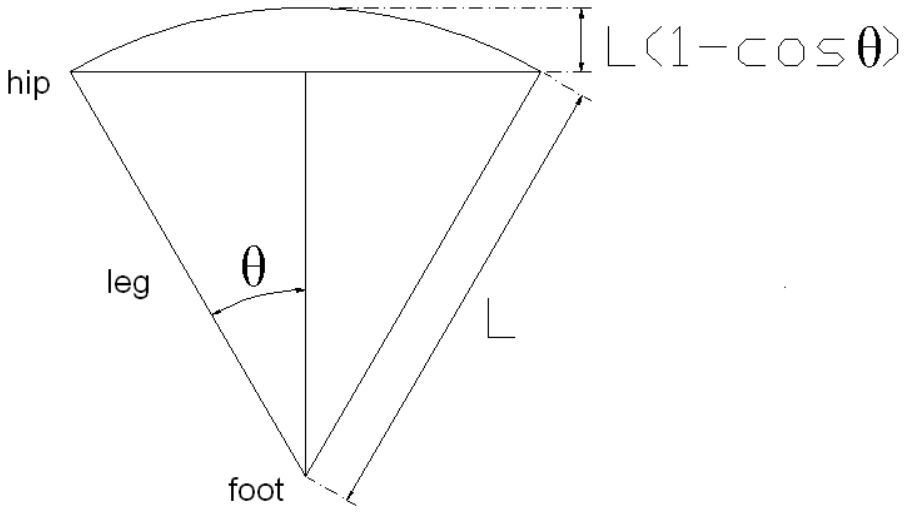

Figure 11 The inverted pendulum model for walking

Based on this model,

$$L_{step} = 2l_0 \sin\theta \tag{3-1}$$

where l_0 is the leg length, and L_{step} is the step length.

The walking speed is the step frequency multiplied by step length, viz.

$$V = \frac{\omega_b}{2\pi} \cdot L_{step} \tag{3-2}$$

where ω_b is the step frequency in radial frequency.

Assuming the trajectory of CoM can be described as a sinusoidal curve (Saunders, Inman et al. 1953), the amplitude of this sinusoidal curve Y is

$$Y = \frac{1}{2} l_0 (1 - \cos\theta) \tag{3-3}$$

Substituting equation (3-1) and (3-2) into (3-3) yields

$$Y = \frac{1}{2} l_0 \left(1 - \sqrt{1 - \left(\frac{\pi V}{l_0 \omega_b} \right)^2} \right) \tag{3-4}$$

Equation (3-4) shows the relation between walking speed and the magnitude of CoM with a certain walking cadence.

During each stride, the pelvis rotates along all three directions (Perry 1992). This mechanism reduces the magnitude of vertical displacement of torso (Figure 12). The average maximum rotation in the transverse plane is about 5° with normal walking (Murray, Drought et al. 1964). From the anthropometry data, the mean distance between hip joints is 19.1% of the stature (about 33cm in average) (Clauser, McConville et al.

1969; Roebuck, Kroemer et al. 1975). Thus, within one step length the forward distance caused by transverse rotation of pelvis (L_p) can be calculated as

$$L_p = 33cm \cdot \sin(5^\circ) = 2.9cm \tag{3-5}$$

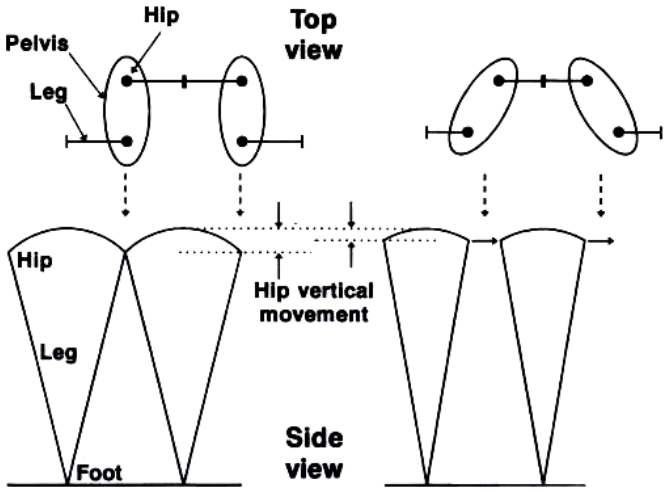

Figure 12 Graphical representation of pelvis rotation in transverse plane (adopted from Whittle MW, 1996)

The pelvic rotation then contributes about $\frac{2.9cm}{77.5cm} = 3.7\%$ to one step length during normal walking as the mean step length is 77.5cm (Whittle 1996). This ratio is suitable under most walking conditions because the pelvic rotation is approximately proportional to the step length (Lamoreux 1971). Therefore, the leg swing contributes to 96.3% of the step length during normal walking. The equation (3-1) is then modified as

$$0.96 \times L_{step} = 2l_0 \sin\theta \tag{3-6}$$

And the equation of amplitude of vertical fluctuation (3-4) is modified to

$$Y = \frac{1}{2} l_0 \left(1 - \sqrt{1 - \left(\frac{0.963\pi V}{l_0 \omega_b} \right)^2} \right) \tag{3-7}$$

In the normal walking, the pelvis is tilted downward on the side of the swing leg (Figure 13). The angular displacement of this collateral drop is about 7° (Perry 1992). The effect of pelvic tilt is to lower the CoM during mid-stance. The anthropometry data showed that the ratio of hip joints width to leg length is about 0.27 (Clauser et al. 1969). The reduction of the maximum vertical displacement is calculated as

$$Y_{tilt} = \frac{1}{2}\left(\frac{0.27 l_0}{2} \times \sin 7^\circ \right) = 0.00792 l_0 \tag{3-8}$$

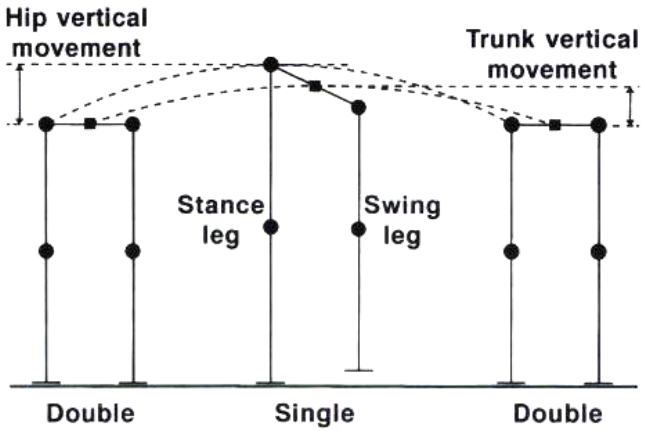

Figure 13 Graphical representation of pelvis tilt (adopted from Wittle MW, 1996)

The knee flexion during the mid-stance shortens the leg length and reduces the height of the hip joints (Figure 14, left). The knee angle is about 12° when the hip joint reaches the apex (Whittle 1996), and the height of the hip joint / knee joint is 53% / 28.5% of the stature (Roebuck, Kroemer et al. 1975). Based on the law of cosines, the shortened amplitude is:

$$\begin{aligned} Y_{knee} &= \frac{0.53H - \sqrt{(0.285H)^2 + (0.245H)^2 - 2 \times 0.285H \times 0.245H \times \cos(12^\circ)}}{2} \\ &= 0.00289H / 2 \\ &= 0.00272 l_0 \end{aligned} \tag{3-9}$$

The mechanism of the ankle is to elevate the hip joint by lengthening the effective leg length during the initial contact (Figure 14, right). Assuming that the ankle joint is on the middle of the foot, with the anthropometry data that the foot length is 15.2% of the stature, (Roebuck, Kroemer et al. 1975) , the amplitude shortened by ankles is

$$\begin{aligned} Y_{ankle} &= \frac{\sqrt{(0.53H)^2 + \left(\frac{0.152H}{2}\right)^2} - 0.53H}{2} \\ &= 0.00542H/2 \\ &= 0.00511l_0 \end{aligned} \tag{3-10}$$

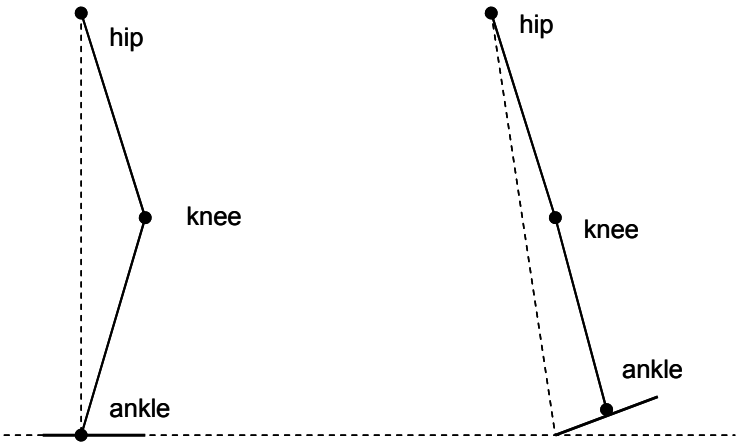

Figure 14 Graphical representation of knee flexion (left) and the mechanism of the ankle (right).

Therefore, considering all the mechanisms mentioned above, the equation (3-7) becomes

$$\begin{aligned} Y &= \frac{1}{2}l_0\left(1-\sqrt{1-\left(\frac{0.963\pi V}{l_0\omega_b}\right)^2}\right) \text{-}0.00792l_0 - 0.00272l_0 - 0.00511l_0 \\ &= \frac{1}{2}l_0\left(1-\sqrt{1-\left(\frac{0.963\pi V}{l_0\omega_b}\right)^2}\right) - 0.0157l_0 \end{aligned} \tag{3-11}$$

In equation (3-11), walking speed V and cadence ω_b are two variables that influence the magnitude of fluctuation. However, with normal walking, there is approximately an exponential relationship between step frequency and relative walking speed. In the research of Grieve et al. (1966), such a relationship could be described by the equation (3-12) below,

$$f = 2 \times 64.8 \left(\frac{V}{S} \right)^{0.57} (\text{min}^{-1}) \tag{3-12}$$

where S is the stature of the subjects

In order to be consistent with equation (3-11), the above equation (3-12) is represented with radial frequency as:

$$\omega_b = \frac{4\pi \times 64.8 \left(\frac{V}{S} \right)^{0.57}}{60} (\text{sec}^{-1}) \tag{3-13}$$

To reduce the number of variables in the model, stature is replaced by leg length. Anthropometry data showed that leg length accounts for 53% of stature (Roebuck, Kroemer et al. 1975). Therefore, the equation (3-13) could be written as

$$\omega_b = 2\pi \times 1.504 \left(\frac{V}{l_0} \right)^{0.57} (\text{sec}^{-1}) \tag{3-14}$$

Substitution of this into equation (3-11) yields

$$Y = \frac{1}{2} l_0 \left(1 - \sqrt{1 - \left(\frac{0.963V}{l_0 \times 2 \times 1.504 \left(\frac{V}{l_0} \right)^{0.57}} \right)^2} \right) - 0.0157 l_0 \qquad (3\text{-}15)$$

which represents the magnitude of the torso excitation as a function of leg length and walking velocity.

Because the torso leans forward while carrying the backpack, and only the movement along the frame has an effect on the springs, the effective vertical excitation reduced to $Y\cos\alpha$ (Figure 15), where α is the angle between the vertical plane and the torso coronal plane. The vertical component of the displacement of the payload along the frame can be expressed as:

$$x_f^v(t) = \omega_n Y \cos^2\alpha \sqrt{\frac{\omega_n^2 + (2\zeta\omega_b)^2}{(\omega_n^2 - \omega_b^2)^2 + (2\zeta\omega_n\omega_b)^2}} \cos\left(\omega_b t - (\theta_1 + \theta_2)\right) \qquad (3\text{-}16)$$

It should be noticed that due to the oblique nature of the frame, the equivalent spring stiffness enlarges to $k\sec\alpha$. All the spring stiffness and natural frequency presented below is based on this enlarged spring stiffness. On the other hand, the displacement of the payload perpendicular to the frame ($y_{f\perp}$) is same as the perpendicular component of the frame movement. The vertical component of this displacement is:

$$y_{f\perp}^v(t) = \omega_n Y \sin^2\alpha \sin(\omega_b t) \qquad (3\text{-}17)$$

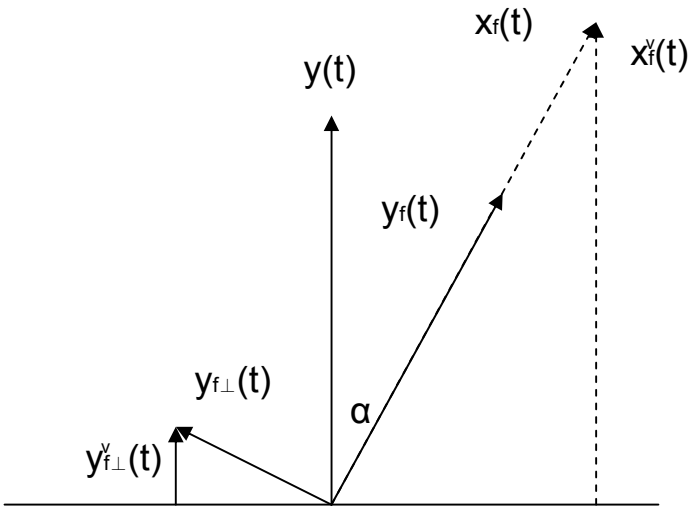

Figure 15 Schematic of the payload and the backpack frame movement.

Considering there is phase shift between $x_f(t)$ and $y_{f\perp}(t)$, the magnitude of the vertical displacement of payload is calculated as below:

$$X^v = \sqrt{X_f^{v2}(t) + Y_{f\perp}^{v2}(t) - 2X_f^v Y_{f\perp}^v \cos\left(\theta_1 + \theta_2 + \frac{\pi}{2}\right)} \tag{3-18}$$

where X_f^v and $Y_{f\perp}^v$ is the amplitude in equation (3-16) and (3-17), respectively. Figure 16 is the graphic representation of this vector summation

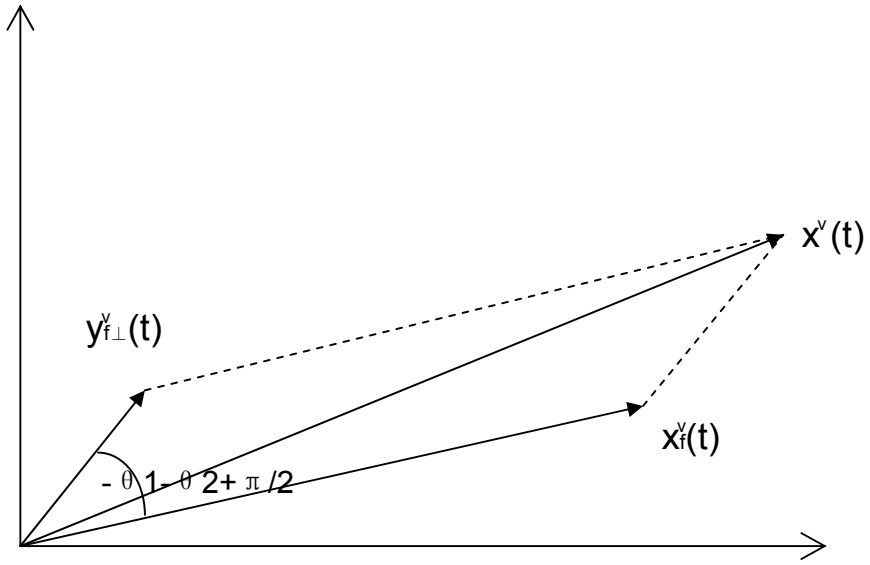

Figure 16 Graphical representation of the summation of the movements in vertical direction

3.1.2 Output Power Analysis

The goal of the backpack generator is to produce electricity, using the relative movement between the payload and the backpack frame. For a generator, by Faraday's law

$$e = B \cdot l \cdot v \tag{3-19}$$

where e is motional electromotive force, B is the flux density, l is the effective length, and v is the velocity. Since the output voltage is proportional to the velocity, it is important to ensure that the relative velocity between the payload and the backpack frame is large enough to generate enough power. From equation (0-4), the velocity of the base along the direction of frame is

$$\dot{y}_f(t) = \omega_b Y \cos\alpha \cos\omega_b t \tag{3-20}$$

and the velocity of the payload along the frame is

$$\dot{x}_f(t) = -\omega_n \omega_b Y \cos\alpha \left[\frac{\omega_n^2 + (2\zeta\omega_b)^2}{(\omega_n^2 - \omega_b^2)^2 + (2\zeta\omega_n\omega_b)^2} \right]^{\frac{1}{2}} \sin(\omega_b t - \theta_1 - \theta_2) \qquad (3\text{-}21)$$

Thus, the relative velocity between the payload and the frame $\dot{x} - \dot{y}$ is

$$\dot{x}_f - \dot{y}_f = -\omega_n \omega_b Y \cos\alpha \left[\frac{\omega_n^2 + (2\zeta\omega_b)^2}{(\omega_n^2 - \omega_b^2)^2 + (2\zeta\omega_n\omega_b)^2} \right]^{\frac{1}{2}} \sin(\omega_b t - \theta_1 - \theta_2) - \omega_b Y \cos\alpha \cos\omega_b t \qquad (3\text{-}22)$$

The magnitude of the relative velocity V_{bp} is then expressed as

$$V_{bp} = \sqrt{\dot{X}_f{}^2 + \dot{Y}_f{}^2 - 2\dot{X}_f \dot{Y}_f \cos\left(\theta_1 + \theta_2 - \frac{\pi}{2}\right)} \qquad (3\text{-}23)$$

where $\dot{X}_f$ and $\dot{Y}_f$ are the amplitude of $\dot{x}_f$ and $\dot{y}_f$. Figure 17 shows the relative velocity between the payload and the backpack frame as the function of the walking speed and the mass of the payload, while the leg length is 0.94m and the damping coefficient is set to 0.25.

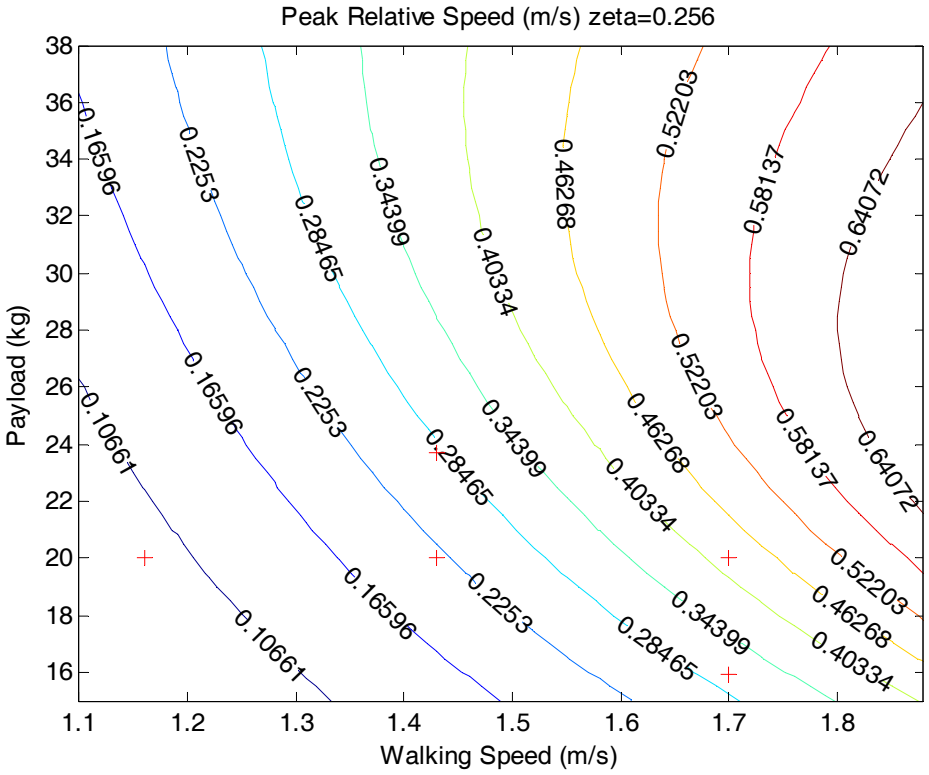

Figure 17 The contour of the peak relative velocity between the payload and the backpack frame as the function of the walking speed and the mass of the payload (leg length = 0.94m, zeta=0.256, α=30°). Five red crosshairs represent the conditions tested in the pilot study.

3.1.3 Ground Reaction Force

By applying Newton's second law to the base, which is the torso in this research, the dynamics of base movement can be described as

$$-m_{subject}\ddot{y} = F_{gr}(t) - m_{subject}g - mg - F_{bp}(t) + m\ddot{y}\sin^2\alpha \qquad (3\text{-}24)$$

where $F_{gr}(t)$ is the ground reaction force, $F_{bp}(t)$ is the vertical reaction force transmitted to torso from the payload, m is the mass of the payload, and $m_{subject}$ is the mass of the subject. By rearranging equation (3-24), the ground reaction force is

$$F_{gr}(t) = F_{bp}(t) + mg - (m_{subject} + m\sin^2\alpha)\ddot{y} + m_{subject}g \qquad (3\text{-}25)$$

The acceleration of the base $\ddot{y}$ can be obtained by calculating the second order derivative of the base displacement:

$$\ddot{y} = -\omega_b^2 Y \sin \omega_b t \tag{3-26}$$

Since it is assumed that base moves harmonically, the transmitted force can be expressed using equation (3-27)

$$F_{bp}(t) = m\omega_b^2 \omega_n Y \cos^2 \alpha \left[\frac{\omega_n^2 + (2\zeta\omega_b)^2}{(\omega_n^2 - \omega_b^2)^2 + (2\zeta\omega_n\omega_b)^2} \right]^{\frac{1}{2}} \cos(\omega_b t - \theta_1 - \theta_2) \tag{3-27}$$

Substituting (3-26) and (3-27) into (3-25) yields the expression of ground reaction force,

$$\begin{aligned} F_{gr}(t) = {} & m\omega_b^2 \omega_n Y \cos^2 \alpha \left[\frac{\omega_n^2 + (2\zeta\omega_b)^2}{(\omega_n^2 - \omega_b^2)^2 + (2\zeta\omega_n\omega_b)^2} \right]^{\frac{1}{2}} \cos(\omega_b t - \theta_1 - \theta_2) \\ & + mg + (m_{subject} + m\sin^2 \alpha)\omega_b^2 Y \sin \omega_b t + m_{subject} g \end{aligned} \tag{3-28}$$

Because the two sinusoidal terms in the equation above have phase shift, the magnitude of the ground reaction force is calculated as:

$$\begin{aligned} |F_{gr}| = {} & \\ & \sqrt{|F_{bp}|^2 + \left((m_{subject} + m\sin^2 \alpha)\omega_b^2 Y\right)^2 - 2F_{bp}(m_{subject} + m\sin^2 \alpha)\omega_b^2 Y \cos\left(\theta_1 + \theta_2 - \frac{\pi}{2}\right)} \\ & + mg + m_{subject} g \end{aligned} \tag{3-29}$$

where $|F_{bp}|$ is the amplitude of $F_{bp}(t)$ in equation (3-27). Figure 18 shows the peak ground reaction force as the function of the walking speed and the mass of payload, while the leg length is 0.94m and the damping coefficient is set to 0.256.

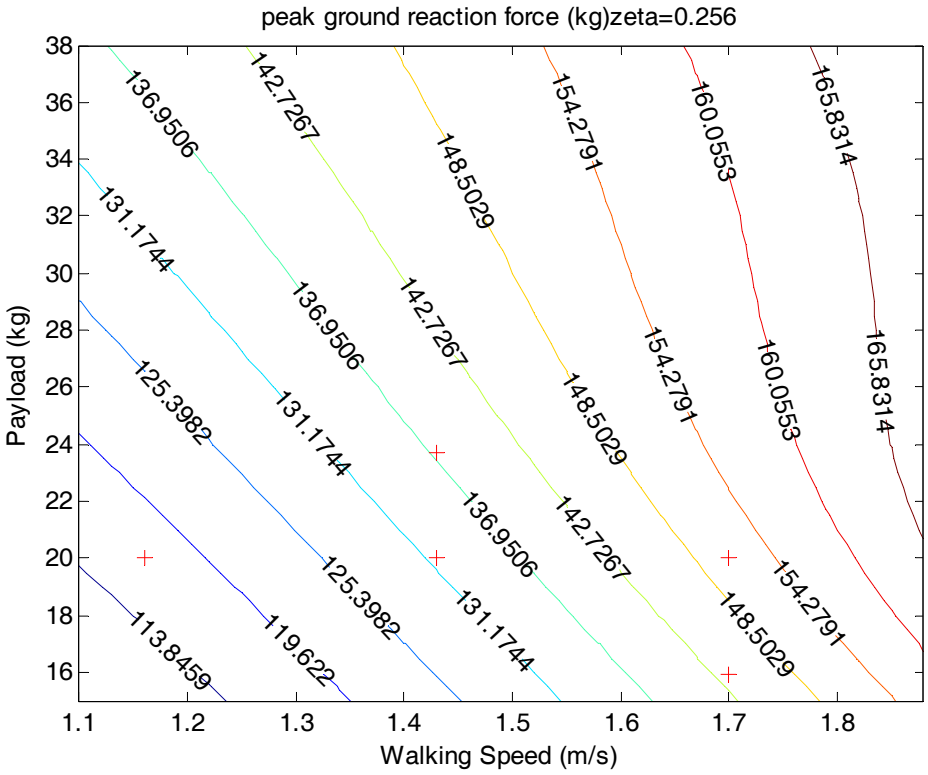

Figure 18 The contour of the peak ground reaction force as the function of the walking speed and the mass of the payload (leg length = 0.94m, zeta=0.256, α=30°) Five red crosshairs represent the conditions tested in the pilot study.

To demonstrate the effects of the damping coefficient, Appendix A shows the magnitudes of relative velocity and the GRF with zeta = 0.01, 0.1, 0.256, 0.5, 0.7. The larger the damping coefficient is, the contour of relative velocity and the contour of GRF are more similar. That means if the output energy is increased by a faster walking speed or by a heavier payload, the corresponding ground reaction force and joint load will also increase. On the other hand, since they are not exactly identical for any damping coefficient, a trade-off between energy scavenging and joint force may exist for a set of walking speeds and payload masses corresponding to relatively low GRF and high output energy. However, before analyzing the trade-off, the accuracy of the model needs to be validated.

To summarize, the model has two folds: the first fold is the inverted pendulum model, which is used to predict the magnitude of the torso oscillation base on the walking speed and the leg length; the second fold is the base excitation model, which predicts the movement of the backpack and the ground reaction force during walking based on the natural frequency of the system and the amplitude of the excitation output from the first fold. Figure 19 is the flowchart of the whole model. It should be noticed that the outputs of the entire system may have feedback on the structure of the inverted pendulum. The system then will become a time-variant system. However, at this step, only the open-loop model will be investigated because the time-invariant model needs to be evaluated first.

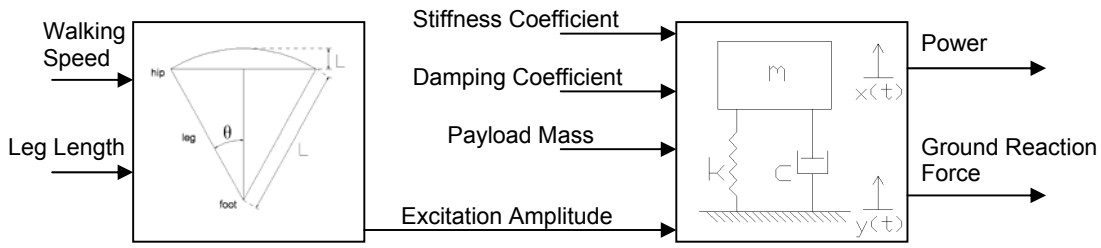

Figure 19 Flowchart of the lumped model of human walking and suspended-load backpack

3.2 Apparatus

Suspended-load Backpack

A military backpack was refitted to a suspended-load backpack by detaching the backpack frame and the sack (Figure 20). An additional frame was built for holding the payload. The original backpack frame was used to fix the whole backpack system to the body torso through the shoulder belts and the hip belt. The additional frame was then connected with the original one by four screws. The payload (mounted on an aluminum

plate) is suspended by 4 springs and free to move up and down through 4 Teflon bushings constrained to 2 vertical rods of the additional frame. The equivalent spring stiffness was about 4027 N/m, while the equivalent damping coefficient is unknown. The dimension of the frame in length by width by height was 66cm by 32 cm by 9 cm, and the weight was 6.7 kg.

Figure 20 Left: Front view of the suspended-load backpack. Right: Side view of the suspended-load backpack.

Motion Tracking System

The three-dimensional position data of the payload, the backpack frame and the CoM of the subject were captured by an Ascension MotionStar position and orientation measurement system (Flock of Birds MotionStar Model with the extended range transmitter, Ascension Technology, Burlington, VT) and recorded for 60 seconds at the frequency of 60Hz with the Innovative Sports Training Motion Monitor software (ver. 4.10). The magnetic source was placed 90cm away on the right side of the subject, and the front surface of the source was parallel to the sagittal plane of the subject. The center

of the magnetic source was the origin of this three-dimensional reference frame in the space. The x-axis was vertical to the sagittal plane, the y-axis was vertical to the coronal plane, and the z-axis is vertical to the ground and transverse plane. Two motion track sensors were placed on the clear plastic plates connected with the backpack frame and the payload respectively. To avoid the interference of the metal frame on the flock bird sensor, two clear plastic plates with length of 20cm were connected with the backpack frame and the load plate respectively. The sensors were then put on clear plastic plates. Because the link between the torso and the backpack frame was not a rigid link (Ren, Jones et al. 2005), the movement of the frame cannot exactly represent the movement of the torso of the subjects. Therefore, another sensor needs to be placed on the body for capturing the movement of the torso. Considering the displacement pattern of the torso along the spine is almost identical (Cappozzo 1981; Thorstensson, Nilsson et al. 1984), this sensor is placed on the bottom of the subject's sternum where the CoM of the subject is approximately located.

Treadmill

During walking, the ground reaction force data were captured by a Gaitway Instrumented Treadmill (Model 685) and recorded for 60 seconds at the frequency of 100 Hz with Gaitway software (ver. 2.0.8.42). Two force plates are placed below the conveyer and each force plate has four piezoelectric transducers for measuring 3-dimensional forces and moments. The output voltages yielded by the force plate are proportional to the GRF. If the subject places each heel-strike on the front force plate of the treadmill and toe-off on the back one, the components of the left foot and right foot in

the vertical ground reaction force can be distinguished by using the software of the treadmill.

Metronome

In the experiment the subject may change cadence using different step lengths, though the walking speed will be kept unchanged within a trial. This may vary the excitation frequency and invalidate the model. To keep the excitation frequency constant, a metronome (SEIKO, DM-20) was used and the subject was asked to step on the beat of the metronome. The rhythm of the metronome was calculated by equation (3-12).

3.3 Procedure

Upon arrival, anthropometry data of the subject, including weight, stature, and leg length were measured. The subject was then given a 5-minute warm-up designed to prepare the legs and the torso muscles for the experiment. The suspended-load backpack was then placed on the back of the subject and the shoulder belts and hip belt were fastened so that the movement between the torso and the backpack frame was constrained. In order to let the subject become familiar with the load level and the speed level used in the experiment, he was asked to hold a 22kg load without walking and to walk on the treadmill at 2.6 and 3.8 mph (the speeds used in the experiment) without carrying any additional load. A short walking trial was given to train the subject to place each heel-strike on the front force plate of the treadmill and toe-off on the back one. The flock of bird sensors were then mounted on the subject's CoM (around the bottom of the sternum) and the clear plastic plates connecting with the backpack frame and the load plate. Figure 21 demonstrates the subject walking on the treadmill with the suspended-load backpack.

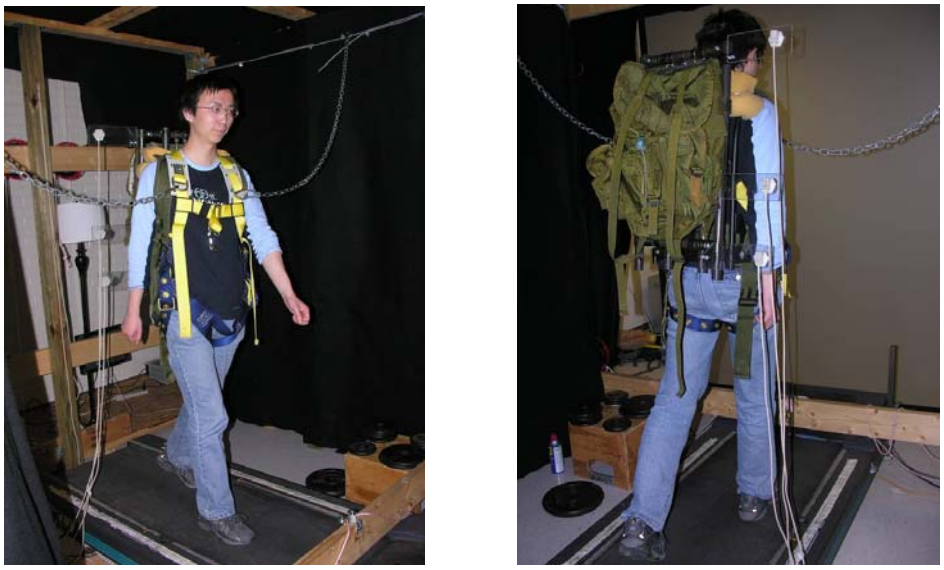

Figure 21 Left: Front view of the subject walking on the treadmill. Right: Back view of the subject walking on the treadmill.

During the experiment, five different conditions (Table 4) were tested in a random sequence:

Table 4 The configuration of each trial in the pilot study

Trail No.	Walking Speed (mph)	Walking Speed (m/s)	Payload (kg)	Cadence (/min)
1	3.8	1.70	20	126
2	2.6	1.16	20	102
3	3.2	1.43	21.8	115
4	3.2	1.43	20	115
5	3.8	1.70	15.9	126

The cadence (step frequency) for each trial was calculated by equation (3-12) and a metronome was placed beside the subject to help him step with the specific frequency. Each trial was performed for 70 seconds and the last one minute was monitored by the motion tracking system and the instrumented treadmill. The captured kinematics parameters included the space position of the subject's CoM, the backpack frame and the

payload and the kinetic parameters included the 3-dimensional GRF. To reduce the effect of fatigue, there was a ten-minute break between each trial.

3.4 Data Processing

Figure 22 shows the vertical oscillation of the CoM of the subject, the backpack frame, and the payload in a trial with 3.8 mph walking speed and 20 kg payload. Figure 23 shows the single side spectrum of the payload oscillation in that trial. Since the component of the dominant frequency (walking frequency) accounts for the majority of the oscillation and the low frequency component is not able to excite a large displacement on the payload (Figure 8), the amplitude at the walking frequency is used as an index to quantify the displacement of the oscillations. A Matlab program was written to extract the amplitude of the vertical position of the subject's CoM, the vertical position of the backpack frame, the vertical position of the load plate, and the velocity of the payload relative to the frame, using fast Fourier transformation (FFT).

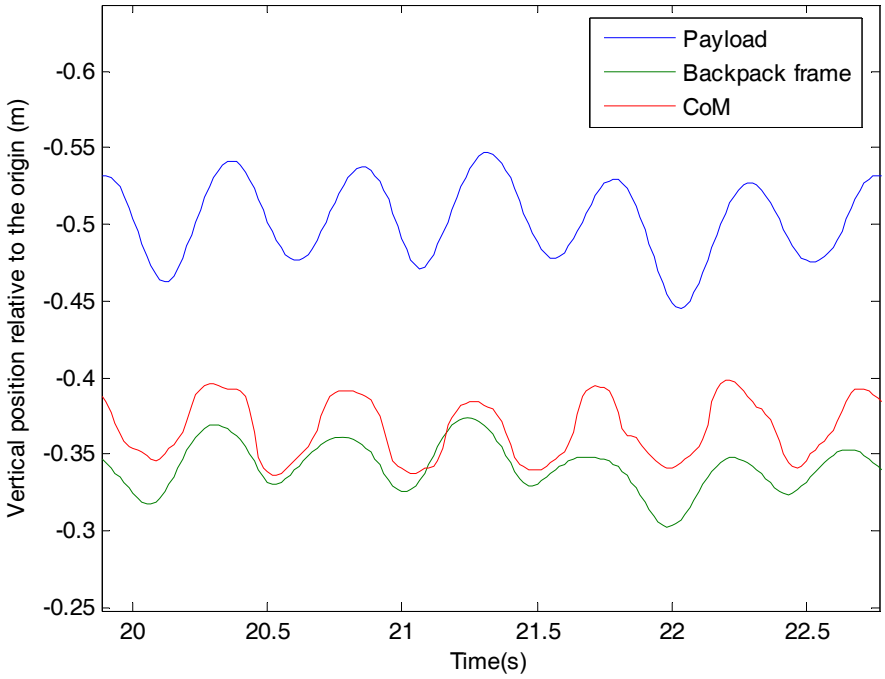

Figure 22 The vertical oscillation of the CoM of the subject, the backpack frame, and the payload in the trial of 3.8mph walking speed and 20 kg payload.

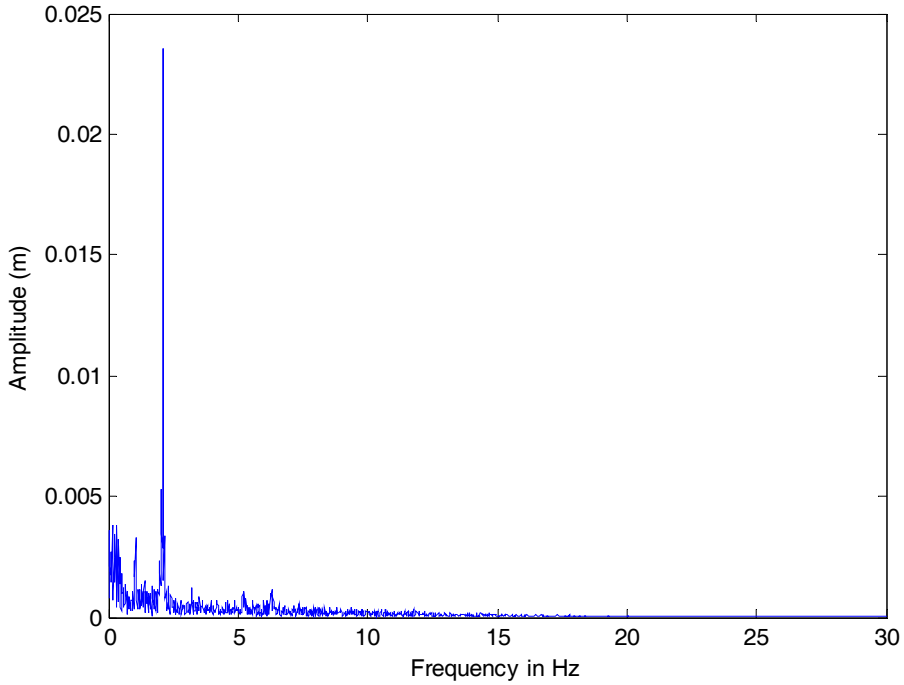

Figure 23 The single side spectrum of the payload oscillation in that trial of 3.8mph walking speed and 20 kg payload

Because it was found that the displacement of backpack frame is not as large as that of CoM, the oscillation of the torso may not be fully transferred to the backpack frame due to the relative movement between them. Thus, to evaluate the inverted pendulum model, both the amplitude of the subject's CoM and the backpack frame were calculated and compared with the predicted value. In addition, since the model has two folds (inverted pendulum model and base excitation model), the error from the first fold may influence the final predicted value. To validate the base excitation model, the measured relative movement between the payload and the backpack frame was compared not only with the predicted value of the entire model, but also with the predicted value using the measured frame oscillation as the input in the base excitation model. This latter predicted value can be used to evaluate the accuracy of the base excitation model without interference from the error of the inverted pendulum model.

In terms of the kinetics parameter, Figure 24 and Figure 25 show the oscillation of the GRF on the time domain and frequency domain. The amplitude at the walking frequency is also used to describe the displacement of the force oscillation. Another Matlab program was developed to extract the amplitude of the vertical GRF for each trial.

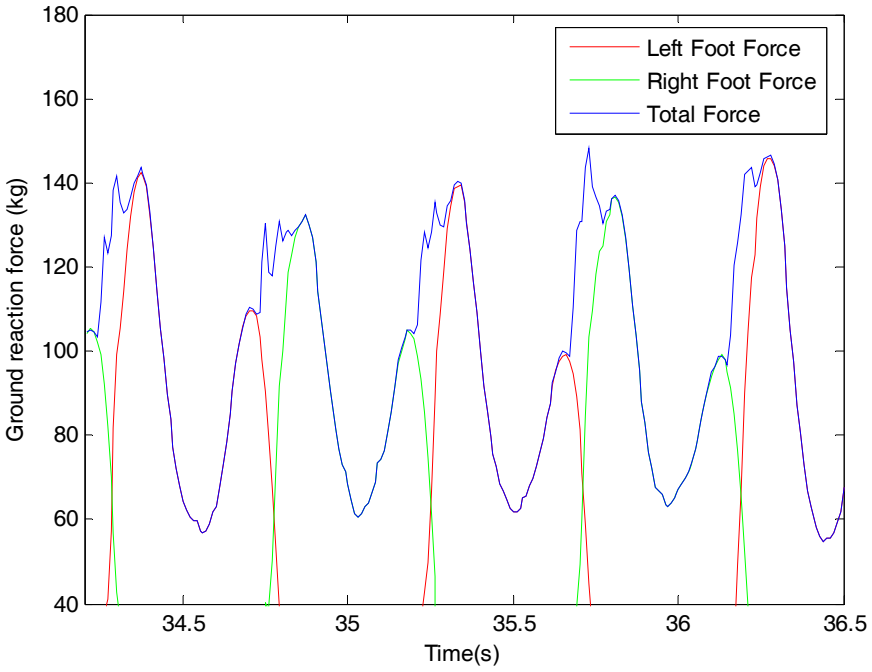

Figure 24 The oscillation of the ground reaction force in the trial of 3.8mph walking speed and 20 kg payload

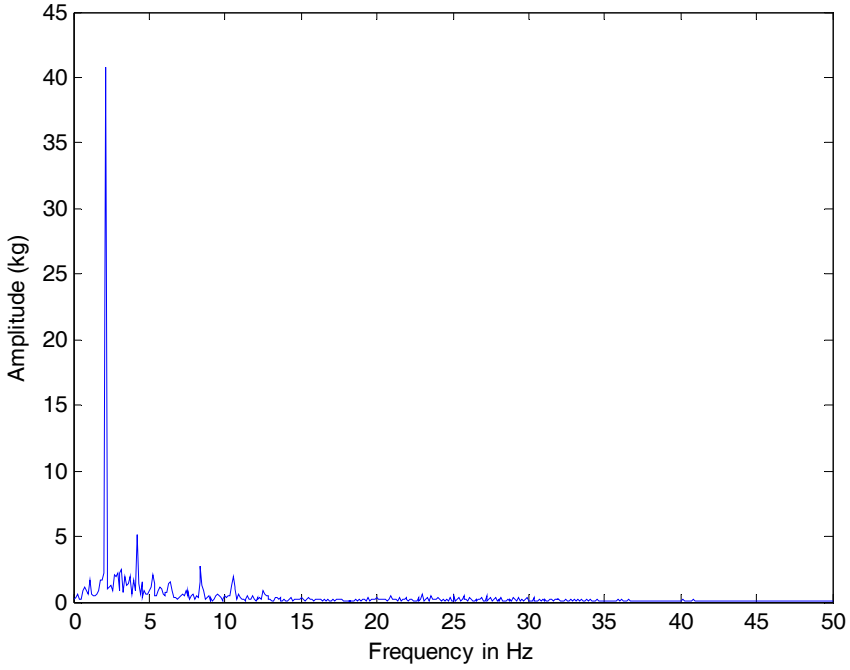

Figure 25 The single side spectrum of the ground reaction force in the trial of 3.8mph walking speed and 20 kg payload

In addition, displacement ratio of each trial was calculated to estimate the unknown damping coefficient ζ, based on equation (0-15). It was found that the mean damping ratio was 0.256, which was then input into the vibration model. Since the mass, the damping coefficient, and the stiffness coefficient are known, the suspended-load backpack system can be expressed in Laplace domain as

$$G(s) = \frac{cs + k}{ms^2 + cs + k}$$

(assuming that the backpack oscillates vertically, without leaning forward). The frequency domain properties of this transfer function are demonstrated in Appendix C.

3.5 Result

3.5.1 Vertical Displacement of the Torso and Backpack Frame

Table 5 shows the measured vertical displacement of the backpack frame and the torso (subject's CoM) and the predicted vertical displacement of the torso in all 5 trials.

Table 5 Comparison among the measured vertical displacement of the backpack frame and torso (subject's CoM) and the predicted vertical displacement of the torso

Trail No.	Walking Speed (mph)	Payload (kg)	Frame Vertical Disp. (m)	CoM Vertical Disp. (m)	Predicted Vertical Disp. (m)
1	3.8	20	0.017	0.024	0.024
2	2.6	20	0.014	0.016	0.012
3	3.2	23.7	0.018	0.026	0.018
4	3.2	20	0.015	0.019	0.018
5	3.8	18.1	0.020	0.023	0.024

To illustrate the effect of the walking speed, Figure 26 shows the trials with same mass of the payload (20 kg) and different walking speeds.

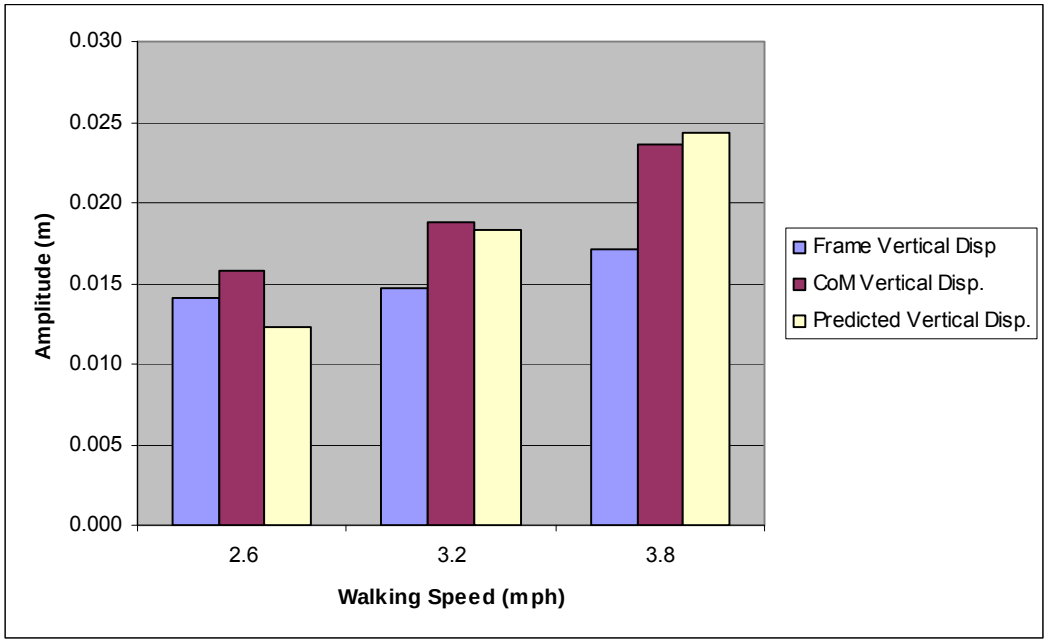

Figure 26 The comparison among the measured vertical displacement of the backpack frame, the measured vertical displacement of subject's CoM, and the predicted vertical displacement for 20 kg payload with different walking speeds.

Figure 27 shows the trials, which have the same walking speed (3.2mph and 3.8 mph) with different payload.

Figure 27 The comparison among the measured vertical displacement of the backpack frame, the measured vertical displacement of subject's CoM, and the predicted vertical displacement for different mass of payload with same walking speeds.

3.5.2 Output Power Analysis

Table 6 shows the measured relative speed between the frame and the payload, the predicted relative speed by using measured frame amplitude, and the predicted relative speed with using an inverted pendulum model in all 5 trials.

Table 6 Comparison among the measured relative speed, the predicted relative speed using measured frame amplitude, and the predicted relative speed using inverted pendulum model

Trail No.	Walking Speed (mph)	Payload (kg)	Measured Relative Speed (m/s)	Predicted Relative Speed Using Frame Amp. (m/s)	Predicted Relative Speed (m/s)
1	3.8	20	0.365	0.296	0.421
2	2.6	20	0.103	0.103	0.091
3	3.2	23.7kg	0.320	0.278	0.279
4	3.2	20	0.191	0.173	0.217
5	3.8	18.1kg	0.272	0.298	0.366

To illustrate the effect of the walking speed and the mass of payload on the relative speed, Figure 28 shows the trials with same payload mass (20 kg) and Figure 29 shows the trials with same walking speed (3.2 mph and 3.8 mph).

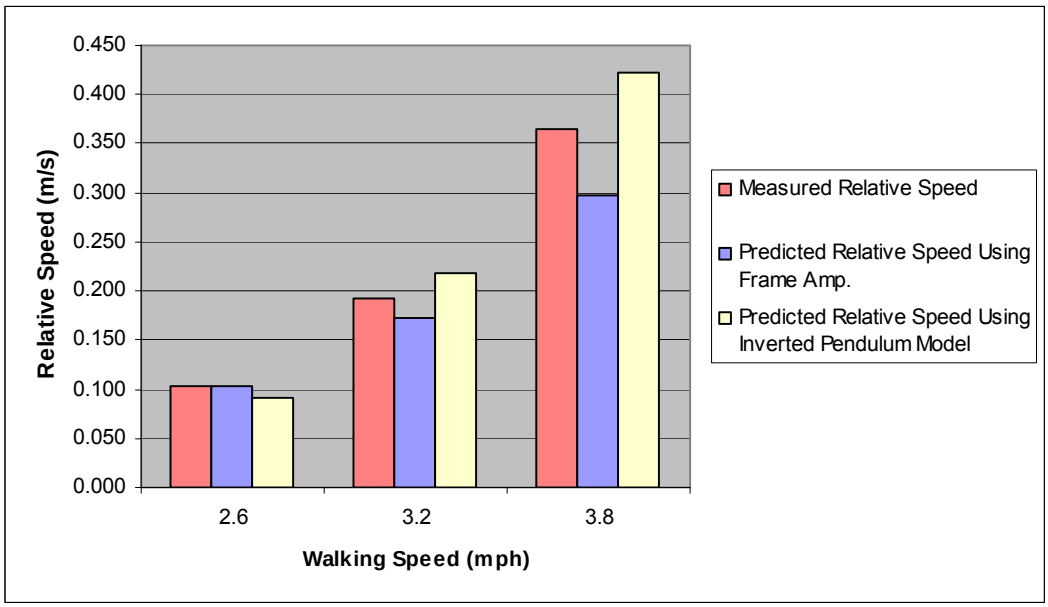

Figure 28 The comparison among the measured relative speed, the predicted relative speed using frame amplitude, and the predicted relative speed using inverted pendulum model for 20 kg payload with different walking speed

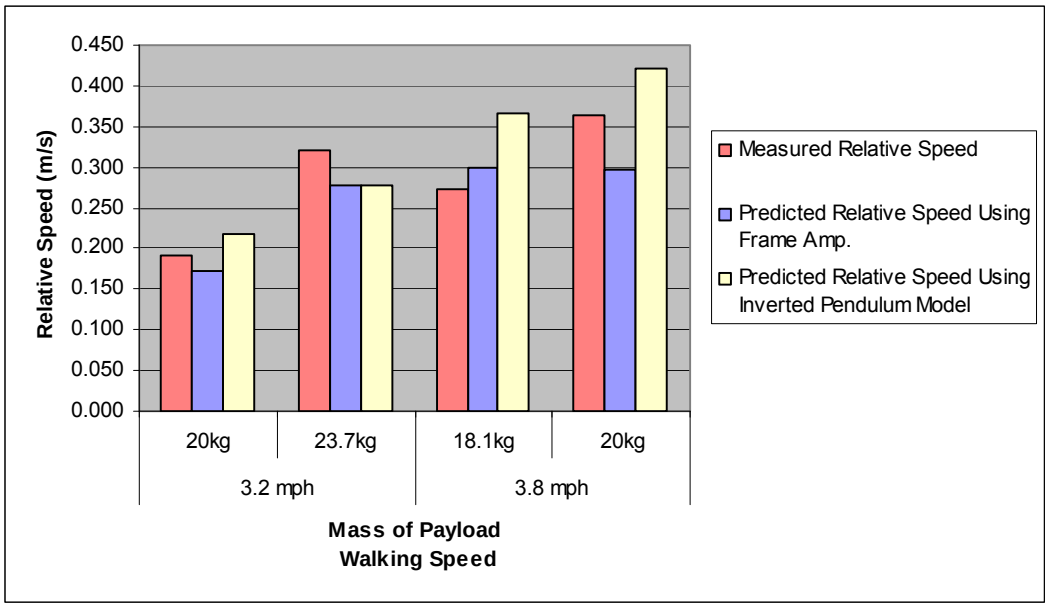

Figure 29 The comparison among the measured relative speed, the predicted relative speed by using frame amplitude, and the predicted relative speed with using inverted pendulum model for same walking speed with different mass of the payload

3.5.3 Ground Reaction Force

Table 7 shows the measured and the predicted peak vertical GRF in all 5 trials. Figure 30 shows the trials with same payload mass (20 kg) and different walking speed, while Figure 31 shows the trials with same walking speed (3.2 mph and 3.8 mph) and different mass of payload.

Table 7 The comparison between the measured and the predicted peak vertical ground reaction force in all 5 trials

Trail No.	Walking Speed (mph)	Payload (kg)	Measured Peak Force (kg)	Predicted Peak Force (kg)
1	3.8	20	143.6	151.1
2	2.6	20	119.7	117.0
3	3.2	23.7kg	137.8	137.6
4	3.2	20	125.3	131.9
5	3.8	18.1kg	137.0	147.8

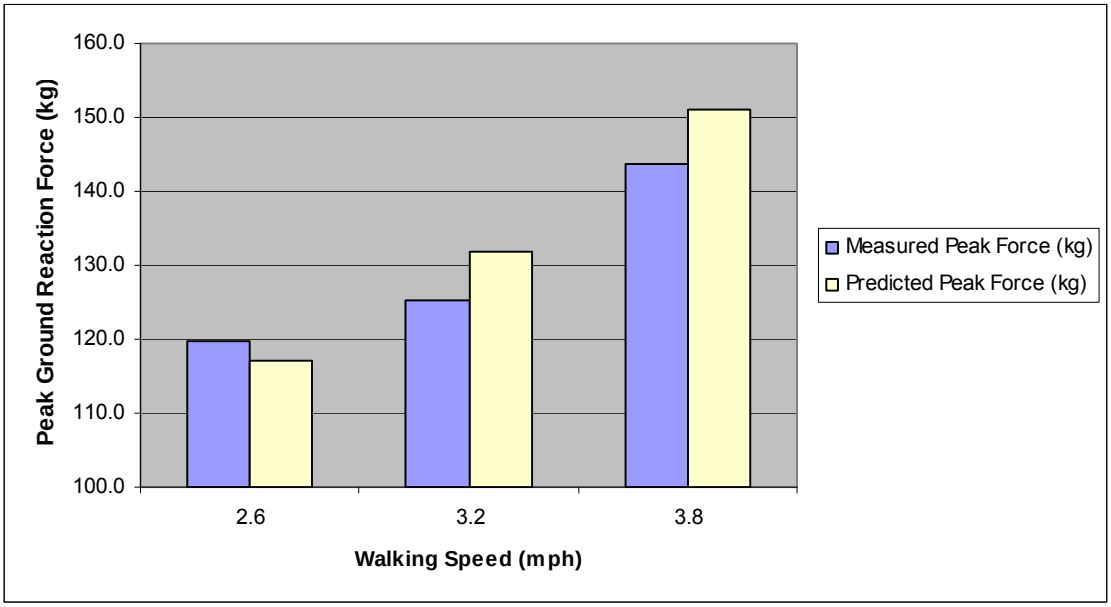

Figure 30 The comparison between the measured and the predicted peak vertical ground reaction force for 20 kg payload with different walking speed

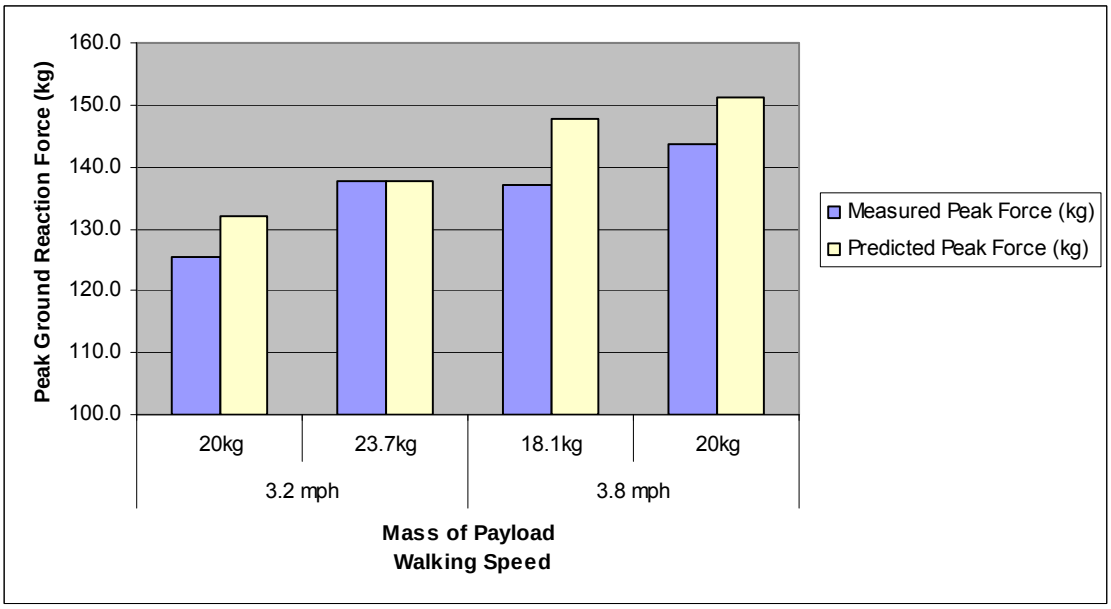

Figure 31 The comparison between the measured and the predicted peak vertical ground reaction force for same walking speed with different mass of the payload

3.6 Pilot Work Discussion

Figure 26 indicates that the vertical displacement of the subject's CoM has a clear growing trend when the walking speed increases. This trend is consistent with the results of previous studies on the vertical displacement of the torso during human walking (Cappozzo 1981; Thorstensson, Nilsson et al. 1984). Figure 27 shows that while walking at 3.8 mph, the vertical displacement of the CoM did not change much with a 2 kg increase at the payload. This unchanged displacement was consistent with the assumption that the vertical movement of the torso was not influenced by the payload. However, the trials with 3.2 mph walking speed did not show such consistency. The movement of CoM with 23.7 kg payload was considerably larger than that with 20 kg. One possible explanation is that before the trial with 23.7 kg started, the subject was told that this trial was the heaviest one in the experiment, which may lead to overreacting of the subject during walking. Therefore in the experiment, subjects were only told the approximate weight before the experiment rather than the exact weight before each trial.

With respect to the accuracy of the inverse pendulum model, the predicted vertical displacement is approximately equal to the measured vertical displacement of the subject's CoM, except the trial with 3.2mph walking speed and 23.7 kg payload. Because 1 out 5 trials had a relatively large error between the predicted and the measured displacement, more subjects were run in the further investigation to validate the accuracy of the model. On the other hand, Figure 26 and Figure 27 show that the vertical displacement of the backpack frame is smaller than that of the subject's CoM, which indicates that there is some relative movement between the backpack and the torso. After looking back at the video of the trials, it was found that for the two-layer frame the one

connecting to the torso was not rigidly linked to the one holding the weight due to the slackness of the screws. The movements of the torso then cannot be fully transmitted to the backpack through this loose link. To ensure that the torso movements fully excite the load-suspended backpack, two buckles were added between the original frame and the additional one to secure the whole backpack frame for the full experiment.

Figure 28 indicates that with a constant 20 kg payload, the measured amplitude of the relative speed has a growing trend when the walking speed increases. Based on Figure 29, the predicted relative speed also increases as the mass of the payload increases with a constant walking speed. Thus the observed trend is consistent with the model. The model also indicates that with a constant walking speed, the relative speed between the payload and the backpack frame is a function of the payload weight is not monotonic (Figure 17). However, the trials tested in the pilot study are located in a monotonic region, which means that the relative speed would only increase when the payload weight increases. This prediction is consistent with the measured relative speed show in Figure 29. To solely evaluate the base excitation model, the measured frame oscillation was input instead of the vertical displacement predicted by the inverted pendulum model. Thus in Figure 28 and Figure 29, there are two predicted relative speeds, one for evaluating the whole model and one for evaluating the base excitation part of the model. Since the measured frame oscillation is less than the predicted vertical displacement (Figure 26), the relative speed predicted by the measured frame oscillation is also less. The five trials in the pilot study showed that the measured relative speeds were close to these two sets of predicted relative speeds.

With respect to the kinetics variable, Figure 30 indicates that the peak ground reaction force increases as walking speed increases. This trend is in accord with the predicted trend and the magnitude of the force is similar to the predicted magnitude. Figure 31 demonstrates the effect of changing the mass of payload and adding mass on the payload increased the peak ground reaction force. All these results indicate that the model has predictability and the further study is necessary for investigating the accuracy. A revised methodology is presented in the next section as the main proposed method in this dissertation.

4 Methods

The goal of this research was to develop and validate a model that is capable of predicting the amount of utilizable energy generated by a load-suspended backpack during human walking and estimating the peak ground reaction force of walking with such a backpack under various speeds and payloads. This section includes the methodology used in the experiment, refined from the pilot study.

4.1 Subject

Ten subjects were recruited from North Carolina State University student body on a voluntary basis. The subject group had a mean age of 26.3 (SD 1.5) years, height 177 (SD 4.2) cm, leg length 95 (SD 1.9) cm, and body mass 70.8 (SD 12.0) kg. To control inter-gender differences in anthropometry and physiology, only male subjects were tested. Each subject was fully informed that he should be in good health and have no current or chronic back injury. He signed the Informed Consent Form approved by North Carolina State University Institutional Review Board.

4.2 Apparatus

The apparatus that were used in the experiment were approximately identical to those used in the pilot study (section 3.2). Since it was found that the backpack frame was slightly deformed by the weight loading, two buckles were added between the original frame and the additional frame to secure the whole structure of the backpack frame and ensure that the torso movement could be fully transmitted to the backpack frame and excite the payload (Figure 32). Because the pilot subject reported that walking with the

metronome was not comfortable and might not well represent normal human walking, the metronome was discarded in the experiment. Instead, the subjects were allowed to choose a comfortable cadence. Generally, the apparatus include a reinforced suspend-loaded backpack carried by the subjects, a treadmill with two force plates placed under the conveyor recording the GRF, and three sensors of motion tracking system rigidly fixed on the backpack and subjects' torso to record the vertical displacement.

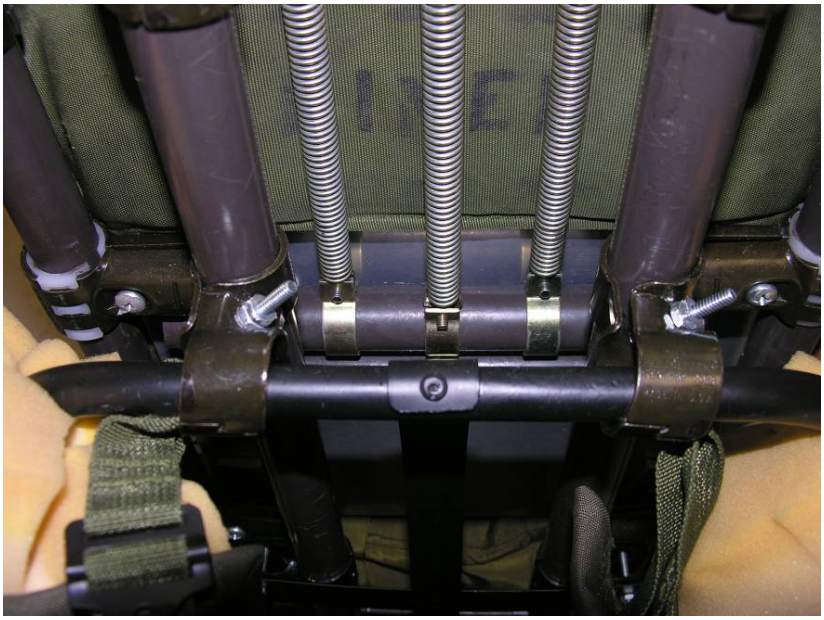

Figure 32 Adjusted backpack frame with two buckles between the original frame and the additional frame

4.3 Experimental Variables

4.3.1 Independent Variables

The independent variables in this study included the walking speed and the mass of payload. As mentioned by Whittle (1996), the 95% range of walking speed is from 0.90 m/s to 1.62 m/s. Under experiment conditions the walking speeds were roughly set from 0.89 m/s to 1.78 m/s (Table 1), which reflect reality. In the current experiment,

considering the resolution of the treadmill is 0.1 mph (0.0447 m/s), three walking speeds (1.16, 1.44 and 1.70 m/s) were used to approximately reflect slow walking, normal walking, and fast walking. In terms of the mass of payload, there is no obvious definition of the maximal load. For military groups, load usually range from 20 to 50 kg, and for industrial tasks the load is up to 40 kg (Haisman 1988). In the current research, due to the mechanism of the suspended-load backpack, the force exerted on the torso oscillates and the peak force is proportionally magnified based on the mass of payload. To ensure that the peak force does not exceed 40 kg, two levels of the mass (15.9 and 22.7 kg) which represented light load carriage and normal load carriage were tested. The independent variables are listed below:

A. Walking Speed / Cadence (within subjects)

1. 2.6 mph (1.16 m/s)

2. 3.2 mph (1.43 m/s)

3. 3.8 mph (1.70 m/s)

B. Mass of Payload (within subjects)

1. No payload

2. 35 lb (15.9 kg)

3. 50 lb (22.7 kg)

4.3.2 Dependent Variables

Since the goal of the current research was to predict the scavenged energy and to investigate the changes on walking pattern, the dependent variables consist of two parts. In the first part, vertical movement of the subject and the backpack were measured to

evaluate the accuracy of the inverted pendulum model and the base excitation model. The bottom of the sternum was used to represent the position of the subjects. As mentioned in previous research (Cappozzo 1981; Thorstensson, Nilsson et al. 1984), the oscillation magnitude of the neck, shoulder, and pelvis are about equal during walking. Thus, with respect to construct validity, using the position of the sternum can well reflect the oscillation of the torso. In the second part, based on the previous research listed in Table 2, double support time and single limb stance time were collected to investigate the walking stability. First peak force, second peak force, mid-support force, weight acceptance rate, and push off rate were collected to investigate gait kinetics and energy consumption. The dependent variables are listed below:

A. Vertical position of the CoM of the subjects and the backpack frame

B. The relative velocity between the payload and the backpack frame

C. Gait Parameters

C1. Cycle time (CT)

C2. Single limb stance time (SST)

C3. Double support time (DST)

C4. Normalized weight acceptance force (NWAF)

C5. Normalized push off force (NPOF)

C6. Normalized mid-support force (NMSF)

4.4 Experimental Procedure

Before the scheduling of the experiment, the subjects attended a familiarization period. This program familiarized the subjects with different walking speeds and the

payload levels. Anthropometry data of the subject, such as weight, stature, and leg length, were collected. A short walking training trial with the treadmill was provided to ensure that the subject put each heel-strike on the front force plate of the treadmill and toe-off on the back one during walking. The subject was then given a 5-minute warm-up designed to prepare the legs and torso muscles.

To begin the experimental session, the suspended-load backpack was placed on the back of the subject and the shoulder belts and hip belt were fastened to eliminate the movement between the torso and the backpack frame. The flock of bird sensors were mounted on the subject's CoM (around the bottom of the sternum) and the clear plastic plates connecting with the backpack frame and the load plate. During the experiment, the subjects walked on the treadmill with their preferred cadence under 3 different load levels (no backpack, 15.9 kg, and 22.7 kg) and 3 different walking speeds (1.16 m/s, 1.43 m/s and 1.70 m/s). Thus, there will be 9 conditions (3 payload mass X 3 walking speed = 9 conditions) for each subject. Each condition was performed for 1.5 minutes and the last one minute was monitored by the motion tracking system and the instrumented treadmill. To ensure internal validity, all the subjects were recruited from those who had never carried suspended-load backpacks to eliminate a history effect, and all experimental conditions were conducted in a random order with a 5-minute break between each trial, given to reduce the effect of fatigue.

4.5 Data Processing

A Matlab program was written to extract the position of the subject's CoM, the position of the backpack frame, the position of the load plate, and the relative velocity of the payload of each trial. Note that in the pilot study, after transformation with FFT, 1-

minute data only yielded one value for the amplitude of dominant frequency, and the variability within each trial cannot be detected. Thus, these one-minute time series were separated into six 10-second segments, as 6 repetitions of each trial. Since it was possible for the subjects to change their cadence within each trial, the dominant walking frequency of each repetition was determined by FFT. In terms of ground reaction force, the time series was also separated into six segments. However, with missing steps in each trial, the length of a segment in each trial depended on the number of missing steps. All ground reaction force parameters were normalized by dividing by the bodyweight

4.6 Model Validation

First, the effect of the load and the walk speed on the output energy (represented by the relative velocity between the frame and the payload) was tested using ANOVA over all conditions. If the independent variables had a significant effect, the paired t-test was used to see the difference between every two conditions. To validate the accuracy of the mechanical model, the fitted amplitude of the output energy was compared with the model predicted amplitude. The percentage error (PE) was used to quantify the accuracy of the model, and it is calculated as:

$$PE_i = \frac{\hat{A}_i - A_i}{A_i} \tag{4-1}$$

where $\hat{A}_i$ is the amount of energy predicted by the model with condition i, A_i is the measured value. Similarly, amplitude of predicted GRF was compared with the measured GRF.

4.7 Statistical Analysis

Since the the walking pattern may vary for different walking / carrying conditions, the statistical analysis was performed to find the effect of the conditions on the model and the walking pattern.

$$y_{ijkl} = \mu + \tau_i + \lambda_j + \beta_k + \tau\lambda_{ij} + \varepsilon_{ijkl} \quad (4\text{-}2)$$

where

y_{ijk} corresponds to the gait parameters, including CT, SST, DST, NWAF, NPOF, and NMSF.

μ corresponds to the overall mean

τ_i corresponds to the walking speed (i=1,2,3)

λ_j corresponds to the carrying level (j=1,2,3)

β_k corresponds to the subjects (k=1,2,…,10)

$\tau\lambda_{ij}$ corresponds to the interaction between the walking speed and the carrying level

ε_{ijkl} corresponds to the error term (l=1,2,…,6)

For the effects of the payload on walking pattern, Kinoshita (1985) demonstrated that with fixed walking speed, the step length was quite similar for carrying different masses of payloads. However, he found that the single support period decreased and the double support period increased while the payload mass increased. As mentioned by Attwells et al. (2006), this increased double support period is able to provide greater stability. In addition, Kinoshita found that the magnitude of the first peak force and the second peak force significantly increased as the mass of payload increased, while the

time to reach the first and the second peak force did not change. He then stated that the GRF were magnified in proportion to the increase of the mass of the payload. Consequently, it is hypothesized that the increased load will result in an increased DST and a decreased SST, and will increase NWAF, NPOF, and NMSF.

In terms of the effect of walking speed on walking pattern, some research (Mann and Hagy 1980; Winter 1991) showed that with faster walking speed, the deviations of the GRF from the body weight will increase. Thus, it is hypothesized that in this research the increased walking speed will result in increased NWAF, NPOF, and NMSF. It is clear that with a fast walking, the SST and DST will decrease.

5 Results

One participant showed difficulty in maintaining reliable gait because he was not accustomed to walking on the treadmill. Therefore, his data was not used in the analyses. Since a no-load walking condition did not yield any output energy, 54 trials (9 subjects $\times$ 6 walking conditions) were available for assessing the validity of the model of energy output. All of the 81 trials (9 subjects $\times$ 9 walking conditions) were available for analyzing the peak GRF and the effect of the backpack on the gait parameters.

5.1 Assessment of the model validity and performance

The ANOVA result showed that the load mass ($p=0.0022$) and the walking speed ($p<0.0001$) had a significant effect on the average relative velocity between the load and the frame, while their interaction did not have a significant effect.

The absolute percentage error is 24.2%. Figure 33 is the scatter plot for the measured average velocity of the load (relative to the frame) vs. the predicted velocity. The closer the points are to the diagonal line, the more precise the model is.

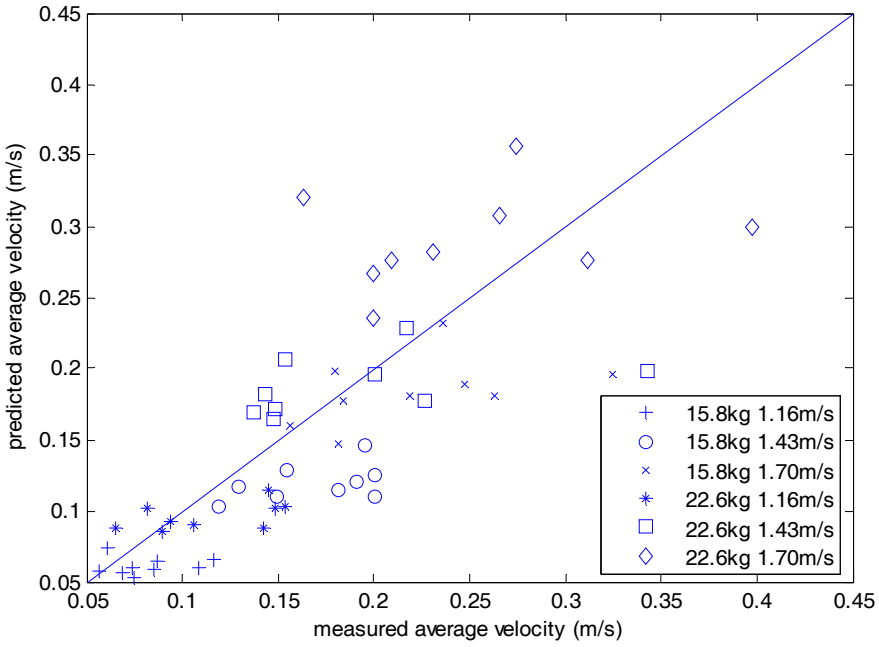

Figure 33 The scatter plot for the measured average velocity of the load vs. the predicted.

Figure 34 showed the comparison between the measured and predicted average velocity of the load under each condition. It also showed the post-hoc analysis on the effect of walking speed and load. Capital letters (A-B) were used to indicate the statistical difference on load (between the two subplots), and small letters (a-c) were used to indicate the statistical difference on walking speed (within each subplot)

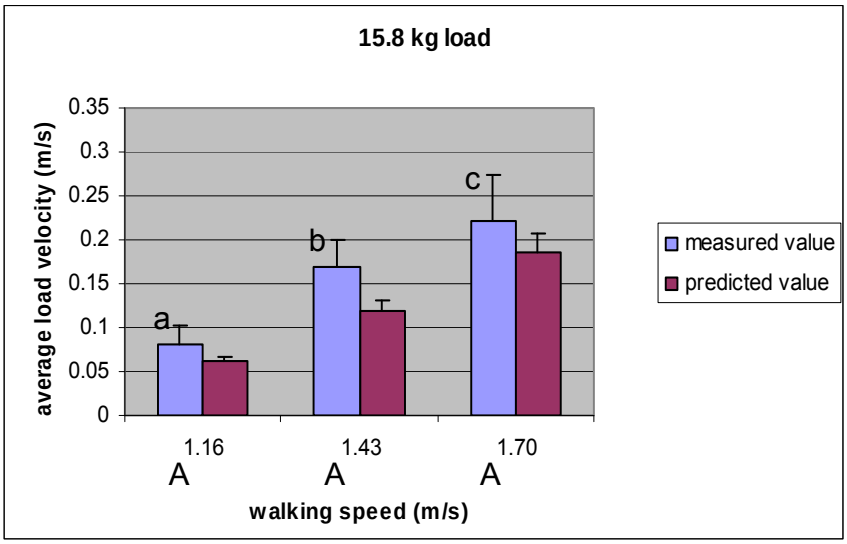

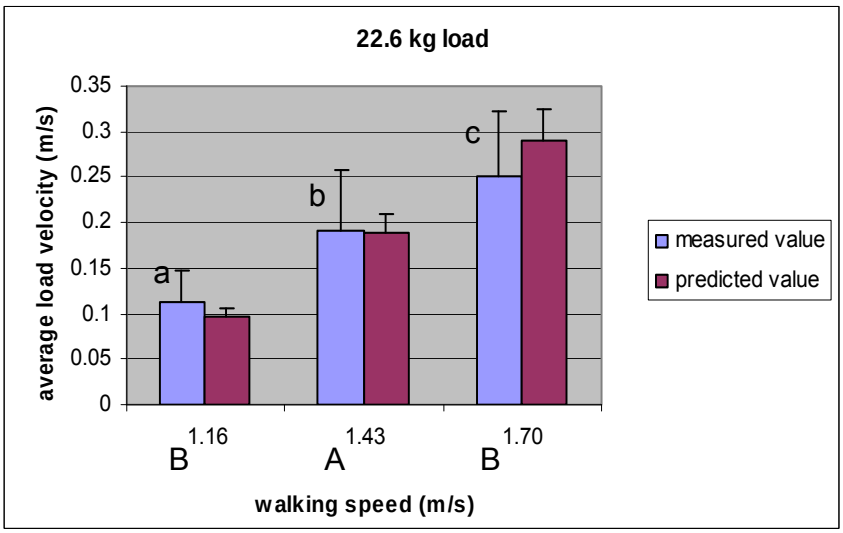

Figure 34 The comparison between the measured and the predicted average velocity of the oscillating load and the post-hoc analysis on the measured average velocity. Capital letters (A-B) were used to indicate the statistical difference on load (between the two subplots), and small letters (a-c) were used to indicate the statistical difference on walking speed (within each subplot)

In terms of gait kinetics, The ANOVA result showed that the load mass ($p<0.0001$), the walking speed ($p<0.0001$), and their interaction ($p=0.0492$) had significant effect on the peak GRF.

The absolute percentage error of peak GRF is 10.9%. Figure 35 is the scatter plot for the measured peak GRF vs. the predicted peak GRF.

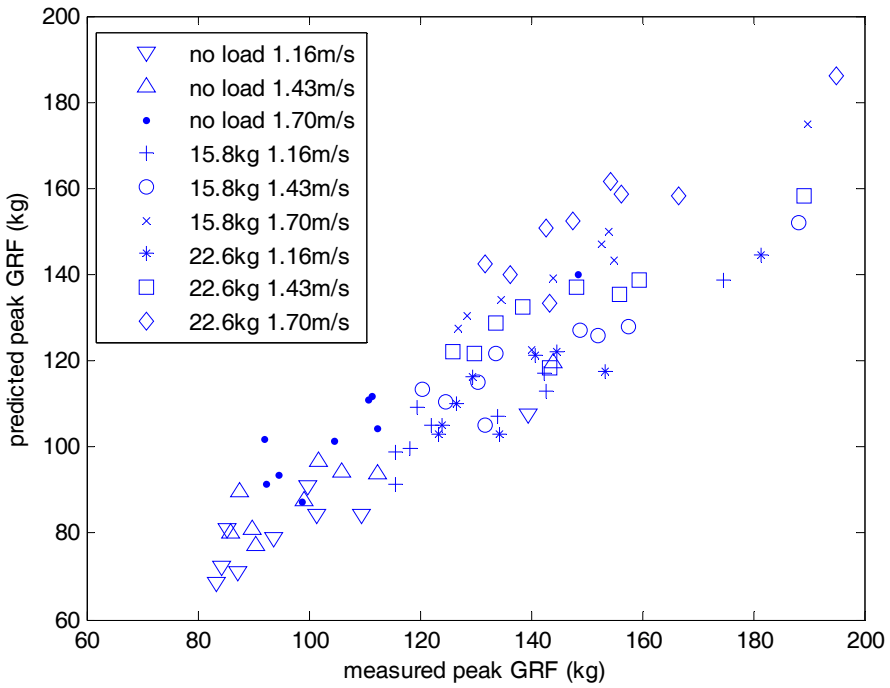

Figure 35 The scatter plot for the measured peak GRF of the load vs. the predicted.

Figure 36 shows the comparison between the measured and predicted peak GRF under each condition. It also shows the post-hoc analysis on the effect of walking speed and load. Capital letters (A-B) were used to indicate the statistical difference on load (between the three subplots), and small letters (a-c) were used to indicate the statistical difference on walking speed (within each subplot)

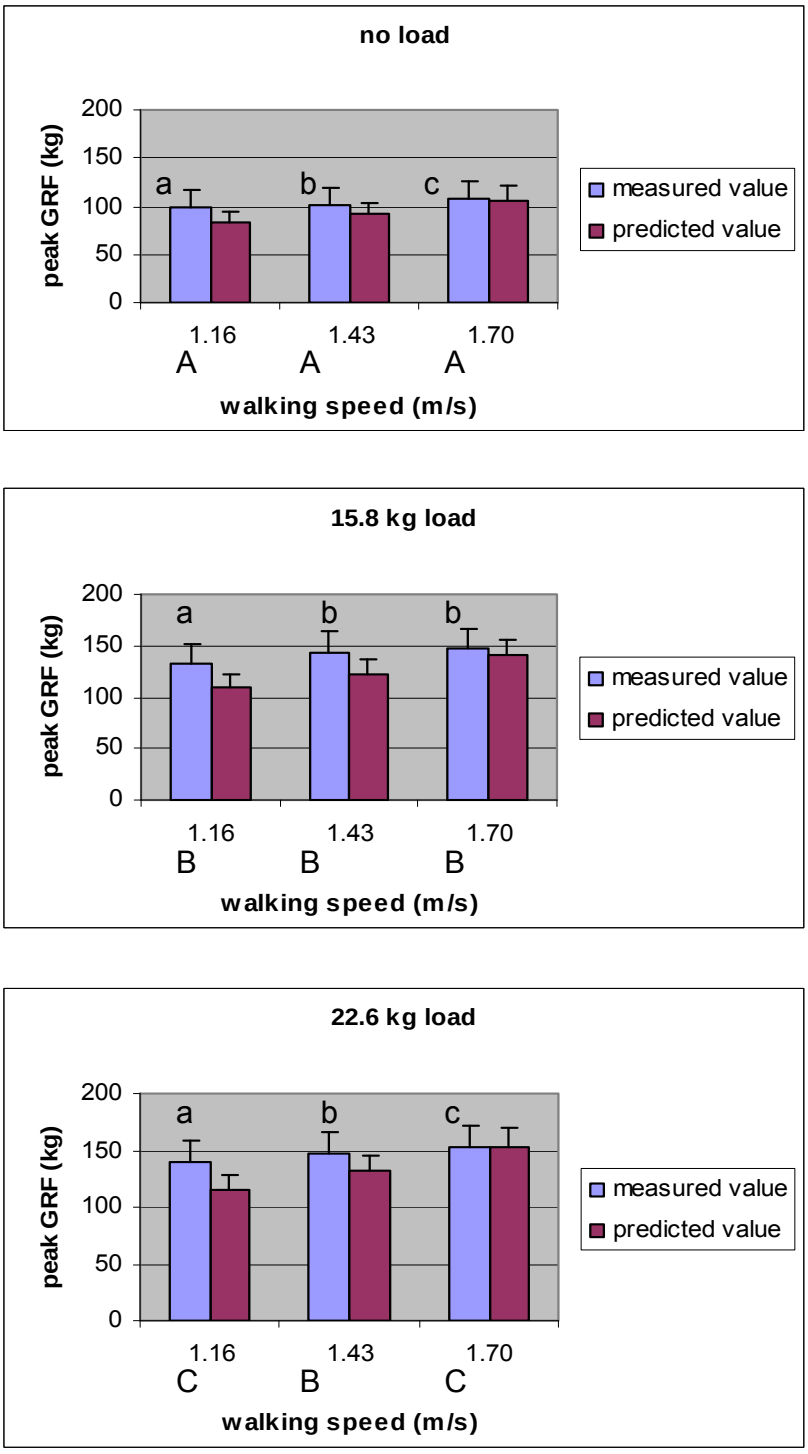

Figure 36 The comparison between the measured and the predicted peak GRF and the post-hoc analysis on the measured average velocity. Capital letters (A-B) were used to indicate the statistical difference on load (between the two subplots), and small letters (a-c) were used to indicate the statistical difference on walking speed (within each subplot)

5.2 Statistical analysis on the gait parameters

The MANOVA was performed on the temporal variables and kinetic variables separately. The results indicated that load and walking speed were significant on temporal and kinetic variables while the interaction between load and walking speed was significant only on kinetic variables. An ANOVA was then performed to identify which dependent variables accounted for the significant effect.

5.2.1 Temporal variables

Table 8 presents the MANOVA of load and walking speed for the CT, SST, and DST. ANOVA results revealed highly significant effects of walking speed on CT, SST, and DST. Load level only affected SST and DST. Figure 37 to Figure 39 show the temporal variables for each load level and walking speed combination (error bars represent one standard deviation on each response measure). For Figure 37 to Figure 42, capital letters (A-C) were used to indicate the statistical difference on loading condition, and small letters (a-c) were used to indicate the statistical difference on walking speed

Table 8 MANOVA and ANOVA results of temporal variables

	MANOVA		CT		SST		DST	
	F	p	F	p	F	p	F	p
Load	31.98	<.0001*	1.64	0.2017	8.93	0.0004*	16.96	<.0001*
Vel	71.54	<.0001*	247.28	<.0001*	42.19	<.0001*	14.11	<.0001*
Load*Vel	0.91	0.5596	-	-	-	-	-	-

An * indicates significant effect

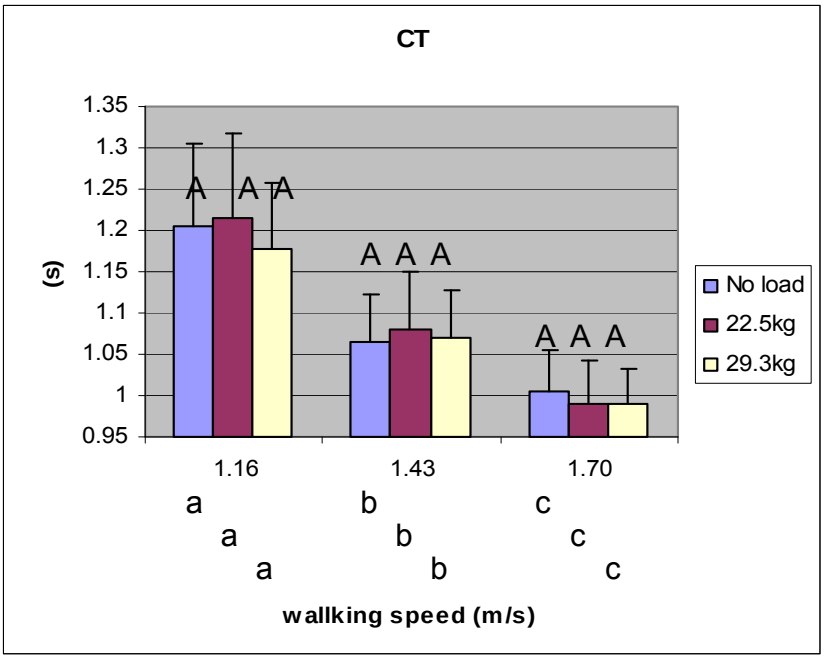

Figure 37 Effect of load and walking speed on the CT. Capital letters (A-C) were used to indicate the statistical difference on loading condition, and small letters (a-c) were used to indicate the statistical difference on walking speed

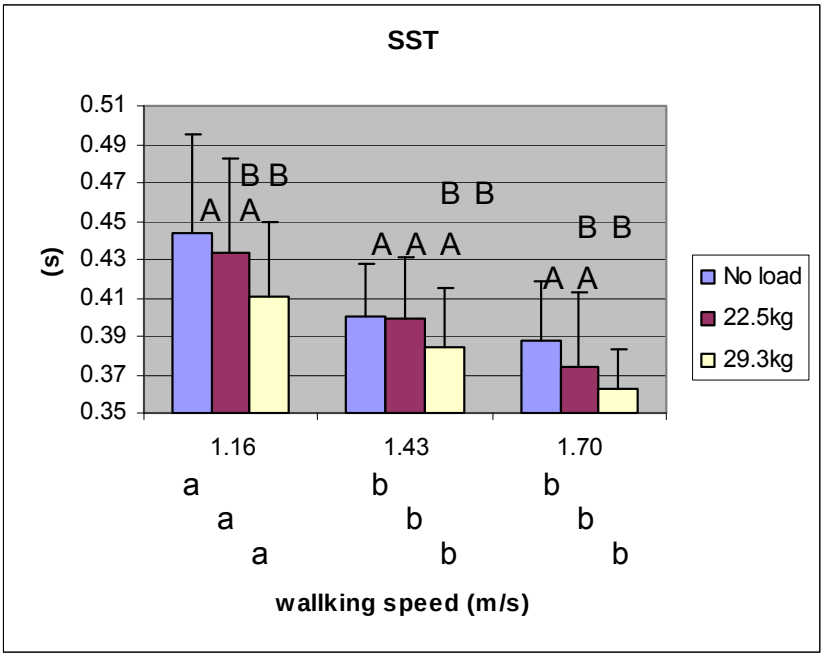

Figure 38 Effect of load and walking speed on the SST. Capital letters (A-C) were used to indicate the statistical difference on loading condition, and small letters (a-c) were used to indicate the statistical difference on walking speed

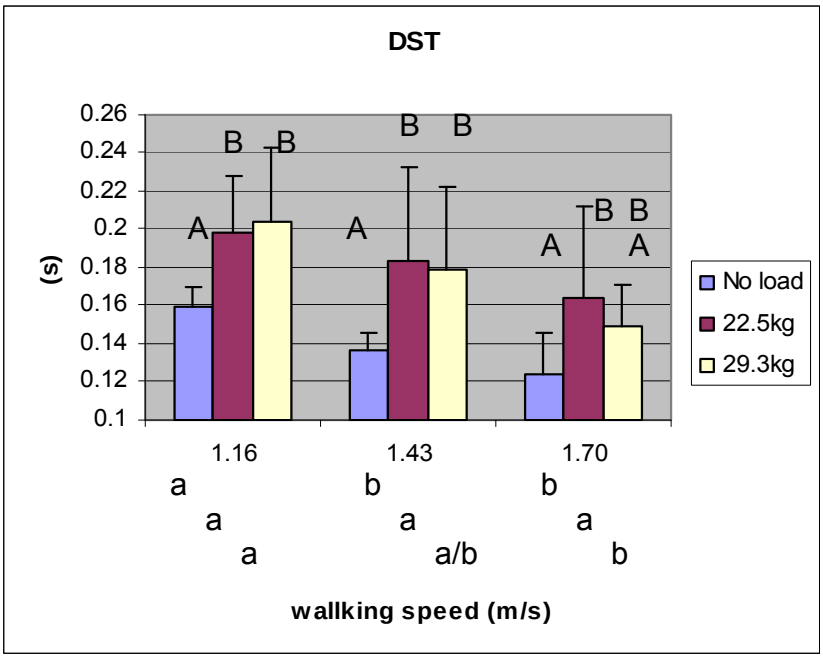

Figure 39 Effect of load and walking speed on the DST. Capital letters (A-C) were used to indicate the statistical difference on loading condition, and small letters (a-c) were used to indicate the statistical difference on walking speed

5.2.2 Kinetic variables

The following table (Table 9) presents the MANOVA of load and walking speed for NWAF, NPOF, and NMSF. ANOVA results revealed highly significant effects of load, walking speed, and their interaction on NWAF, NPOF, and NMSF. Figure 40 to Figure 42 show the kinetic variables for each load level and walking speed combination (error bars represent one standard deviation on each response measure).

Table 9 MANOVA and ANOVA results of kinetic variables

	MANOVA		NWAF		NPOF		NMSF	
	F	p	F	p	F	p	F	p
Load	128.37	<.0001*	720.44	<.0001*	147.32	<.0001*	136.92	<.0001*
Vel	48.92	<.0001*	209.36	<.0001*	18.99	<.0001*	44.37	<.0001*
Load*Vel	7.16	<.0001*	7.2	0.0058	16	<.0001*	5.88	0.0189*

An * indicates significant effect

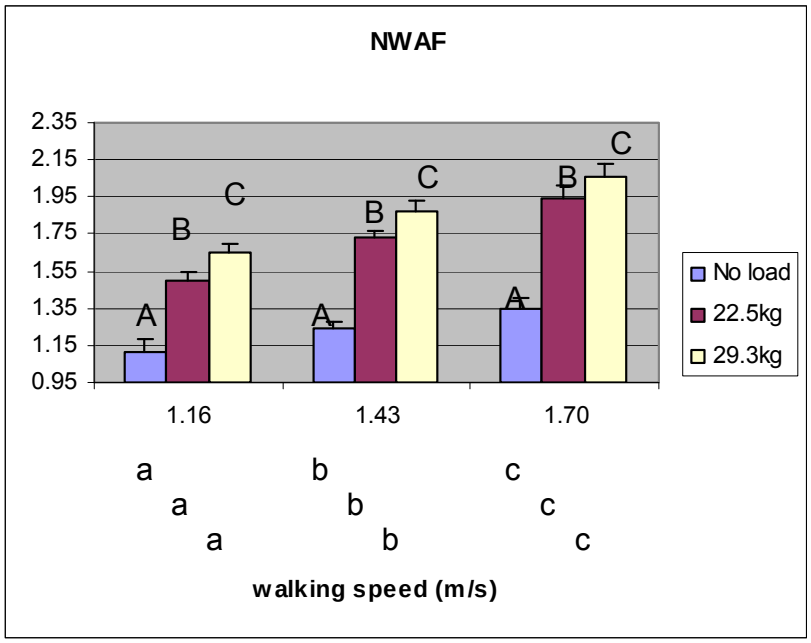

Figure 40 Effect of load and walking speed on the NWAF. Capital letters (A-C) were used to indicate the statistical difference on loading condition, and small letters (a-c) were used to indicate the statistical difference on walking speed

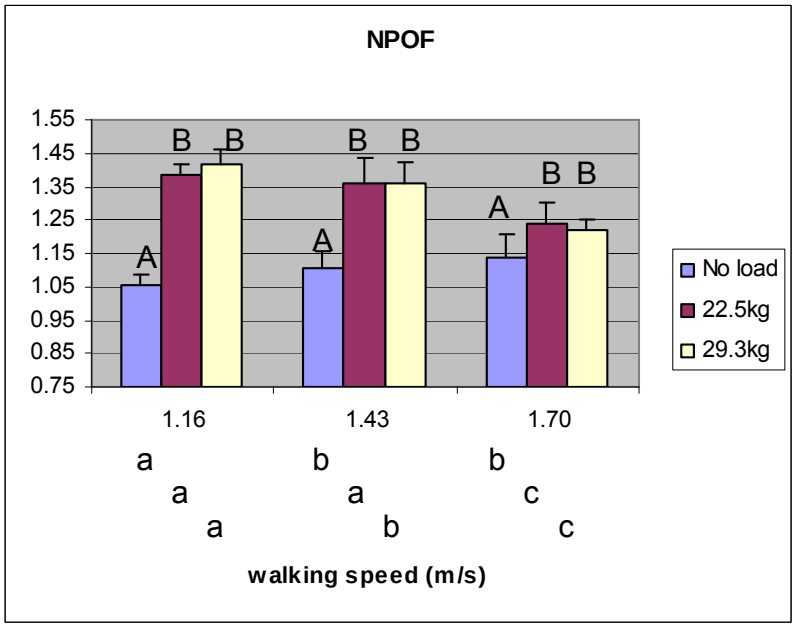

Figure 41 Effect of load and walking speed on the NPOF. Capital letters (A-C) were used to indicate the statistical difference on loading condition, and small letters (a-c) were used to indicate the statistical difference on walking speed

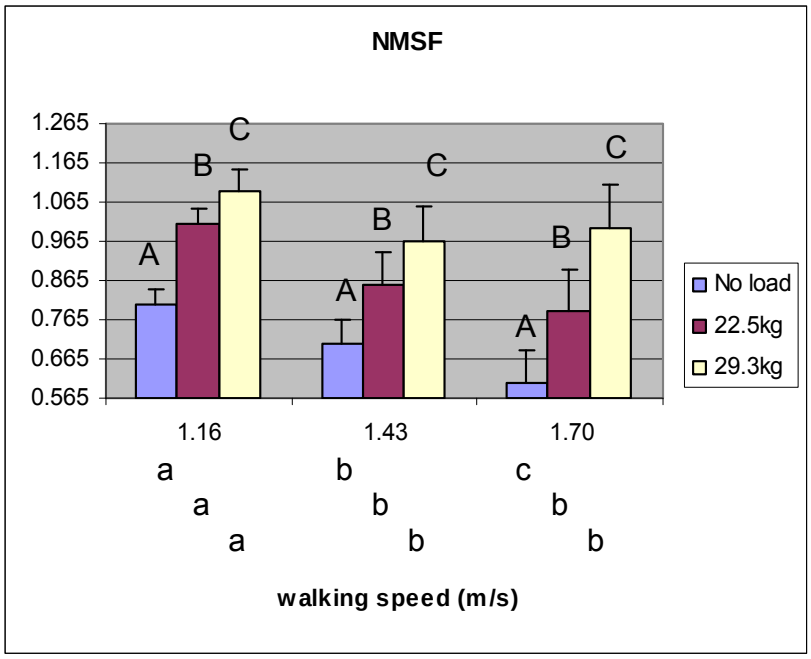

Figure 42 Effect of load and walking speed on the NMSF. Capital letters (A-C) were used to indicate the statistical difference on loading condition, and small letters (a-c) were used to indicate the statistical difference on walking speed

6 Discussion

A suspended-load backpack generator in which a load was hung by springs was invented to harvest energy from human walking (Rome et al. 2005). Owing to the fact that the CoM of the human body moves up and down periodically during walking, the hung load in the backpack excitedly oscillates up and down. The relative movement between body and load can be a source of harvesting energy. The energy generated by a suspended-load backpack is sufficient to drive many portable electronic devices (Rome et al. 2005). However, the previous research is not capable of calculating the amount of the output energy, nor does it investigate the effects of such suspended-load backpacks on human walking. Therefore, a biomechanical model was built to predict the output energy and to analyze the influence of the suspended-load backpack on the human walking pattern.

6.1 Model performance and validity

Given the walking speed and the mass of the load, the proposed model is capable of predicting the relative velocity of the suspending load and the peak GRF. From Figure 33 and Figure 35, it is clear that there is a general agreement between the experimental data and the predicted value. The model indicates that the load velocity and the peak GRF are basically determined by two sets of variables. The first set consists of anthropometric data and gait parameters including leg length, walking speed, and cadence. The second set consists of the mechanical parameters of the backpack including the load weight, the spring stiffness and the damping coefficient. The bridge between the two variable sets is

the movement of the torso which is determined by human performance and plays a role as the excitation source of the backpack.

Both the empirical data and the model show that under the experimental walking condition, the average velocity of the load increases with faster walking speed or heavier load. Since faster average load velocity indicates more mechanical energy, this result is consistent with the finding of Rome et al. (2005) in which the power scavenged from a suspended-load backpack increased with faster walking and heavier load. However, it may not be correct to state that walking faster and carrying heavier loads can necessarily lead to a faster average load velocity. According to the base excitation model, the excited magnitude increases as the base frequency is increased from zero to the natural frequency of the system. As the base frequency exceeds the natural frequency, the excited magnitude starts decreasing. In this study, the natural frequency of the backpack system can be easily influenced by changing the load weight. The relationship between load velocities and walking speed / load weight may be non-monotonic. To clarify this question, a simplified model in section 3.1.2 is helpful. Consider that for a specific suspended-load backpack, the spring coefficient and damping coefficient are fixed. Assuming that the walking cadence is related only to leg length and walking speed, the load velocity can be written as a function of load weight and walking speed for a specific subject:

$$V_{rms} = f_{k,\zeta,l_0}(m,V) \tag{6-1}$$

Figure 47, Figure 49, Figure 51, Figure 53, and Figure 55 in Appendix A demonstrate that with the different system configurations (stiffness, damping ratio, and leg length), the load velocity can change from a non-monotonic function of load weight / walking speed

to a monotonic one. For example, the shape of this function becomes more linear as the damping coefficient increases. Since the damping ratio of the frame tested in the current research is about 0.256, Figure 51 approximately represents the actual function of the load velocity in the experiment. Although it is not globally monotonic, it is still consistent with the experimental data because all of the conditions tested in this study are in a monotonic area.

Similarly, based on the discussion in section 3.1.3, the peak GRF can be expressed as a function of load weight and walking speed:

$$F = f'_{k,\zeta,l_0}(m,V) \tag{6-2}$$

Figure 48, Figure 50, Figure 52, Figure 54, and Figure 56 in Appendix A showed that with different system configurations, the monotonicity of the function also changes, and the shape of this function becomes more linear with an increased damping coefficient. Since the damping ratio of the frame is about 0.256, Figure 52 approximately represents the actual function of the peak GRF in the experiment. Figure 50 demonstrates that when the damping ratio is small enough, the effect of carrying a heavy load is similar to carrying a light load in terms of the peak GRF. For instance, assuming that the walking speed is 1.6 m/s, the peak GRF of carrying 20 kg load is similar to carrying 36 kg. This inference is consistent with the previous work, namely Kram (1991), who found that peak GRF was only slightly changed when weights were carried with bamboo poles. Since the bamboo poles are springy and the friction on the load is very small, carrying a load with poles can be simplified to the model proposed in the current research with a very small damping ratio. However, it should be noted that all these carrying tools only help reduce the peak GRF rather than the energy consumption. When the phase shift between the load

and the torso decreases the peak GRF, it also lengthens the contact time (Kram 1991), which leads to an increased cumulative GRF (time integral of the GRF) and energy consumption.

In terms of the accuracy of the model, the results indicate that with a light load the measured load velocity tends to be larger than the predicted value (Figure 34). One possible reason is that the bushings on the backpack frame are not pure damping elements. When the load is light, only a small moment is generated on the bushings. The contact between the bushings and the rods is loose, which leads to a reduced damping coefficient. Based on the excitation model, the reduced damping coefficient then yields a large amplitude of load oscillation (Figure 8). In the proposed model, the damping coefficient is fixed and derived from the pilot study in which a heavy load (20 kg) was used. Since a heavy load leads to a large damping coefficient, the predicted value is smaller than the measured value. The results also indicate that with slow walking speed, the peak GRF tends to be underestimated (Figure 36). Consider that during walking, the motion of the CoM is consecutive arcs and the CoM is redirected in the double support phase as the maximum peak GRF occurs. In the current model, it is assumed that this path redirection is as smooth as a sinusoidal wave. Based on the inverted pendulum model, however, the redirection is suddenly changed. Although the walking determinants smooth this sudden change of the CoM, the effect of the smoothing is weakened during slow walking (Lamoreux 1971). In consequence, the sudden redirection during the slow walking may yield a large peak GRF.

6.2 Trade-off between the output energy and the peak GRF

Because the extreme GRF may lead to foot blisters, metatarsalgia, stress fractures, etc. (Knapik, Harman et al. 1996), it would be interesting to know what the minimum peak GRF is to achieve a specific power output level. Consider that both the load velocity and the peak GRF are two-variable functions of load weight and walking speed (Eq. 6-1 and Eq. 6-2). Different configurations of load weight and walking speed may yield the same magnitude of load velocity while the magnitude of peak GRF varies. Thus, to find the configuration that yields the minimum peak GRF, this problem becomes a nonlinear programming (NLP) problem with a nonlinear constraint, in which the peak GRF is the objective function and the load velocity is the constraint:

$$\min\ F = f'_{k,\zeta,l_0}(m,V)$$
$$s.t.\ V_{rms} = f_{k,\zeta,l_0}(m,V) = V_0$$

where V_0 is the load velocity for a specific task. In Figure 43, all the points on the red curve (the constraint) represent the same amount of power generation while the corresponding GRFs are different. Using NLP, the minimum GRF along the constraint is 155.3 kg when the walking speed is 1.54 m/s and the payload is 28.4 kg.

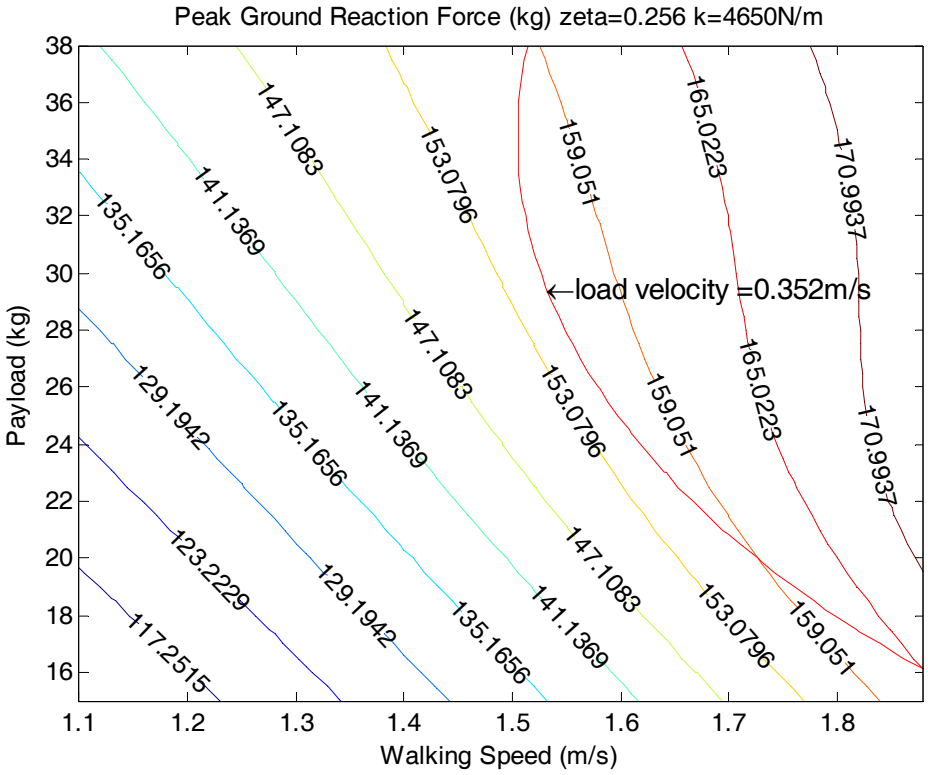

Figure 43 An NLP in which the peak GRF is the objective function and the load velocity is the constraint

On the other hand, if the upper limit of the peak GRF is given for a task, the maximum power output also can be found by using NLP:

$$\max \; V_{rms} = f_{k,\zeta,l_0}(m,V)$$
$$s.t.\; F = f'_{k,\zeta,l_0}(m,V) = F_0$$

where F_0 is the peak GRF for a specific task. In Figure 44, all the points on the red curve (the constraint) represent the same peak GRF a while the corresponding amounts of power generation are different. Using NLP, the maximum power generation along the constraint is 0.315 m/s when the walking speed is 1.50 m/s and the payload is 27.6 kg.

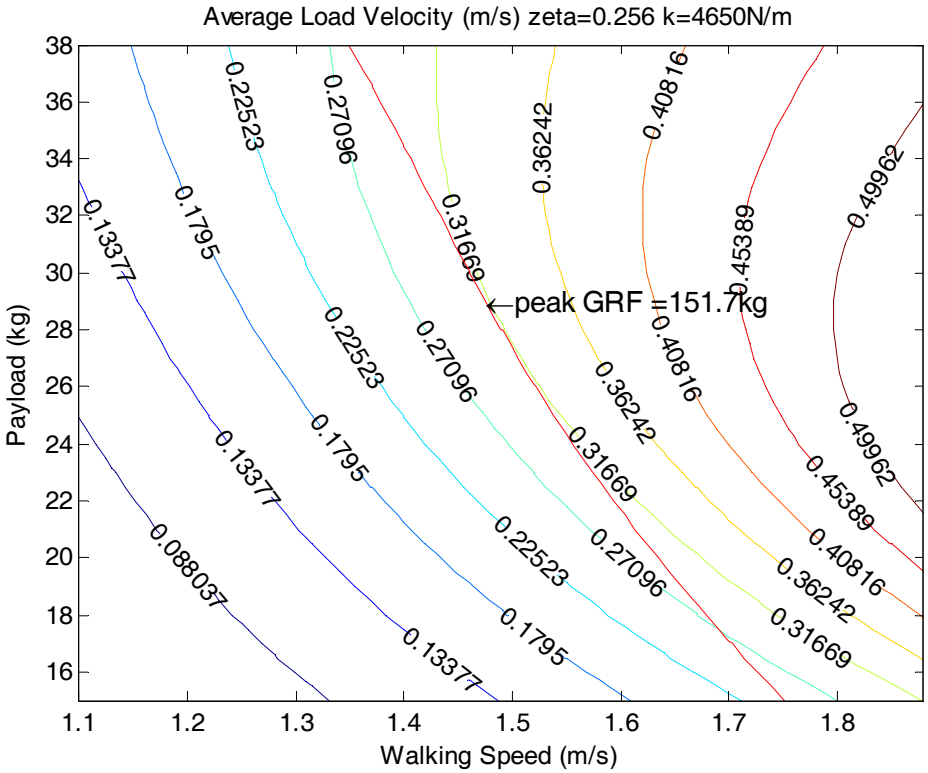

Figure 44 An NLP in which the load velocity is the objective function and the peak GRF is the constraint

6.3 Effect on human walking pattern

Because of the associated high walking cadence, it was not surprising to see that SST, DST and CT significantly decreased with a faster walking speed (Grieve and Gear 1966). The results also showed that the subjects had decreased SST and increased DST when the load level increased from no backpack to heavy-load condition, whereas the total cycle time were not significantly affected by the load conditions. As suggested by Wang et al. (2001), a lengthened DST indicated that the subjects tried to avoid instability by distributing the load on both legs during walking. These results are consistent with the findings of the research conducted by Kinoshita (1985) and Wang et al. (2001) on the

effect of conventional backpacks. Therefore, it is reasonable to speculate that the effects of suspended-load backpacks are similar to a regular backpack in terms of temporal parameters of gait.

With respect to the control of push-off or roll-off, analysis on the kinetic parameters of the gait revealed that with the suspended-load backpack the NPOF decreased when the walking speed increased. This finding was not consistent with Hsiang and Chang (2002). The result of their study showed that with a regular backpack the peak push-off force significantly increased with an increased walking speed. The inconsistency between the two studies appears to be mainly due to the effect of the mechanism of the suspend-load backpack. Based on the inverted pendulum model of human walking, the center of gravity of a human reaches the lowest position and the vertical ground reaction force reaches the maximum during the double support phase. With a conventional backpack the movement of the fixed load in the backpack is roughly in-phase with the movement of the torso, and the downward force exerted by the load also reaches the maximum during the double support phase. However, the suspended load has a phase shift from the movement of the torso due to the friction of the spring-damper system. This phase shift may defer the maximum force transferred from the load to the torso, which in consequence reduces the peak push-off force. This result supports the suggestion of Kuo (2005) that the suspended-load backpack can reduce the energy cost of muscles during the step-to-step transition of human walking.

Finally, the effect of a suspended-load backpack on NWAF and NMSF and the effect of the walking speed on all kinetic variables are in agreement with the findings of

Hsiang and Chang (2002). Because the friction was not controlled in the current research, little can be discussed about the effect of changing the phase shift on the kinetic variables.

6.4 Limitations

There are a number of limitations of the current study that limit the generalization of the results. First, the model was constructed based on the anthropometric data and ignored the inter-subject variability among each individual. For example, from one subject to another, the ratio of leg length to stature or the gait pattern may be different. Thus, the model only yields a rough estimate of torso movement rather than an accurate value.

A second limitation factor is that based on the inverted pendulum model the locus of CoM is successive arcs rather than a perfect sinusoidal curve. The curve in the double support phase is not as smooth as that in the single support phase. Since the input of the backpack system has little deviation from a purely sinusoidal oscillation, the prediction of load velocity with the base excitation model may vary from the actual value.

The third limitation of this work is that the suspended-load backpack used in the experiment was not a pure time-invariant second order system. The spring stiffness and damping coefficient tend to change during the load oscillating because of the swing of the torso and the abrasion of the Teflon bushing. Figure 45 represents the phase plots of the movement of a subject's CoG and the corresponding movement of the backpack in a gait cycle. Based on Equation 2-11, if the system is time-invariant, the phase shift (the difference on the phase angles between the two phase plots) should be a constant. Figure 46 demonstrates that although the movement of CoG always leads the movement of the backpack, the phase shift in the gait cycle keeps changing over time. This indicates the

system is time-variant. However, it would be very challenging to exactly determine how these parameters change over time.

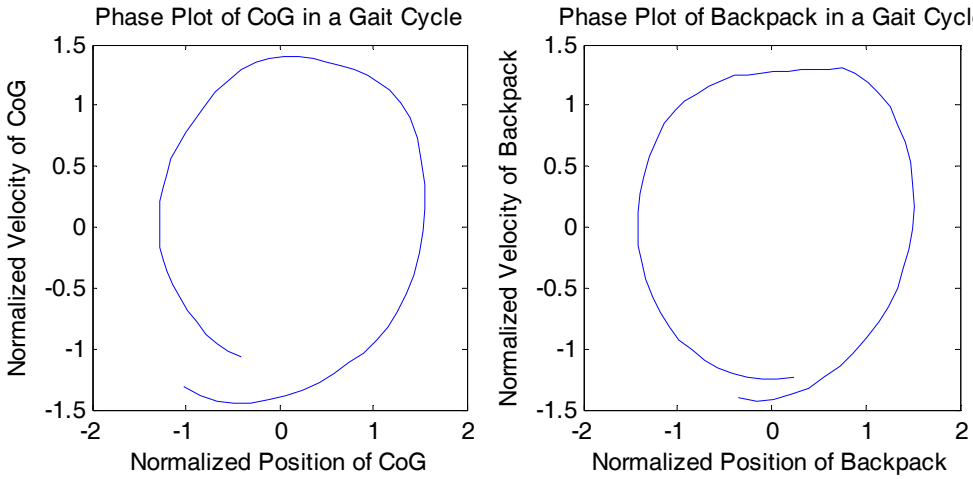

Figure 45 The phase plots of the movement of CoG and the corresponding movement of the load in a gait cycle. All values were subtracted by the mean value and then divided by the standard deviation of the trial (the original data were transformed to their z-score)

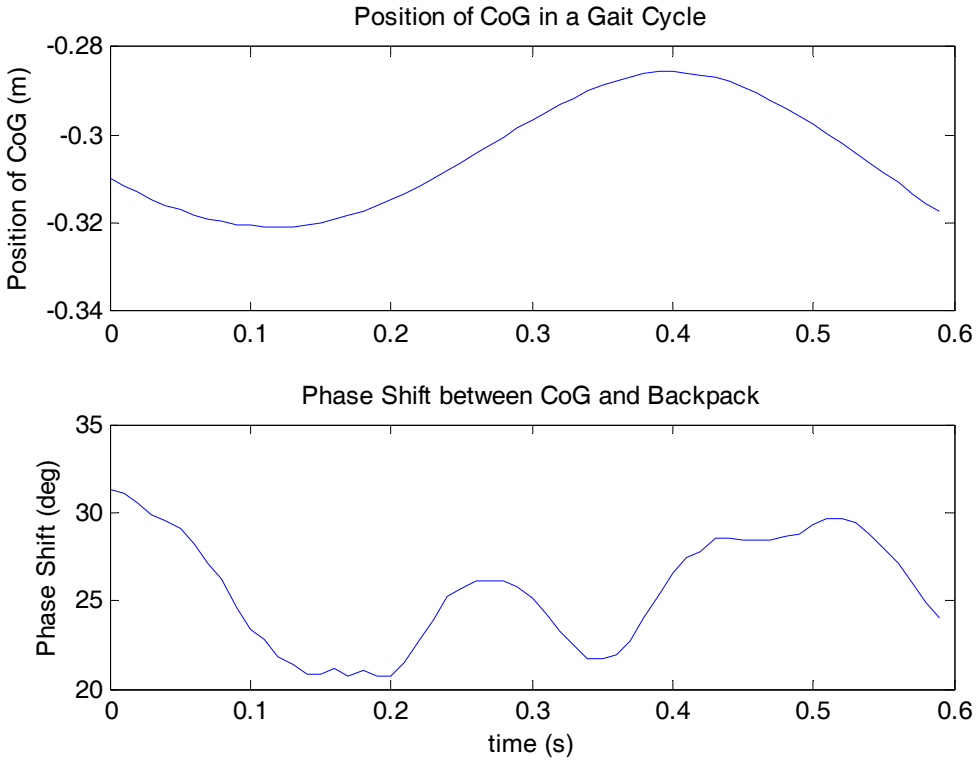

Figure 46 The phase shift between CoG and backpack. For comparison, the corresponding movement of CoG is plotted above the phase shift plot

The last limitation is that the load velocity may not represent the output energy very well. Once the mechanical energy is transferred to electrical energy, the resistance of the generator will influence the movement of the mass. The lighter the load is, the stronger it is influenced. In that case, the load weight also needs to be considered as an index for representing energy. Consequently, it should be noted that all the limitations mentioned here result in the reduction of the predictability of the model.

6.5 Future research

Extending this basic research, future studies should investigate the following areas. To use such suspended-load backpacks in industrial applications, the interaction between the power generator and the suspending load should be considered, and how this interaction influences the human walking pattern needs to be investigated. Since the output power may need to be modified frequently, the backpack frame should be redesigned so that the stiffness and the damping coefficient can be replaced easily.

In the current research, only 5 of 6 walking determinants were considered. Since it is unclear whether the lateral swing (the 6^{th} determinant) of the torso is beneficial for energy scavenging, the effect of it should be examined.

In addition, because the suspended-load backpack is a novel invention, very few, if any, research studies have focused on it. Thus, some conventional study, such as investigating the effect of fatigue and training, should also be considered. In terms of gait pattern, future research directions should include study on the sensitivity of gait parameters to the stiffness and damping ratio of the suspended load.

7 Conclusion

A century ago, Frank and Lilian Gilbreth (1916) said "…that organization is best that has the best quality of workers. No organization can continue to be of first quality whose workers are over-fatigued". Since then, the main two objectives of ergonomist are to enhance the effectiveness of the work and to improve the working condition, including safety (Sanders and McCormick, 1993). When these two objectives cannot be satisfied at the same time, the balance between them needs to be determined so that the overall benefit can be maximized. With these ergonomics principles in mind, the main purposes of this research were to build a model on a suspended-load backpack to 1) predict the amount of the scavenged energy and the GRF, and 2) to find the trade-off between them.

The results showed that the relative velocity between the load and the frame, as an index of power generation, was influenced by many variables. Specifically, for an individual load carrier with a particular suspended-load backpack, the load velocity was mainly influenced by the walking speed and the load weight. Although it was observed that the load velocity increased approximately linearly with faster walking speed and heavier load weight, the model indicated that the relationship may be non-monotonic and it depended on the damping coefficient. On the other hand, the model revealed that the peak GRF was also a function of the walking speed and the load weight. The function contour of peak GRF is similar but not exactly the same as that of the load velocity. Thus, NLP can help find the trade-off between the output energy and the GRF. Findings in the present study provide some quantitative insights into the mechanism of the suspended-load backpack and may help configure the backpack for the task with a specific energy requirement or peak GRF limit.

This study also investigated the effect of the suspended-load backpack on gait pattern. Based upon the findings, the following conclusions may be drawn. First, similar to the effect of a fixed load, the suspended-load changed the temporal variables of gait parameters in order to maintain the walking stability. Second, the suspended-load backpack impacted the gait pattern in different ways than a conventional backpack in terms of the kinetic variables. It is recommended that when applying the suspended-load backpack to energy scavenging, it is necessary to consider how the oscillating load influences the way of human walking.

In summary, this study has accomplished the proposed objectives and made the following contributions:

- A physical model was developed for depicting human carrying a suspended-load backpack during walking based on the nature of the human gait and the backpack.
- With known gait parameters and the mechanical configuration of the backpack, the amount of the scavenged energy and the GRF can be predicted through the proposed model.
- When the lower limit on scavenged energy is known, the minimum GRF can be found by applying NLP on the model in order to improve the safety.
- When the upper limit on the GRF is known, the maximum scavenged energy can be found by applying NLP on the model in order to improve the productivity.

8 References

Alexander, R. M. (1976). "Mechanics of bipedal locomotion." Perspectives in experimental biology **1**: 493-504.

Alexander, R. M. (1980). "Optimum walking techniques for quadrupeds and bipeds." Journal of Zoology (London) **192**(1): 97-117.

Alexander, R. M. (1992). "A Model of Bipedal Locomotion on Compliant Legs." Philosophical Transactions of the Royal Society of London Series B-Biological Sciences **338**(1284): 189-198.

Alexander, R. M. (1995). "Simple Models of Human Movement." Applied Mechanics Reviews **48**(8): 461-469.

Andriacchi, T. P., J. A. Ogle, et al. (1977). "Walking Speed as a Basis for Normal and Abnormal Gait Measurements." Journal of Biomechanics **10**(4): 261-268.

Attwells, R. L., S. A. Birrell, et al. (2006). "Influence of carrying heavy loads on soldiers' posture, movements and gait." Ergonomics **49**(14): 1527-1537.

Bloom, D. and A. P. Woodhull-McNeal (1987). "Postrual adjustments while standing with two types of loaded backpack." Ergonomics **30**(10): 1425-1430.

Bobet, J. and R. W. Norman (1984). "Effects of Load Placement on Back Muscle-Activity in Load Carriage." European Journal of Applied Physiology and Occupational Physiology **53**(1): 71-75.

Cappozzo, A. (1981). "Analysis of the Linear Displacement of the Head and Trunk During Walking at Different Speeds." Journal of Biomechanics **14**(6): 411-425.

Charteris, J. (1998). "Comparison of the effects of backpack loading and of walking speed on foot-floor contact patterns." Ergonomics **41**(12): 1792-1809.

Clauser, C. E., J. T. McConville, et al. (1969). Weight, volume, and center of mass of segments of the human body. Dayton, Ohio, Aerospace medical research laboratory.

Datta, S. R. and N. L. Ramanathan (1971). "Ergonomic comparison of seven modes of carrying loads on the horizontal plane." Ergonomics **14**(2): 269-278.

Evans, W. J., F. R. Winsmann, et al. (1980). "Self-Paced Hard Work Comparing Men and Women." Ergonomics **23**(7): 613-621.

Gard, S. A., S. C. Miff, et al. (2004). "Comparison of kinematic and kinetic methods for computing the vertical motion of the body center of mass during walking." Human Movement Science **22**(6): 597-610.

Gilbreth F. B. and L. M. Gilbreth (1916). Fatigue Study. New York, NY, Sturgis & Walton Company.

Grieve, D. W. and R. J. Gear (1966). "Relationships between Length of Stride Step Frequency Time of Swing and Speed of Walking for Children and Adults." Ergonomics **9**(5): 379-&.

Haisman, M. F. (1988). "Determinants of Load Carrying Ability." Applied Ergonomics **19**(2): 111-121.

Harman, E., K. H. Han, et al. (1992). "The Effects of Gait Timing Kinetics and Muscle Activity of Various Loads Carried on the Back." Medicine and Science in Sports and Exercise **24**(5 SUPPL): S129.

Holewijn, M. and W. A. Lotens (1992). "The Influence of Backpack Design on Physical Performance." Ergonomics **35**(2): 149-157.

Hsiang, S. M. and C. C. Chang (2002). "The effect of gait speed and load carrying on the reliability of ground reaction forces." Safety Science **40**(7-8): 639-657.

Inman, D. J. (2001). Engineering Vibration. Upper Saddle River, Prentice-Hall.

Inman, R. T., H. J. Ralston, et al. (2006). Human Locomotion. Human Walking. J. Rose and J. G. Gamble. Philadelphia, PA, Lippincott Williams & Wilkins.

Inman, V. T. (1966). "Human Locomotion." Canadian Medical Association Journal **94**(20): 1047-1054.

Kay, B. A. and W. H. Warren (1998). A dynamical model of the coupling between posture and gait. Timing of Behavior. D. A. Rosenbaum and C. E. Collyer. Cambridge, The MIT Press**:** 293-322.

Kinoshita, H. (1985). "Effects of Different Loads and Carrying Systems on Selected Biomechanical Parameters Describing Walking Gait." Ergonomics **28**(9): 1347-1362.

Knapik, J., E. Harman, et al. (1996). "Load carriage using packs: A review of physiological, biomechanical and medical aspects." Applied Ergonomics **27**(3): 207-216.

Kram, R. (1991). "Carrying Loads with Springy Poles." Journal of Applied Physiology **71**(3): 1119-1122.

Kuo, A. D. (2005). "Harvesting energy by improving the economy of human walking." Science **309**(5741): 1686-1687.

Lamoreux, L. W. (1971). "Kinematic measurements in the study of human walking." Bulletin of prosthetics research **10-15**: 3-84.

Legg, S. J. and A. Mahanty (1985). "Comparison of Five Modes of Carrying a Load Close to the Trunk." Ergonomics **28**(12): 1653-1660.

Levine, L., W. J. Evans, et al. (1982). "Prolonged Self-Paced Hard Physical Exercise Comparing Trained and Untrained Men." Ergonomics **25**(5): 393-400.

Mann, R. A. and J. Hagy (1980). "Biomechanics of Walking, Running, and Sprinting." American Journal of Sports Medicine **8**(5): 345-350.

Martin, P. E. and R. C. Nelson (1986). "The Effect of Carried Loads on the Walking Patterns of Men and Women." Ergonomics **29**(10): 1191-1202.

McGeer, T. (1990). "Passive Dynamic Walking." International Journal of Robotics Research **9**(2): 62-82.

McMahon, T. A. and G. C. Cheng (1990). "The Mechanics of Running - How Does Stiffness Couple with Speed." Journal of Biomechanics **23**: 65-78.

Mochon, S. and T. A. McMahon (1980a). "Ballistic Walking." Journal of Biomechanics **13**(1): 49-57.

Mochon, S. and T. A. McMahon (1980b). "Ballistic Walking - an Improved Model." Mathematical Biosciences **52**(3-4): 241-260.

Murray, M. P., A. B. Drought, et al. (1964). "Walking Patterns of Normal Men." Journal of Bone and Joint Surgery-American Volume **46**(2): 335-360.

Obusek, J. P., E. A. Harman, et al. (1997). "The relationship of backpack center of mass location to the metabolic cost of load carriage." Medicine and Science in Sports and Exercise **29**(5 SUPPL.): S205.

Paradiso, J. A. and T. Starner (2005). "Energy scavenging for mobile and wireless electronics." Ieee Pervasive Computing **4**(1): 18-27.

Pascoe, D. D. and D. E. Pascoe (1999). "Bookbags help to shoulder the burden of school work." Teaching elementary physical education **10**: 18-20.

Perry, J. (1992). Gait Analysis. Thorofare, NJ, SLACK Incorporated.

Pierrynowsi, M. R., R. W. Norman, et al. (1981). "Mechanical Energy Analyses of the Human During Load Carriage on a Treadmill." Ergonomics **24**(1): 1-14.

Ren, L., R. K. Jones, et al. (2005). "Dynamic analysis of load carriage biomechanics during level walking." Journal of Biomechanics **38**(4): 853-863.

Roebuck, J. A., K. H. E. Kroemer, et al. (1975). Engineering anthropometry methods. New York, Wiley-interscience.

Rome, L. C., L. Flynn, et al. (2005). "Generating electricity while walking with loads." Science **309**(5741): 1725-1728.

Rose, J. and J. G. Gamble (2006). Human Walking. Philadelphia, PA, Lippincott Williams & Wilkins.

Sanders, M. S. and E. J. McCormick (1993). Human Factors in Engineering and Design. New York, NY, McGraw-Hill.

Saunders, J., V. T. Inman, et al. (1953). "The Major Determinants in Normal and Pathological Gait." Journal of Bone and Joint Surgery-American Volume **35-A**(3): 543-558.

Selles, R. W., J. B. J. Bussmann, et al. (2001). "Comparing predictive validity of four ballistic swing phase models of human walking." Journal of Biomechanics **34**(9): 1171-1177.

Shenck, N. S. and J. A. Paradiso (2001). "Energy scavenging with shoe-mounted piezoelectrics." Ieee Micro **21**(3): 30-42.

Smith, B., K. M. Ashton, et al. (2006). "Influence of carrying a backpack on pelvic tilt, rotation, and obliquity in female college students." Gait & Posture **23**(3): 263-267.

Smith, K. U., C. D. McDermid, et al. (1960). "Analysis of the temporal components of motion in human gait." American Journal of Physical Medicine **39**: 142-151.

Soule, R. G., K. B. Pandolf, et al. (1978). "Energy-Expenditure of Heavy Load Carriage." Ergonomics **21**(5): 373-381.

Srinivasan, M. and A. Ruina (2006). "Computer optimization of a minimal biped model discovers walking and running." Nature **439**(7072): 72-75.

Starner, T. (1996). "Human-powered wearable computing." Ibm Systems Journal **35**(3-4): 618-629.

Stuempfle, K. J., D. G. Drury, et al. (2004). "Effect of load position on physiological and perceptual responses during load carriage with an internal frame backpack." Ergonomics **47**(7): 784-789.

Thorstensson, A., J. Nilsson, et al. (1984). "Trunk movement in human locomotion." Acta Physiologica Scandinavica **121**: 9-22.

Wang, Y. T., D. D. Pascoe, et al. (2001). "Evaluation of book backpack load during walking." Ergonomics **44**(9): 858-869.

White, H. J. and S. Tauber (1969). System Analysis, W. B. Saunders Company.

Whittle, M. W. (1996). Gait Analysis An Introduction. Oxford, Butterworth-Heinemann.

Winter, D. A. (1991). The Biomechanics and Motor control of Human Gait. Waterloo, Ontario, Unversity of Waterloo Press.

Appendix

9 Appendices

9.1 Appendix A The Predicted Peak Relative Velocity and Peak GRF with Different Damping Coefficient

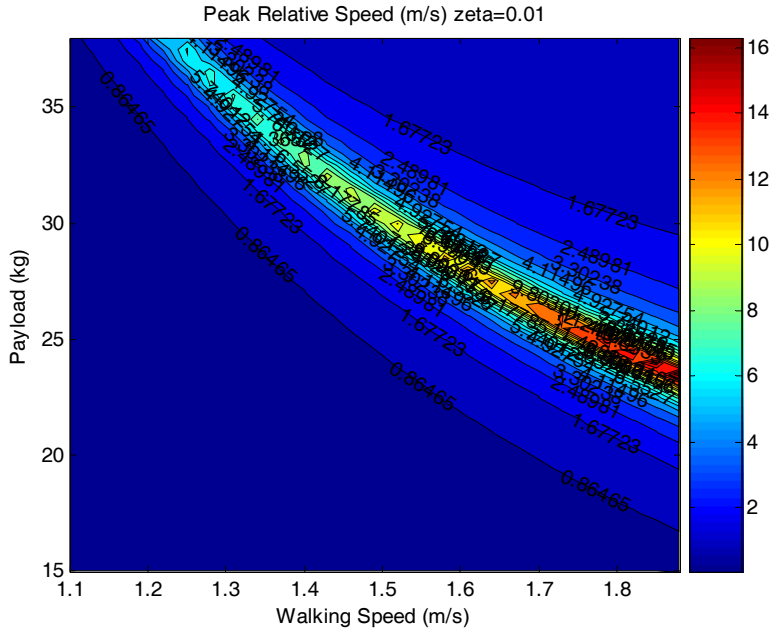

Figure 47 The predicted peak relative velocity for different payload mass and walking speed with damping coefficient = 0.01

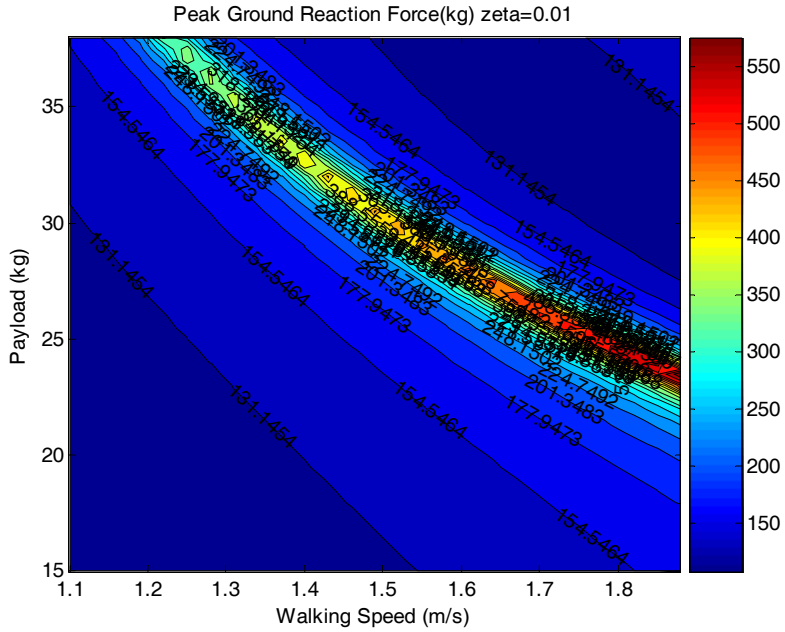

Figure 48 The predicted GRF for different payload mass and walking speed with damping coefficient = 0.01

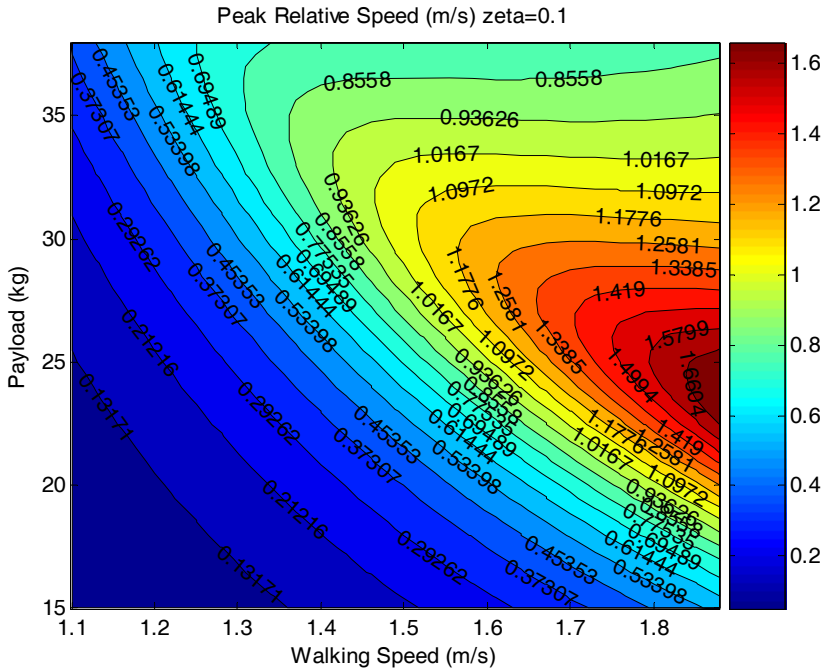

Figure 49 The predicted peak relative velocity for different payload mass and walking speed with damping coefficient = 0.1

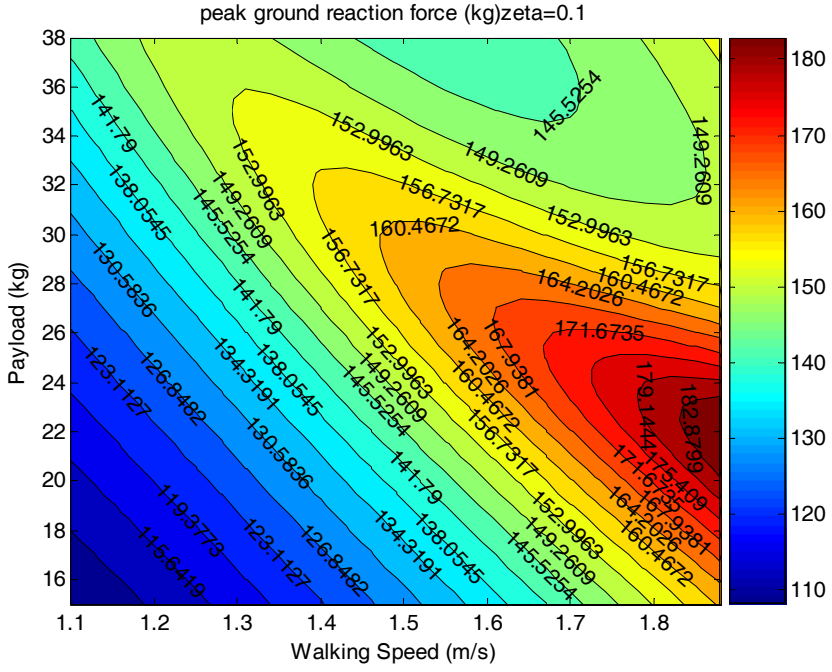

Figure 50 The predicted GRF for different payload mass and walking speed with damping coefficient = 0.1

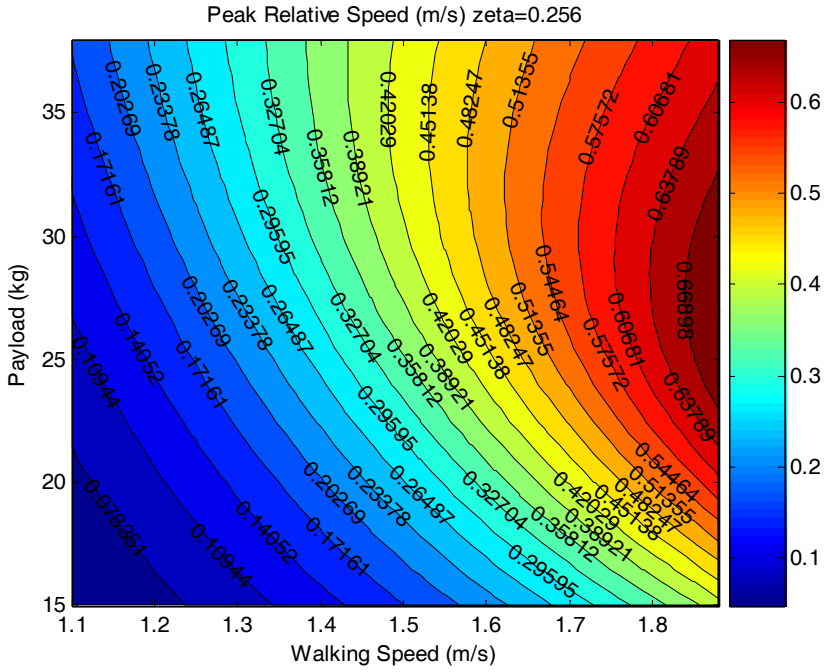

Figure 51 The predicted peak relative velocity for different payload mass and walking speed with damping coefficient = 0.256

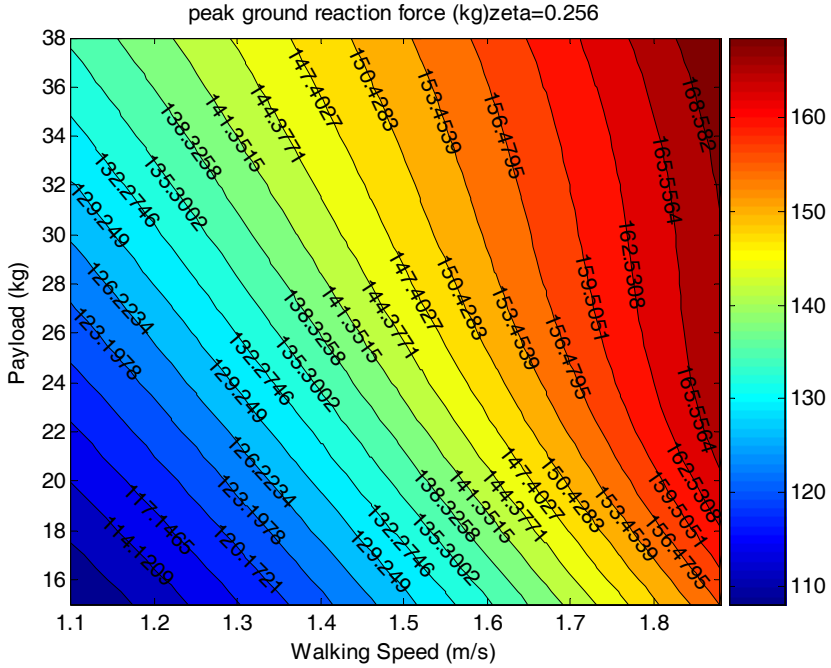

Figure 52 The predicted GRF for different payload mass and walking speed with damping coefficient = 0.256

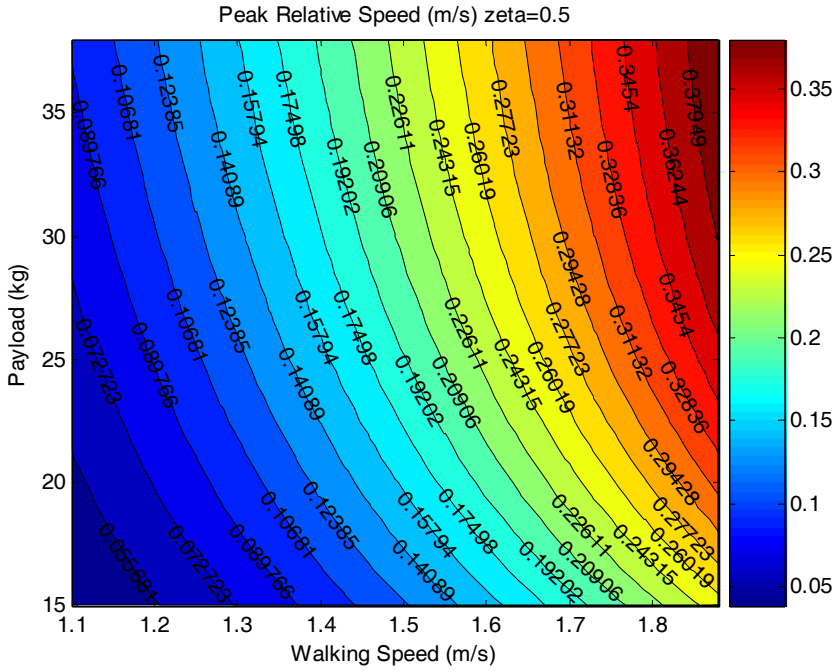

Figure 53 The predicted peak relative velocity for different payload mass and walking speed with damping coefficient = 0.5

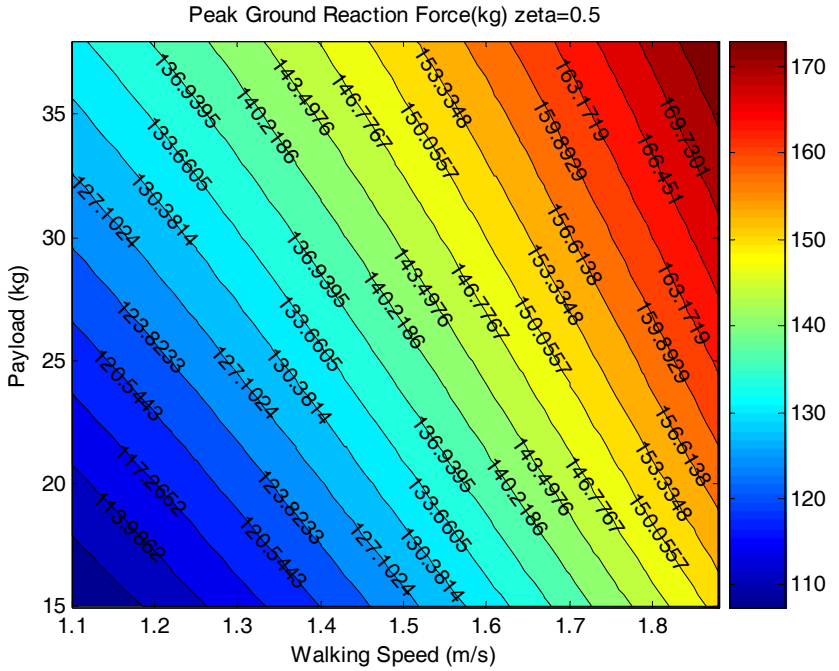

Figure 54 The predicted GRF for different payload mass and walking speed with damping coefficient = 0.5

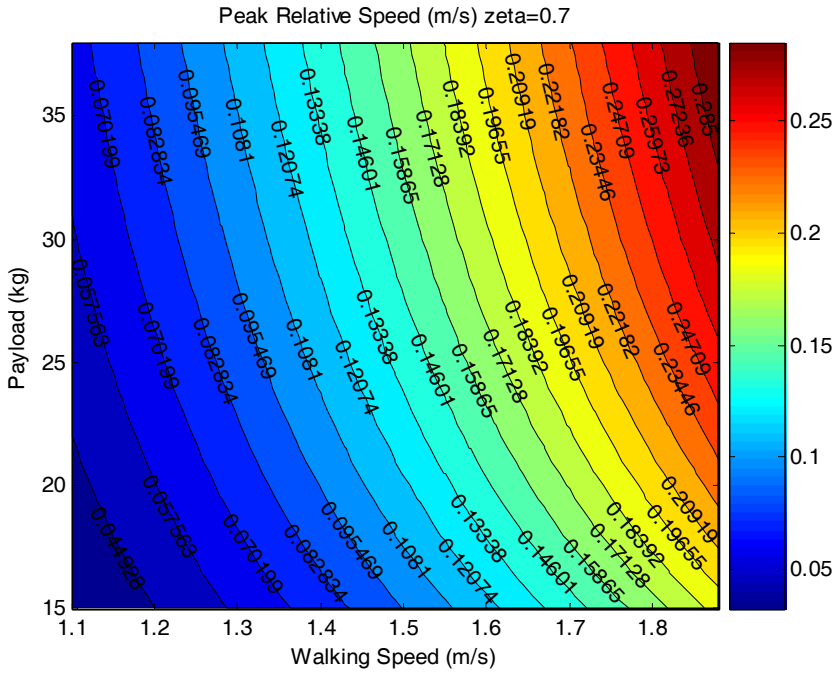

Figure 55 The predicted peak relative velocity for different payload mass and walking speed with damping coefficient = 0.7

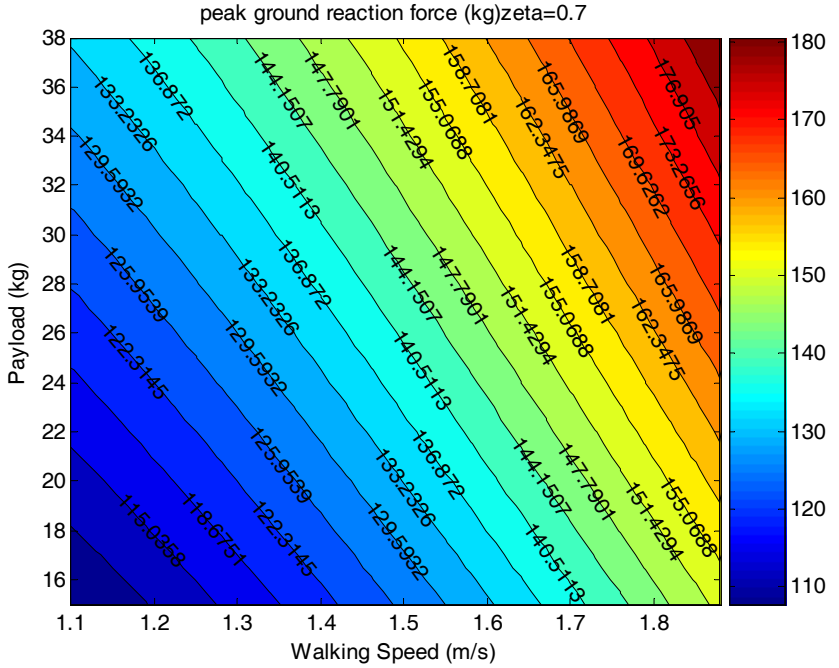

Figure 56 The predicted GRF for different payload mass and walking speed with damping coefficient = 0.7

9.2 Appendix B ANOVA Assumption

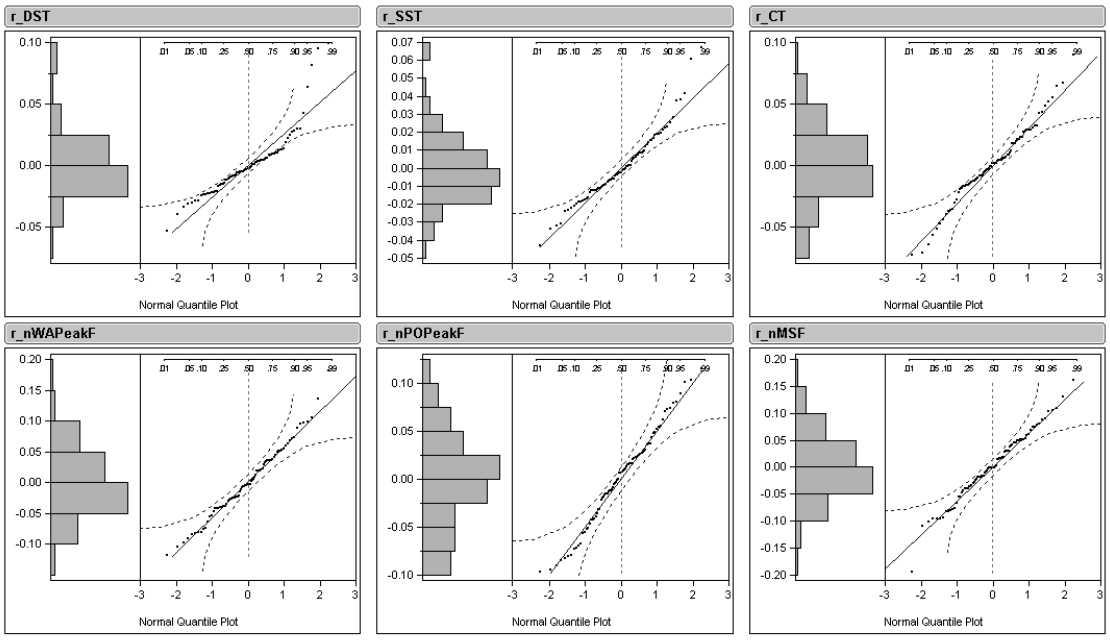

Figure 57 The normal quantile plot of the residuals for the dependent variables

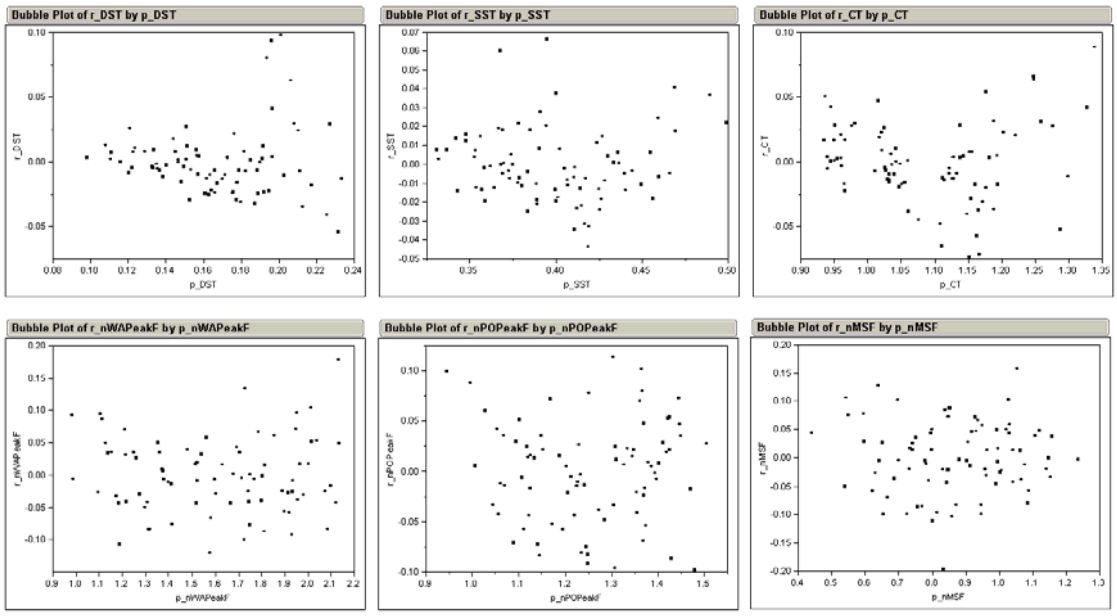

Figure 58 The scatter plot of the residuals vs. the predicted values of the dependent variables

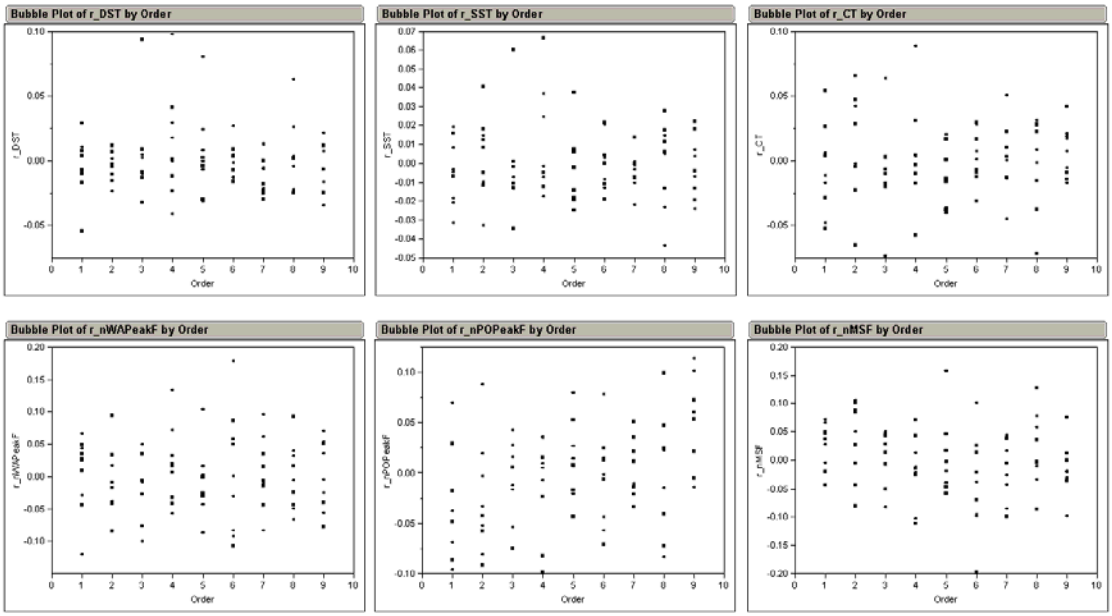

Figure 59 The scatter plot of the residuals to test the independence between trials for the dependent variables

9.3 Appendix C Frequency Domain Properties

All figures below demonstrate the frequency domain properties of the

system: $G(s) = \dfrac{152s + 4027}{20s^2 + 152s + 4027}$

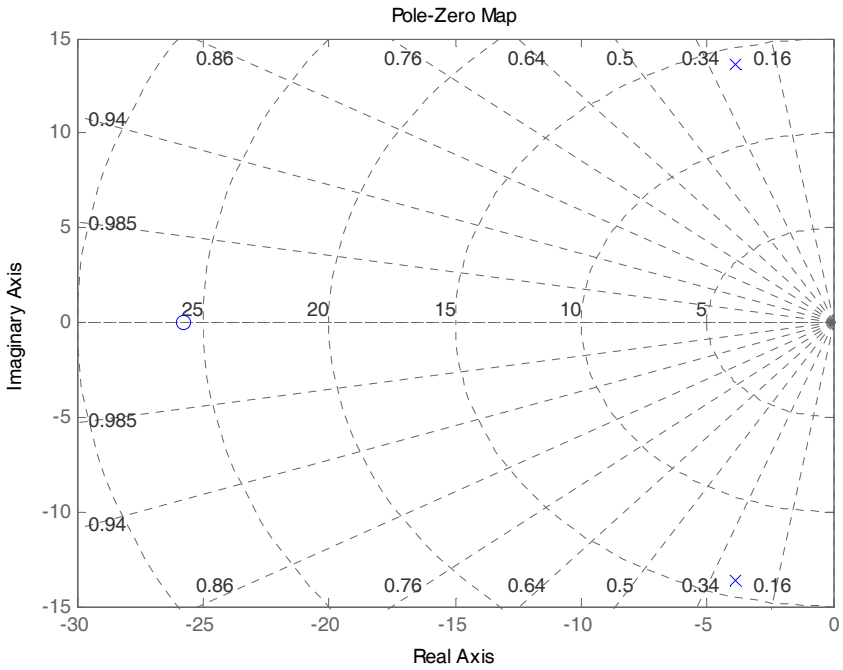

Figure 60 Pole-zero map of the backpack system

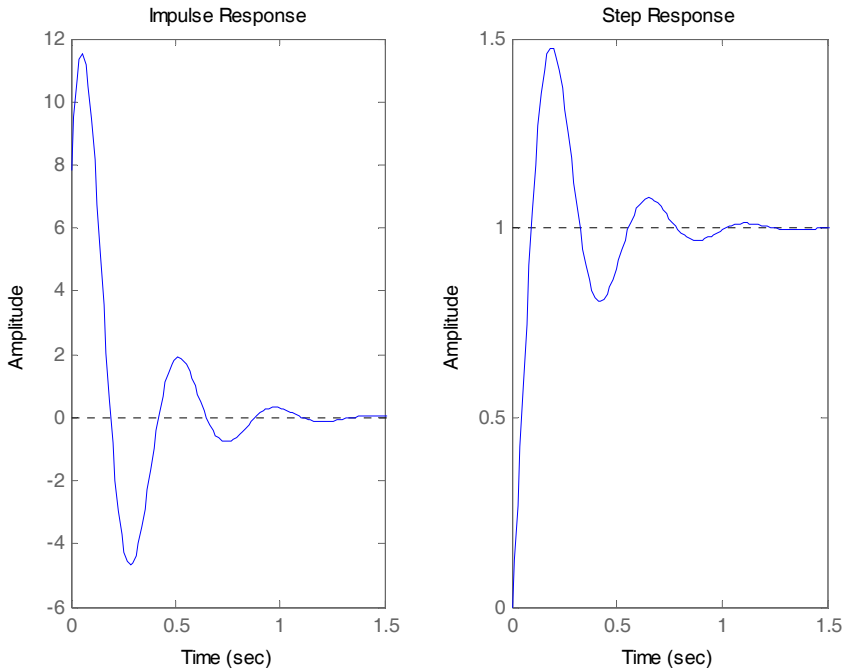

Figure 61 Impulse response and step response of the backpack system

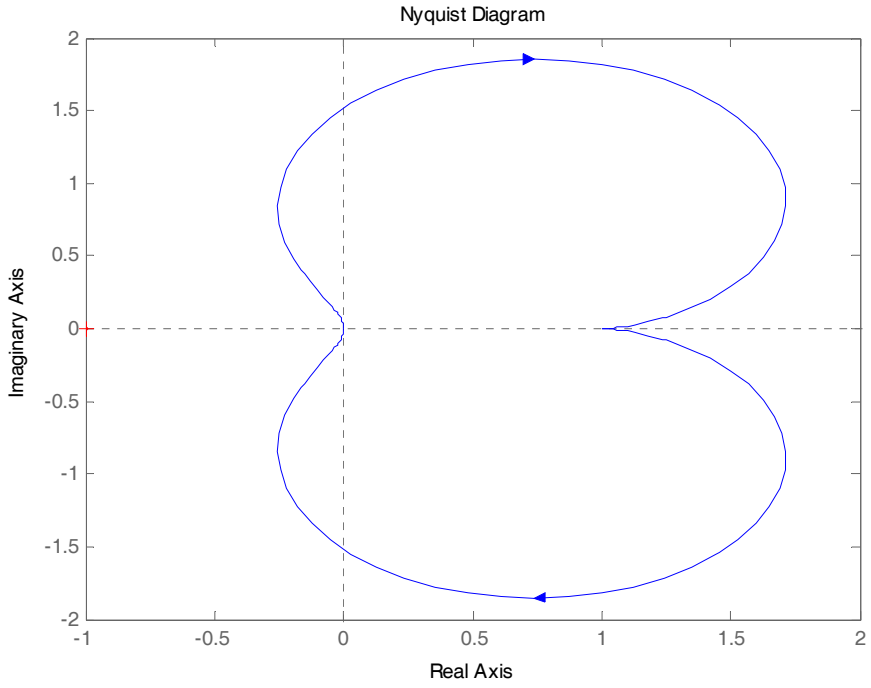

Figure 62 Nyquist plot of the backpack system

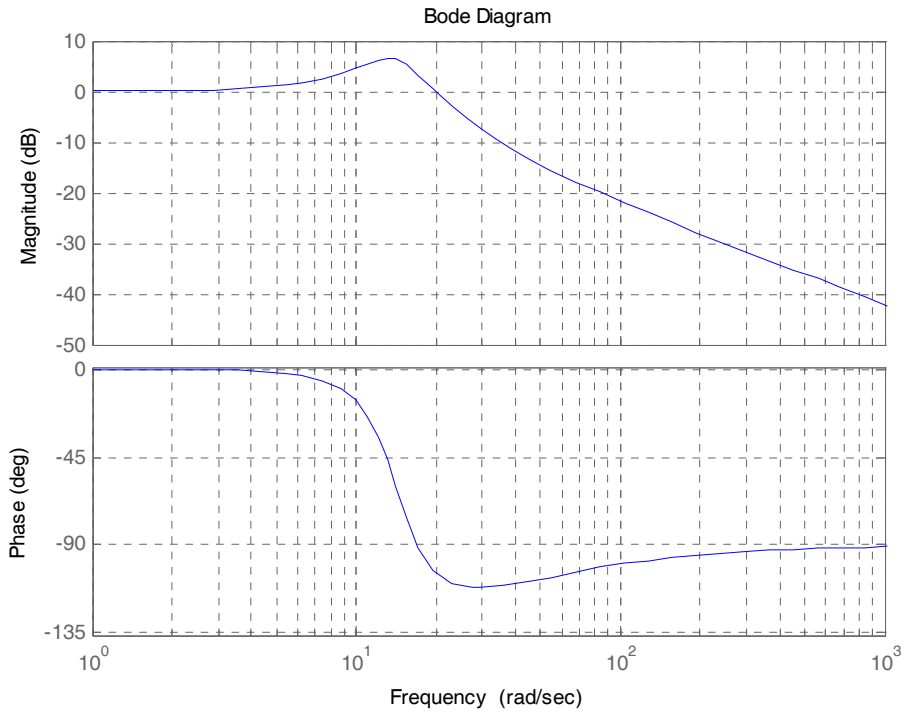

Figure 63 Bode plot of the backpack system

9.4 Appendix D Informed Consent Form

North Carolina State University
INFORMED CONSENT FORM for RESEARCH

Title of Study: **Evaluation of Suspended-load Backpack during Human Walking**

Principal Investigator: Xu Xu Faculty Sponsor: Dr. Simon Hsiang

We are asking you to participate in a research study. The purpose of this study is to investigate how walking speed and payload mass influence the amount of energy generated by the suspended-load backpack. You should not participate in this study if you have any chronic or current problems/discomfort in your back and upper extremity. If you do NOT have such an injury or disease, please initial here: _____.

INFORMATION
If you agree to participate in this study, you will be asked to do the following tasks.

1. You will be asked to do light warm-up and stretching exercises to prepare the muscles involved in the experiment (5 min).
2. Several measurements will be recorded including your age, height, weight, shoulder height, and leg length. Then all of the following procedures will be videotaped for data analysis.
3. Before the experimental session, the suspended-load backpack will be put on your back and the shoulder belts and hip belt will be fastened to eliminate the movement between the trunk and the backpack frame. To let you get familiar with the treadmill, you will be asked to walk on the treadmill with 1.16 m/s, 1.43 m/s and 1.70 m/s for 1 minute. The preferred cadence for different walking speeds will be recorded and used as the reference during the experiment.
4. A flock of bird sensors that can monitor positional coordinates and orientation angles will be mounted on your center of gravity (around the bottom of the sternum) by using an elastic belt. Another three sensors will be mounted on the backpack frame.
5. In the task, you will be asked to walk on the treadmill with 3 different load levels (0 kg, 15.9 kg, and 22.7 kg) and 3 different walking speeds (1.16 m/s, 1.43 m/s and 1.70 m/s). Thus, there will be 9 conditions (3 payload mass X 3 walking speed = 9 conditions) in this experiment. Each condition will be performed 1.5 minute. To reduce the effect of fatigue, there will be a five-minute break between each trial.
6. Total for your participation time is 2 hours approximately.

RISKS
Since the tasks need some physical exertion with load carrying, there might be residual muscle soreness for several days after the experiment due to the physical nature of the muscle. There also is a smaller risk of more serious injury to the musculoskeletal system, such as back fatigue, knee pain, foot blister, and rucksack palsy (rucksack palsy is due to the straps of a heavy backpack compressing the nerve and may lead to numbness in the hands). To prevent risks, warm-up and stretching period will be given prior to experiments and frequent rest breaks will be given between each trial. The total load-carrying time for each is limited within 15 minutes to reduce the risks. If at any time during the experiment you feel pain/ discomfort, let the researchers know and we will stop the experiment.

BENEFITS
You will receive an ErgoLab T-shirt. You may also derive some indirect benefits including an understanding of ergonomics research method.

CONFIDENTIALITY
The information in the study records will be kept strictly confidential. Subject's data will be recorded only with an assigned ID number. The list of the subjects' name, numbers and corresponding videotapes will be

locked in a cabinet in the lab. All electronic data and ID numbers will be stored in a computer protected by the password which is only known by researchers. The purpose of keeping the list and videotape is that in case there is a problem with a set of data, we can contact that subject to see if s/he is willing to help figure out the problem, or we can review the videotape to figure out the problem. No reference will be made in oral or written reports which could link the subjects to the study. After completion of data analysis, all written record, electronic data and videotape will be destroyed.

EMERGENCY MEDICAL TREATMENT (if applicable)
There is no provision for free medical care for you in the event that you are injured during the course of this study. In the event of an emergency, the researcher will contact the Student Health Service (for students only) medical services at 515-3333 for necessary care or through the 911 emergency response service.

CONTACT
If you have questions at any time about the study or the procedures, you may contact Dr. Simon Hsiang, at 437 DANIELS HALL, or 919-513-7208. If you feel you have not been treated according to the descriptions in this form, or your rights as a participant in research have been violated during the course of this project, you may contact Dr. David Kaber, Chair of the NCSU IRB for the Use of Human Subjects in Research Committee, Box 7514, NCSU Campus (919-515-3086) or Mr. Matthew Ronning, Assistant Vice Chancellor, Research Administration, Box 7514, NCSU Campus (919-513-2148).

PARTICIPATION
Your participation in this study is voluntary; you may decline to participate without penalty. If you decide to participate, you may withdraw from the study at any time without penalty and without loss of benefits to which you are otherwise entitled. If you withdraw from the study before data collection is completed your data will be returned to you or destroyed at your request.

CONSENT
"I have read and understand the above information. I have received a copy of this form. I agree to participate in this study with the understanding that I may withdraw at any time."

Subject's signature_____ **Date** _____

Investigator's signature_____ **Date** _____

9.5 Appendix E Matlab Code

```
function [pGF mGF oGF1 Y X relV r]=backpack5_Y(x,k,zeta,m_body,L)
%for calculate fmean fosc Y, NOT for fmincon
%x(1)~m (kg)
%x(2)~V (m/s)
%k~stiffness coefficient of the springs
%L0~leg length
%Y~vertcial displacement of base
%X~vertical displacement of backpack
%relV~relative speed between frame and payload, along the frame
%w~base excitation frequency (rad)

Y=body_amp(x(2),L); %get the amplitude of CoM, vertical, viz. Y(t) in
base excitation model
%Y=Y1*cos(30/180*pi);%get the amplitude along the frame

%Y=0.0171;

w=walk_freq(x(2));%get walking frequency
r=w/sqrt(k/x(1));%displacement ratio

%Calculate phase shift
theta1=atan(2*zeta*r/(1-r^2));
if theta1<0
    theta1=theta1+pi;
end
theta2=atan(1/(2*zeta*r));

%Calculate the amplitude of backpack, vertical, viz. X(t) in base
%excitation model
X1=Y*(cos(30/180*pi))^2*(((1+4*zeta^2*r^2)/((1-
r^2)^2+4*zeta^2*r^2))^(1/2));
X2=Y*(sin(30/180*pi))^2;
X=sqrt(X1^2+X2^2-2*X1*X2*cos(theta1+theta2+pi/2));

%Calculate peak relative velocity,along the frame
%phase shift on position is -theta1-theta+pi/2
%phase shift on velocity is -theta1-theta-pi/2
%using pi-(phase shift) in law of cosines for vector summation
relV1=-w*Y*cos(30/180*pi)*((1+4*zeta^2*r^2)/((1-
r^2)^2+4*zeta^2*r^2))^(1/2);
relV2=-w*Y*cos(30/180*pi);
% relV=Y*cos(30/180*pi)*x(1)*w^3/(k-x(1)*w^2);
relV=sqrt(relV1^2+relV2^2-2*relV1*relV2*cos(theta1+theta2-pi/2));

%Calculate the ground reaction force due to the oscillation
oGF1=k*Y*r^2*cos(30/180*pi)*cos(30/180*pi)*((1+4*zeta^2*r^2)/((1-
r^2)^2+4*zeta^2*r^2))^(1/2); %Force due to weight oscillation
oGF2=Y*(m_body+6.7+x(1)*sin(30/180*pi)*sin(30/180*pi))*w^2;%Force due
to acceleration
oGF=sqrt(oGF1^2+oGF2^2-2*oGF1*oGF2*cos(theta1+theta2+pi/2));
```

```
%Calculate peak ground reaction force
pGF=(oGF+...
    +x(1)*9.8...                %Force due to load weight
    +9.8*(m_body+6.7))/9.8;      %Force due to fixed load (body weight
and frame weight)


%Calculate mean ground reaction force
mGF=x(1)*9.8+(m_body+6.7)*9.8;

    function w=walk_freq(V)
        w=(1.504*(V/(L*0.53))^0.57)*60/60*2*pi;
    end

    function Y=body_amp(V,L)
        L0=L*0.53;
        Y=L0/2*(1-(1-(0.963*pi*V/( L0*walk_freq(V)))^2)^(1/2))-
0.0157*L0;
    end

end
```

```
clear

%NLP, calculate the minimum peak GRF, given energy output
options=optimset;
opt1=optimset(options,'TolCon',1e-5,'TolX',1e-8,'MaxFunEvals',100000,...
    'MaxIter',100000,'LargeScale','off');

k=4650;L0=0.94;m_body=74.3;zeta=0.256;L=1.76;
[x,fval]=fmincon(@(x)backpack_MinGRFNLP(x,k,zeta,m_body,L),[20,1.463]',
[],[],[],[],...

[11.36;1.1],[30;1.82],@(x)backpack_MinGRFcon(x,k,zeta,m_body,L),opt1)


function pGF=backpack_MinGRFNLP(x,k,zeta,m_body,L)
[pGF1 mGF oGF1 Y X relV r]=backpack5_Y(x,k,zeta,m_body,L);
pGF=pGF1;


function relV=backpack_NLPcon(x,k,zeta,m_body,L)
[pGF mGF oGF1 Y X relV1 r]=backpack5_Y(x,k,zeta,m_body,L);
relV=relV1;


function [c,ceq]=backpack_MinGRFcon(x,k,zeta,m_body,L)
%constraint function on output power
%x(1)~load weight (kg)
%x(2)~walking speed (m/s)
%k~stiffness coefficient of the springs
%L~body height
%L0~leg length
L0=0.53*L;
Y=body_amp(x(2),L0); %get the amplitude of CoM, viz. Y(t) in base
excitation model
w=walk_freq(x(2));%get walking frequency

c=[x(1)-1000];%inequalility constraint
ceq=[0.352-0.707*backpack_NLPcon(x,k,zeta,m_body,L)];%equalility
constraint on output power

    function w=walk_freq(V)
        w=round((1.504*(V/L0)^0.57)*60)/60*2*pi;
    end

    function Y=body_amp(V,L)

        Y=L0/2*(1-(1-(0.96*pi*V/( L0*walk_freq(V) ))^2)^(1/2))-
0.0157*L0;
    end
end
```

```
clear

%NLP, calculate the maximum energy output, given peak GRF
options=optimset;
opt1=optimset(options,'TolCon',1e-5,'TolX',1e-8,'MaxFunEvals',100000,...
    'MaxIter',100000,'LargeScale','off');

k=4650;L0=0.94;m_body=74.3;zeta=0.256;L=1.76;
[x,fval]=fmincon(@(x)backpack_MaxRVNLP(x,k,zeta,m_body,L),[20,1.463]',[
],[],[],[],...
    [11.36;1.1],[30;1.82],@(x)backpack_MaxRVcon(x,k,zeta,m_body,L),opt1)

function relV=backpack_MaxRVNLP(x,k,zeta,m_body,L)
[pGF mGF oGF1 Y X relV1 r]=backpack5_Y(x,k,zeta,m_body,L);
relV=-0.707*relV1;

function [c,ceq]=backpack_MaxRVcon(x,k,zeta,m_body,L)
%constraint function on output power
%x(1)~load weight (kg)
%x(2)~walking speed (m/s)
%k~stiffness coefficient of the springs
%L~body height
%L0~leg length
L0=0.53*L;
Y=body_amp(x(2),L0); %get the amplitude of CoM, viz. Y(t) in base
excitation model
w=walk_freq(x(2));%get walking frequency

c=[x(1)-1000];%inequalility constraint
ceq=[151.7-backpack_MinGRFNLP(x,k,zeta,m_body,L)];%equality
constraint on output power

    function w=walk_freq(V)
        w=round((1.504*(V/L0)^0.57)*60)/60*2*pi;
    end

    function Y=body_amp(V,L)

        Y=L0/2*(1-(1-(0.96*pi*V/( L0*walk_freq(V) ))^2)^(1/2))-
0.0157*L0;
    end
end
```

```
function [CoG_amp_m CoG_amp_p CoG_amp_per...
    relVrms_m relVrms_p relVrms_per
lean12_mean]=fb(Sub,Load,Vel,BW,LL,m_frame)

m_body=BW*0.4536;
zeta=0.26;%k=4027 for vertical position
fb1=importdata(['F:\Backpack
Data\Sub',Sub,'\Activity_',Sub,'_',Load,'lb_',Vel,'mph.exp']);
fb_raw=fb1.data;

CoG=fb_raw(:,[4]);
t=[0.001:0.001:6]';
p=polyfit(t,CoG,10);
CoGd=polyval(p,t);
CoG=CoG-CoGd;
CoG12=reshape(CoG(5:5992),499,12);


%calculate predicted value
%body amplitude
fft_CoG12=abs(fft(CoG12));
vel=str2num(Vel)/10*1609/3600;
[Y12
I12]=max([zeros(6,size(fft_CoG12,2));fft_CoG12(7:493,:);zeros(6,size(ff
t_CoG12,2))]);
w=(I12-1).*(100/size(fft_CoG12,1)*2*pi);%get the dominant frequency of
each fragment

if str2num(Load)==0
    load=0;
    lean12_mean=zeros(1,12);
else
    load=str2num(Load)*0.4536+2.2;
    bp=sqrt((fb_raw(:,[10])-fb_raw(:,[13])).^2+(fb_raw(:,[9])-
fb_raw(:,[12])).^2);
    lean=(atan(fb_raw(:,[12])-fb_raw(:,[6])./(fb_raw(:,[7])-
fb_raw(:,[13])))/pi*180;
    %bp=sqrt((fb_raw(:,[5])-fb_raw(:,[11])).^2+(fb_raw(:,[6])-
fb_raw(:,[12])).^2+(fb_raw(:,[7])-fb_raw(:,[13])).^2);
    rel_vel_1=diff(bp)./(1/100);
    rel_vel_1(abs(rel_vel_1)>1)=0;
    bp12=reshape(bp(5:5992),499,12);
    rel_vel12=reshape(rel_vel_1(5:5992),499,12);
    lean12=reshape(lean(5:5992),499,12);
    lean12_mean=mean(lean12);
    k=4027./cos(lean12_mean./180.*pi);
end

        body_amp(1,i7)=LL/2*(1-(1-
(0.963*pi*vel/( LL*w(1,i7)))^2)^(1/2))-0.0157*LL;

    if load==0
        ;
    else
         r(1,i7)=w(1,i7)/sqrt(k(1,i7)/load);%displacement ratio
        %Calculate phase shift
```

```
        theta1(1,i7)=atan(2*zeta*r(1,i7)/(1-r(1,i7)^2));
        if theta1(1,i7)<0
            theta1(1,i7)=theta1(1,i7)+pi;
        end
        theta2(1,i7)=atan(1/(2*zeta*r(1,i7)));

        %Calculate peak relative velocity,along the frame
        %phase shift on position is -theta1-theta+pi/2
        %phase shift on velocity is -theta1-theta-pi/2
        %using pi-(phase shift) in law of cosines for vector summation
        relV1(1,i7)=-w(1,i7)*body_amp(1,i7)*cos(30/180*pi)*...
            ((1+4*zeta^2*r(1,i7)^2)/((1-
r(1,i7)^2)^2+4*zeta^2*r(1,i7)^2))^(1/2);
        relV2(1,i7)=-w(1,i7)*body_amp(1,i7)*cos(30/180*pi);
        relV(1,i7)=sqrt(relV1(1,i7)^2+relV2(1,i7)^2-...
            2*relV1(1,i7)*relV2(1,i7)*cos(theta1(1,i7)+theta2(1,i7)-
pi/2));
        relVrms_p(1,i7)=relV(1,i7)*sqrt(0.5);
    end

end

%get measured average CoG amplitude
for i8c=1:size(CoG12,2)
    zm1=1;zm2=1;
    for i8r=2:size(CoG12,1)-1
        if (CoG12(i8r,i8c)-CoG12(i8r-1,i8c)>0)&(CoG12(i8r+1,i8c)-
CoG12(i8r,i8c)<0)
            CoG12_max_temp(1,zm1)=CoG12(i8r,i8c);
            zm1=zm1+1;
        elseif (CoG12(i8r,i8c)-CoG12(i8r-1,i8c)<0)&(CoG12(i8r+1,i8c)-
CoG12(i8r,i8c)>0)
            CoG12_min_temp(1,zm2)=CoG12(i8r,i8c);
            zm2=zm2+1;
        end
    end
    CoG_max(1,i8c)=mean(CoG12_max_temp);
    CoG_min(1,i8c)=mean(CoG12_min_temp);
    CoG12_max_temp=[];
    CoG12_min_temp=[];
end
CoG_amp_m=(CoG_max-CoG_min)/2;
CoG_amp_p=body_amp;
CoG_amp_per=(CoG_amp_m-CoG_amp_p)./CoG_amp_m;

%get measured average V-rms
if load==0;
    relVrms_per=zeros(1,12);
    relVrms_m=zeros(1,12);
    relVrms_p=zeros(1,12);
else
    for i9c=1:size(CoG12,2)
        zmv1=1;zmv2=1;
        for i9r=2:size(CoG12,1)-1
            if (rel_vel12(i9r,i9c)-rel_vel12(i9r-
1,i9c)>0)&(rel_vel12(i9r+1,i9c)-rel_vel12(i9r,i9c)<0)...
```

```
                    &rel_vel12(i9r,i9c)>0
                rel_vel12_max_temp(1,zmv1)=rel_vel12(i9r,i9c);
                zmv1=zmv1+1;
            elseif (rel_vel12(i9r,i9c)-rel_vel12(i9r-
1,i9c)<0)&(rel_vel12(i9r+1,i9c)-rel_vel12(i9r,i9c)>0)...
                    &rel_vel12(i9r,i9c)<0
                rel_vel12_min_temp(1,zmv2)=rel_vel12(i9r,i9c);
                zmv2=zmv2+1;
            end
        end
        rel_vel_max(1,i9c)=mean(rel_vel12_max_temp);
        rel_vel_min(1,i9c)=mean(rel_vel12_min_temp);
        rel_vel12_max_temp=[];
        rel_vel12_max_temp=[];
    end
    rel_vel_amp=rel_vel_max-rel_vel_min;

    relVrms_m=sqrt(sum(rel_vel12.^2).*0.01./4.99);
    relVrms_per=(relVrms_m-relVrms_p)./relVrms_m;
end
```

```
function [fp_max_m fp_max_p fp_max_per_mean
fp_min_per_mean]=tm(Sub,Load,Vel,BW,LL,m_frame)
%load is either 30 / 45 lb, not including frame nor aluminum plate
%m_frame is either 0 or 6.7kg (transferred from parent-function)

m_body=BW*0.4536;
k=4650; %k=4027 for vertical position
zeta=0.256;
fp_raw=dlmread(['F:\Backpack
ata\Sub',Sub,'\',Sub,'_',Load,'lb_',Vel,'mph.exp'],...
    '\t',[14,0,6013,2]);
fp_raw(:,4)=fp_raw(:,2)+fp_raw(:,3);

%eliminate the zeros at the ends of the sequence
i1=1;i2=size(fp_raw,1);
while fp_raw(i1,4)<mean(fp_raw(:,4))
    i1=i1+1;
end
while fp_raw(i2,4)<mean(fp_raw(:,4))
    i2=i2-1;
end
fp_1=fp_raw(i1:i2,4);

%eliminate missing steps
%detect zero points
z1=1;z2=1;
for i3=1:length(fp_1)-1
    if (fp_1(i3,1)~=0)&(fp_1(i3+1,1)==0)
        fp_1_idx(1,z1)=i3;
        z1=z1+1;
    elseif (fp_1(i3,1)==0)&(fp_1(i3+1,1)~=0)
        fp_1_idx(2,z2)=i3;
        z2=z2+1;
    end
end


if z1==1&z2==1
    fp_rev=fp_1;
else

    %eliminate zero ponits
    %separate GRF into sub sections
    fp_1_idx2=[1,fp_1_idx(2,:);fp_1_idx(1,:),length(fp_1)];
    fp_sub=cell(size(fp_1_idx2,2),1);
    for i4=1:size(fp_1_idx2,2)
        fp_sub{i4,1}=fp_1(fp_1_idx2(1,i4):fp_1_idx2(2,i4));
    end

    %calculate walking frequency
    fft_fp_1=abs(fft(fp_1));
    [Y,I]=max(fft_fp_1(2:end));
    %calculate forward-moved point for each sub sections
    wfreq=1/(100/length(fp_1)*(I+1))*100;
    ff_idx=fp_1_idx(2,:)-fp_1_idx(1,:);
```

```
    ff_step_idx=fp_1_idx(2,:)-cumsum(round(ceil(ff_idx./wfreq).*wfreq));
    for i5=2:size(fp_1_idx2,2)
        fp_sub{i5,1}=[zeros(ff_step_idx(1,i5-1),1);fp_sub{i5,1}];
    end
    for i6=1:size(fp_1_idx2,2)
        bw_zero=length(fp_sub{end,1})-length(fp_sub{i6,1});
        fp_sub_mat(:,i6)=[fp_sub{i6,1};zeros(bw_zero,1)];
    end
    fp_rev=sum(fp_sub_mat,2);
end

%saparate force into 6 pieces
fp_rev1=fp_rev(1:floor(length(fp_rev)/6)*6);
fp_rev12=reshape(fp_rev1,floor(length(fp_rev)/6),6);
fp_rev12=fp_rev12.*0.4536;
fp_rev1=fp_rev1.*0.4536;

%calculate predicted value
%body amplitude
fft_fp_12=abs(fft(fp_rev12));
vel=str2num(Vel)/10*1609/3600;

if str2num(Load)==0
    load=0;
else load=str2num(Load)*0.4536+2.2; %<--add oscillating part fixed on
the backpack
end

[Y12 I12]=max(fft_fp_12(2:end,:));
w=I12.*(100/size(fft_fp_12,1)*2*pi);

for i7=1:length(w)
    body_amp(1,i7)=LL/2*(1-(1-(0.963*pi*vel/( LL*w(1,i7)))^2)^(1/2))-
0.0157*LL;

    if load==0

oGF(1,i7)=body_amp(1,i7)*(m_body+m_frame+load*sin(30/180*pi)*sin(30/180
*pi))*w(1,i7)^2;
    else r(1,i7)=w(1,i7)/sqrt(k/load);%displacement ratio
        %Calculate phase shift
        theta1(1,i7)=atan(2*zeta*r(1,i7)/(1-r(1,i7)^2));
        if theta1(1,i7)<0
            theta1(1,i7)=theta1(1,i7)+pi;
        end
        theta2(1,i7)=atan(1/(2*zeta*r(1,i7)));

        %Calculate the ground reaction force due to the oscillation

oGF1(1,i7)=k*body_amp(1,i7)*r(1,i7)^2*cos(30/180*pi)*cos(30/180*pi)*...
            ((1+4*zeta^2*r(1,i7)^2)/((1-
r(1,i7)^2)^2+4*zeta^2*r(1,i7)^2))^(1/2); %Force due to weight
oscillation
```

```
oGF2(1,i7)=body_amp(1,i7)*(m_body+m_frame+load*sin(30/180*pi)*sin(30/18
0*pi))*w(1,i7)^2;%Force due to acceleration
        oGF(1,i7)=sqrt(oGF1(1,i7)^2+oGF2(1,i7)^2-...

2*oGF1(1,i7)*oGF2(1,i7)*cos(theta1(1,i7)+theta2(1,i7)+pi/2));
    end

    %Calculate peak ground reaction force
    pGF(1,i7)=(oGF(1,i7)...
        +load*9.8...                %Force due to load weight
        +9.8*(m_body+m_frame))/9.8;      %Force due to fixed load (body
weight and frame weight)
    vGF(1,i7)=(-oGF(1,i7)+load*9.8+9.8*(m_body+m_frame))/9.8;

    %Calculate mean ground reaction force
    mGF(1,i7)=load+(m_body+m_frame);
end

%get measured average peak force
fp_rev1_max=fp_rev1.*(fp_rev1>mean(mGF)*.9);
zm1=1;zm2=1;
for i8=1:length(fp_rev1)-1
    if (fp_rev1_max(i8,1)~=0)&(fp_rev1_max(i8+1,1)==0)
        fp_rev1_idx(1,zm1)=i8;
        zm1=zm1+1;
    elseif (fp_rev1_max(i8,1)==0)&(fp_rev1_max(i8+1,1)~=0)
        fp_rev1_idx(2,zm2)=i8;
        zm2=zm2+1;
    end
end

if fp_rev1_max(1)==0&fp_rev1_max(end)~=0
    fp_rev1_idx(1,:)=[1,fp_rev1_idx(1,1:end-1)];
end
if fp_rev1_max(1)~=0&fp_rev1_max(end)==0
    fp_rev1_idx(:,end)=[];
end
if fp_rev1_max(1)==0&fp_rev1_max(end)==0
    temp1=fp_rev1_idx(1,:);
    fp_rev1_idx(1,:)=fp_rev1_idx(2,:);
    fp_rev1_idx(2,:)=temp1;
end
fp_rev1_idx2=[1,fp_rev1_idx(2,:);fp_rev1_idx(1,:),length(fp_rev1)];

%get measured max force
for i9=1:length(fp_rev1_idx2)
    zms=fp_rev1_idx2(:,i9);
    fp_step_max(1,i9)=max(fp_rev1_max([zms(1,1):zms(2,1)],1));
end
fp_step_max(fp_step_max<mean(mGF)*1.15)=[];
fp_step_max12=reshape(fp_step_max(1:floor(length(fp_step_max)/12)*12),1
2,floor(length(fp_step_max)/12));

%get measured min force
for i10=1:length(fp_rev1_idx)
```

```
    zmins=fp_rev1_idx(:,i10);
    fp_step_min(1,i10)=min(fp_rev1([zmins(1,1):zmins(2,1)],1));
end
fp_step_min(fp_step_min>mean(mGF)*0.9)=[];
fp_step_min12=reshape(fp_step_min(1:floor(length(fp_step_min)/12)*12),1
2,floor(length(fp_step_min)/12));

%PE (percentage error)
for i9_1=1:size(fp_rev12,2)
    fp_max_per12(i9_1,:)=fp_step_max12(i9_1,:)./pGF(1,i9_1)-1;
    fp_min_per12(i9_1,:)=fp_step_min12(i9_1,:)./vGF(1,i9_1)-1;
end
if Sub=='06'&Vel=='38'&Load=='45'
    bp=1;
end
fp_max_per_mean=mean(fp_max_per12');
fp_min_per_mean=mean(fp_min_per12');
fp_max_m=mean(fp_step_max12');
fp_max_p=pGF;

%periodic regression
t12=[0:1/100:size(fp_rev12,1)/100]';
t12(end)=[];
for i11=1:size(fp_rev12,2)
    c=cos(w(1,i11).*t12);
    s=sin(w(1,i11).*t12);
    R=[ones(length(t12),1),c,s];
    coeff(:,i11)=R\fp_rev12(:,i11);
    mag(1,i11)=oGF(1,i11)./9.8./sqrt(coeff(2,i11).^2+coeff(3,i11).^2);
    phi(1,i11)= atan(coeff(2,i11)/coeff(3,i11));
    if phi(1,i11)<0
        phi(1,i11)=phi(1,i11)+pi;
    end
    reg(:,i11)=R*coeff(:,i11);
    mdl(:,i11)=mGF(1,i11)+mag(1,i11).*R(:,2:3)*coeff(2:3,i11);
end
```